
Masters Theses

Student Theses and Dissertations

Fall 2018

Field implementation of cement-based composite strengthening technologies

Michael Andrew Janke

Follow this and additional works at: https://scholarsmine.mst.edu/masters_theses



Part of the [Civil Engineering Commons](#)

Department:

Recommended Citation

Janke, Michael Andrew, "Field implementation of cement-based composite strengthening technologies" (2018). *Masters Theses*. 7823.

https://scholarsmine.mst.edu/masters_theses/7823

This thesis is brought to you by Scholars' Mine, a service of the Missouri S&T Library and Learning Resources. This work is protected by U. S. Copyright Law. Unauthorized use including reproduction for redistribution requires the permission of the copyright holder. For more information, please contact scholarsmine@mst.edu.

FIELD IMPLEMENTATION OF CEMENT-BASED COMPOSITE
STRENGTHENING TECHNOLOGIES

by

MICHAEL ANDREW JANKE

A THESIS

Presented to the Faculty of the Graduate School of the
MISSOURI UNIVERSITY OF SCIENCE AND TECHNOLOGY

In Partial Fulfillment of the Requirements for the Degree

MASTER OF SCIENCE IN CIVIL ENGINEERING

2018

Approved by

John J. Myers, Advisor
Lesley H. Sneed
K. Chandrashekhara

ABSTRACT

With infrastructure continuing to age, technologies are being developed to strengthen structures as a more sustainable option than replacement. The use of fiber-reinforced cementitious matrix (FRCM) strengthening systems is a promising new technology for adding flexural and shear capacity to existing reinforced concrete members. While cement based systems with carbon, PBO, and steel have all been implemented in a lab setting, there is not research data available for installation in the field. FRCM composites have advantages over more widely used fiber reinforced polymer (FRP) composites such as heat resistance and compatibility with concrete substrate. FRP systems have previously been field tested, giving confidence for the growth of FRCM use. This study aimed to validate the use of cement-based systems for field implementation. Missouri Bridge P-0058, a structurally deficient bridge in southern Missouri, was recently selected and six of its twelve girders were strengthened using four different composite systems, three of which are cement-based. A parametric study was conducted to help choose the final design that will give the best information in the future. A pre-strengthening load test was conducted to get a baseline of the bridge's stiffness, so that future tests can capture the change due to the strengthening as well as potential loss of stiffness over time. The Missouri Department of Transportation has agreed to allow the girders to be brought to the campus of Missouri University of Science and Technology when the bridge is decommissioned. On campus, destructive testing will give valuable information about the field strengthened and field conditioned beams.

ACKNOWLEDGMENTS

Pursuing my master's degree has been both challenging and rewarding, and would not be possible without the efforts of several amazing people. First and foremost, I would like to thank my advisor, Dr. John J. Myers. It has been an amazing experience working on such an interesting project under Dr. Myers. I would also like to thank the members of my committee, Dr. Lesley H. Sneed and Dr. K. Chandrashekhara, for their review of this document.

This project would not be possible without the help of fellow graduate students, especially Eli Hernandez, Zuhair Al-Jaberi, Hayder Alghazali, and Ali Al-Khafaji. It has been a pleasure getting to know these students throughout the research project. A massive thank you also to Jason Cox for leading the installation of the strengthening systems.

Another big thank you also goes to Dr. Antonio Nanni and his colleagues at the University of Miami for their support and assistance.

I am also very appreciative of material donations and funding that made this project possible. I gratefully acknowledge the financial support provided by the REsearch on Concrete Applications for Sustainable Transportation (ReCAST) Tier 1 University Transportation Center at Missouri S&T. Thank you to Structural Technologies, Simpson Strong-Tie, Ruredil, and Kerakoll for material contributions.

To my parents Brian and Kim, my brother Nick, and my sisters Elizabeth and Rebecca, thank you for always supporting me in all aspects of life.

TABLE OF CONTENTS

	Page
ABSTRACT.....	iii
ACKNOWLEDGMENTS	iv
LIST OF ILLUSTRATIONS.....	x
LIST OF TABLES.....	xii
NOMENCLATURE	xiii
SECTION	
1. INTRODUCTION.....	1
1.1. BACKGROUND	1
1.2. RESEARCH OBJECTIVE	2
1.3. SCOPE AND LIMITATIONS.....	3
1.4. THESIS ORGANIZATION.....	3
2. LITERATURE REVIEW.....	5
2.1. FIBER-REINFORCED POLYMER STRENGTHENING	5
2.1.1. Types of Externally Bonded FRP Systems	5
2.1.1.1. Wet layup systems	5
2.1.1.2. Prepreg systems	6
2.1.1.3. Precured systems.....	6
2.1.1.4. Near-surface-mounted (NSM) systems.....	6
2.1.2. Constituent Materials and Properties	7
2.1.2.1. Constituent materials	7
2.1.2.2. Physical properties	9

2.1.2.3. Mechanical properties	10
2.1.2.4. Time-dependent properties	11
2.1.3. FRP Failure Modes.....	12
2.1.4. Research on FRP Strengthening Systems	12
2.1.4.1. Holdener, Myers, & Nanni, (2004).....	13
2.1.4.2. Rahman, Kingsley, & Kobayashi (2000).....	16
2.1.4.3. Petrou, Parler, Harries, & Rizos (2008).....	17
2.2. FABRIC-REINFORCED CEMENTICIOUS MATRIX STRENGTHENING	19
2.2.1. Tensile Characterization.....	20
2.2.2. FRCM Failure Modes.....	21
2.2.3. Research on FRCM Strengthening Systems	22
2.2.3.1. Di Tommaso, Focacci, & Mantegazza (2008).....	22
2.2.3.2. D'Ambrisi & Focacci (2011).....	23
2.2.3.3. Loreto, Leardini, Arboleda, and Nanni (2013).....	24
2.2.3.4. Babaeidarabad, Loreto, and Nanni (2014).....	25
2.2.3.5. Ombres (2015)	26
2.2.3.6. Loreto, Babaeidarabad, Leardini, and Nanni (2015)	27
2.3. STEEL REINFORCED GROUT.....	28
2.3.1. Research on SRG Strengthening	29
2.3.1.1. Huang et al. (2003)	30
2.3.1.2. Wobbe et al. (2004).....	30
2.4. NON DESTRUCTIVE TESTING	31
2.4.1. Load Testing.....	31

2.4.2. Surface Roughness	32
2.4.3. Fiber Alignment	33
2.4.4. FRP Delamination	34
3. DESIGN OF STRENGTHENING SYSTEMS	35
3.1. BRIDGE DESCRIPTION.....	35
3.2. MATERIALS USED	37
3.2.1. Fiber-Reinforced Polymer	37
3.2.2. Fabric-Reinforced Cementitious Matrix	38
3.3. ANALYSIS OF EXISTING CAPACITY	39
3.3.1. Flexure.....	40
3.3.2. Shear.....	43
3.4. GIRDER STRENGTHENING DESIGN.....	44
3.4.1. Fiber Reinforced Polymer	46
3.4.1.1. Flexure design.....	47
3.4.1.2. Shear design.....	51
3.4.2. Fiber Reinforced Cementitious Matrix.....	53
3.4.2.1. Flexure design.....	54
3.4.2.2. Shear design.....	55
3.4.3. Summary of Design.....	56
4. INSTALLATION OF STRENGTHENING SYSTEMS	58
4.1. PRE INSTALLATION	58
4.1.1. Substrate Repair	58
4.1.2. Surface Preparation	58

4.2. INSTALLATION	62
4.2.1. Mixing of Resin or Matrix.....	62
4.2.2. Manual Layup.....	63
4.2.3. Curing.....	65
4.2.4. Durability Study	65
5. LOAD TESTING	67
5.1. INSTRUMENTATION	67
5.2. SETUP	69
5.3. PROCEDURE.....	71
5.4. RESULTS AND DISCUSSION.....	74
5.4.1. Data Analysis.	74
5.4.2. Theoretical Modeling.....	75
5.4.3. Results.	77
6. SUMMARY AND CONCLUSIONS.....	84
6.1. SUMMARY.....	84
6.2. FINDINGS AND CONCLUSIONS	85
6.3. RECOMMENDATIONS.....	86
6.4. FUTURE WORK.....	87
APPENDICIES	
A. MODOT DESIGN DRAWINGS	89
B. ANALYSIS OF EXISTING CAPACITY	100
C. PARAMETRIC STUDY OF FLEXURAL STRENGTHENING.....	105
D. SHEAR STRENGTHENING WRAPPING SCHEME.....	124

E. BILL OF MATERIALS.....	126
F. MANUFACTURER’S MATERIAL INFORMATION	129
G. TEE-BEAM ANALYSIS DEFLECTION CALCULATIONS.....	149
REFERENCES	158
VITA	162

LIST OF ILLUSTRATIONS

Figure	Page
2.1. FRP Debonding Modes.....	13
2.2. Location of Bridges Strengthened	14
2.3. Loading Scheme.....	17
2.4. Stress-Strain Curve for Fully-Clamped FRCM in Tension	22
2.5. Debonding Failure Modes.....	22
2.6. Steel Reinforcement.....	29
2.7. Laser Profilometer	33
3.1. Bridge P-0058 Load Posting.....	36
3.2. Bridge P-00585 Approach and Profile View	36
3.3. Fibers Used in FRCM	39
3.4. Cross Sections of Spans.....	41
3.5. Effective Flange Width.....	42
3.6. Internal Stress and Strain Distribution in Flexure.....	48
3.7. Shear Strengthening With FRP Nomenclature	51
4.1. Spalling on Girder.....	59
4.2. Surface Preparation by Sand Blasting.....	60
4.3. Rounding Corners	60
4.4. Mixing Resin and Cementitious Matrix.....	63
4.5. Preparing Sheets in Lab Setting.....	64
4.6. Manual Layup	65
5.1. Span 1 Prism Layout.....	68
5.2. Span 4 Prism Layout.....	68
5.3. Data Acquisition System Setup	70

5.4. Total Station Setup.....	70
5.5. H20 Dump Truck Axle Configuration.....	71
5.6. Load Test Truck Placements.....	72
5.7. Trucks on Span 1 for Load Test.....	73
5.8. Truck on Span 4 for Load Test	74
5.9. Span 1 Stop 1 Vertical Deflection	77
5.10. Span 1 Stop 2 Vertical Deflection	78
5.11. Span 1 Stop 3 Vertical Deflection	78
5.12. Span 1 Stop 1 Interior Girder Deflection Comparison	80
5.13. Span 1 Stop 1 Exterior Girder Deflection Comparison	80
5.14. Span 1 Stop 2 Interior Girder Deflection Comparison	81
5.15. Span 1 Stop 2 Exterior Girder Deflection Comparison	81
5.16. Span 1 Stop 3 Interior Girder Deflection Comparison	82
5.17. Span 1 Stop 3 Exterior Girder Deflection Comparison	82

LIST OF TABLES

Table	Page
2.1. Typical Tensile Properties of Fibers Used in FRP Systems	8
2.2. Typical Densities of FRP Materials.....	9
2.3. FRP Service Load Stress Limits	12
2.4. Details of Five Bridges Strengthened	14
2.5. Girder Strengthening Schedule and Analytical Capacity Increase	15
3.1. CFRP Properties from Manufacturer	37
3.2. FRCM Statistical Properties	38
3.3. Geometrical Properties.....	42
3.4. Flexural Internal Steel Reinforcement at Midspan	42
3.5. Existing Nominal Moment Capacity	43
3.6. Shear Internal Steel Reinforcement	43
3.7. Existing Nominal Shear Capacity.....	44
3.8. Moment Capacity Parametric Data.....	45
3.9. Creep and Fatigue Stress Limits	55
3.10. Summary of Strengthening System Design	57
5.1. Pre Strengthening Load Test Axle Loads	75

NOMENCLATURE

<u>Symbol</u>	<u>Description</u>
a	Depth of equivalent stress block (in)
a/d	Shear span-to-depth ratio (in/in)
A_c	Area of concrete section (in ²)
A_f	Area of FRP/FRCM reinforcement (in ²)
A_{fv}	Area of FRP/FRCM shear reinforcement, with spacing s (in ²)
A_s	Area of longitudinal steel (in ²)
b	Width of rectangular cross section (in)
b_w	Web thickness (in)
b_e	Effective width of the flange
c	Distance from extreme compressive fiber to neutral axis (in.)
C_E	Environmental reduction factor
d	Distance from extreme compression fiber to centroid of steel reinforcement (in)
d_b	Diameter of reinforcing bar (in)
d_f	Distance from extreme compression fiber to centroid of FRP/FRCM reinforcement (in)
d_{fv}	Effective depth of FRP/FRCM shear reinforcement
E_c	Modulus of elasticity of concrete (psi)
E_f	Design or guaranteed modulus of elasticity of FRP/FRCM defined as mean modulus of a sample of test specimens; for FRCM, characterizes cracked behavior (psi)
E_f^*	Uncracked modulus of elasticity for FRCM, obtained from a coupon test (psi)
E_s	Modulus of elasticity of steel (psi)

f_c	Compressive stress in concrete (psi)
f'_c	Specified design concrete compressive strength (psi)
f_f	Stress in FRP/FRCM reinforcement in tension (psi)
f_{fd}	Design stress of FRP/FRCM reinforcement (psi)
f_{fe}	Effective stress in FRP/FRCM, stress level attained at section failure (psi)
f_{fu}	design tensile strength of FRP/FRCM material, considering reductions for service environment (psi)
f^*_{fu}	Guaranteed tensile strength of FRP/FRCM (psi)
f_{fv}	Tensile strength of FRP/FRCM for shear design (psi)
f_{fs}	Stress in FRP/FRCM reinforcement under service load (psi)
f_s	Stress in steel reinforcement (psi)
f_{ss}	Stress in steel reinforcement under service load (psi)
f_y	Specified yield strength of shear reinforcement (psi)
h	Total depth of member (in.)
h_f	Member flange thickness (in)
I	Moment of inertia (in ⁴)
I_{cr}	Moment of inertia of transformed, cracked section (in ⁴)
I_e	Effective moment of inertia (in ⁴)
I_g	Gross moment of inertia (in ⁴)
k	Ratio of depth of neutral axis to reinforcement depth measured from extreme compression fiber
l	Length of span (ft)
l_n	Clear span length (ft)
M_{cr}	Flexural cracking moment (k-ft)

M_n	Nominal flexural capacity of section (k-ft)
M_{nf}	Contribution of FRP/FRCM reinforcement to nominal flexural strength (k-ft)
M_{ns}	Contribution of steel reinforcement to nominal flexural strength (k-ft)
M_u	Factored moment at a section (k-ft)
n	Number of plies of FRP/FRCM reinforcement
n_f	Modular ratio of elasticity between FRP/FRCM and concrete = E_f/E_c
n_s	Modular ratio of elasticity between steel and concrete = E_s/E_c
r	Radius of gyration of a section (in)
s	Center to center spacing of shear reinforcement (in.)
t_f	Nominal thickness of one ply of FRP/FRCM reinforcement (in)
T_g	Glass-transition temperature (degrees Fahrenheit)
V_c	Nominal concrete shear resistance (kips)
V_f	Nominal FRP/FRCM shear resistance (kips)
V_n	Nominal shear resistance (kips)
V_s	Nominal steel shear resistance (kips)
V_u	Factored shear force at section (kips)
w_f	Width of FRP/FRCM reinforcing plies (in)
α	Angle of inclination of shear reinforcement to longitudinal reinforcement (degree)
α_1	Multiplier on f_c to determine intensity of an equivalent rectangular stress distribution for concrete
β_1	Ratio of depth of equivalent rectangular stress block to depth of neutral axis
ϵ_{bi}	Strain level in concrete substrate at time of FRP/FRCM installation (in/in)

ϵ_c	Strain level in concrete (in/in)
ϵ_{cu}	Maximum usable strain in concrete (in/in)
ϵ_f	Strain level in FRP/FRCM reinforcement (in/in)
ϵ_{fd}	Debonding strain of externally bonded FRP/FRCM reinforcement (in/in)
ϵ_{fe}	Effective strain level in FRP/FRCM reinforcement at failure (in/in)
ϵ_{fu}	Design rupture strain of FRP/FRCM reinforcement (in/in)
ϵ^*_{fu}	Ultimate rupture strain of FRP/FRCM reinforcement (in/in)
ϵ_s	Net longitudinal strain at centroid of longitudinal reinforcement (in/in)
ϵ_t	Net tensile strain in extreme tension steel at nominal strength (in/in)
ϵ_y	Strain corresponding with yielding of steel reinforcement (in/in)
λ	Reduction factor for lightweight concrete
ϕ	Strength reduction factor
ϕ_m	Strength reduction factor for flexure
ϕ_v	Strength reduction factor for shear
ρ_f	FRP/FRCM reinforcement ratio
ρ_s	Steel reinforcement ratio of flexural member = A_s/bd
σ	Standard deviation
ψ_f	FRP strength reduction factor
AASHTO	American Association of State Highway and Transportation Officials
ACI	American Concrete Institute
ASCE	American Society of Civil Engineers
C-FRCM	Carbon fabric-reinforced cementitious matrix
CFRP	Carbon Fiber-Reinforced Polymer

DAS	Data Acquisition System
DOT	Department of Transportation
EB	Externally Bonded
FRCM	Fabric-reinforced cementitious matrix
FRP	Fiber-reinforced polymer
LRFD	Load and resistance factored design
LVDT	Linear Variable Differential Transformer / Linear Variable Displacement Transformer
ML	Manual Layup
MoDOT	Missouri Department of Transportation
NDT	Nondestructive Testing
NSM	Near Surface Mounted
PBO	Polyparaphenylene Benzobisoxazole
RC	Reinforced concrete
RE-CAST	Research on Concrete Applications for Sustainable Transportation
SRG	Steel Reinforced Grout
SRP	Steel Reinforced Polymer
WL	Wet Layup

1. INTRODUCTION

1.1. BACKGROUND

Our nation is facing major concerns with an aging infrastructure that is vital to commerce and our economy as well as our quality of life. The American Society of Civil Engineers (ASCE) puts out a yearly infrastructure report card in an attempt to put this issue into terms that the general public can relate to well. In 2017, nationally, bridges received a C+ rating, and Missouri is below average, coming in at a C. A grade of C signifies “mediocre, requires attention.” Missouri has the seventh largest number of bridges of all the states, 12.5% of which are considered structurally deficient (ASCE, 2017). Many factors contribute to bridges becoming structurally deficient, including long-term exposure to harsh environments, poor initial design or construction, increasing traffic loads, changing design standards, increased safety requirements, or catastrophic events such as earthquakes.

Replacing thousands of bridges is both time consuming and expensive, so repairing bridges has emerged as a better, more sustainable option. Strengthening or retrofitting concrete structures can add capacity and increase the service life by several decades. Traditional flexural strengthening techniques include externally bonded steel plates, steel or concrete jackets, external post-tensioning, and other methods. Shear strengthening methods include external stirrups and epoxy bonded steel plates. These methods leave materials exposed to the environment, making them vulnerable to corrosion.

Since the 1980s, composite materials have been an emerging technology as an alternative for strengthening concrete structures in the United States, Japan, Canada, and

Europe. While many research projects have been conducted in university labs, more full-scale and in situ studies are needed, since departments of transportation (DOTs) are still hesitant to implement these innovative materials.

Composite materials consist of fibers that are incased in some sort of matrix. Common fiber types include carbon, glass, aramid, and polyparaphenylene benzobisoxazole (PBO). When a polymeric resin is used, the material is classified as a fiber-reinforced polymer (FRP). When a cementitious material is used, the material is classified as a fiber-reinforced cementitious matrix (FRCM). Both classes of composites have advantages over traditional materials such as corrosion resistance and high tensile strength.

The following thesis describes the design, fabrication, and installation of strengthening systems using FRP and FRCM. This study was one task of the Research on Concrete Applications for Sustainable Transportation (RE-CAST) program project 3C. Task 11 of project 3C consists of field implementation and load testing of an FRCM strengthened bridge. Missouri Bridge P0058 was chosen from several candidates for the project.

1.2. RESEARCH OBJECTIVE

This research study was conducted in an attempt to validate the applicability of several composite systems for strengthening bridge girders in the field and to monitor them over time. The main objective is to demonstrate bridge girder strengthening using the FRCM and SRG technology, which to date have no reported field bridge applications in available literature. Analysis of the structure was completed, and design calculations were prepared for each strengthening system. Design guides by ACI committees 440-08

and 549-13 were used in the design of the systems. These reports also detailed the proper procedure for installation of the strengthening systems. Pre- and post-strengthening load tests were used to monitor the bridge's behavior in service, and how the behavior changed after strengthening.

This study is also allowing for long-term bond performance test bed preparing for future studies of how the strengthening systems are affected by field exposure over time. Some design decisions were made to better prepare for future testing of the bridge.

1.3. SCOPE AND LIMITATIONS

This project is a demonstration of the field installation of composite strengthening systems. The study focuses only on strengthening of the bridge girders. Additionally, only the girders on spans 1 and 4 were strengthened where the girders were accessible for strengthening. Other structural elements such as the slab and bents were not considered. The strengthening system design is not intended to change the posted limitations on the bridge.

1.4. THESIS ORGANIZATION

This thesis is organized into six sections. Section 1 is an introduction to the study, including background information on bridge strengthening, the research objective, and the scope.

Section 2 contains background information that was needed to begin the study. The following subject areas were studied: properties of FRP, properties of FRCM, properties of SRG, strengthening of structural members for flexure and shear, and non-destructive testing of structures.

Section 3 details the design of the strengthening systems. This includes a description of the bridge and materials used, analysis of the pre-strengthened bridge, and the design of each system.

Section 4 describes the installation of composite strengthening systems. This includes the substrate repair and surface preparation needed before strengthening, as well as the installation of each system.

Section 5 describes the load testing done for this study prior to strengthening to provide a baseline to compare future load test data to after strengthening during service life. Instrumentation and other work done in preparation for load testing is described in addition to the pre- and post- strengthening tests.

Section 6 contains the conclusions reached in this study, as well as future research recommendations. Following Section 6 are Appendices A through F, which include supplemental details and information.

2. LITERATURE REVIEW

2.1. FIBER-REINFORCED POLYMER STRENGTHENING

Fiber-reinforced polymer (FRP) is defined by ACI 440.2R as “a composite material comprising a polymer matrix reinforced with fibers in the form of fabric, mat, strands, or any other fiber form.” In a composite, constituent materials remain distinct, but combine to form a material with properties not possessed by any of the constituent materials individually. In general in FRP, the fibers carry load along the length of the fiber to provide strength and stiffness, and the matrix material transfers stresses between the fibers and protects them from environmental and mechanical damages. Advantages of FRP include high strength to weight ratio, high tensile strength, and corrosion resistance. (ACI Committee 440, 2008; Arboleda, 2014; Pino, 2016)

2.1.1. Types of Externally Bonded FRP Systems. There are several forms of FRP systems that are classified by how they arrive onsite and are installed. The best system to use varies based on the application. In some cases, a combination of systems can be used, especially if large strength gains are desired. Following are some common forms for strengthening structural members. (ACI Committee 440, 2008)

2.1.1.1. Wet layup systems. Wet layup (WL) FRP systems consist of dry unidirectional or multidirectional fiber sheets or fabrics that are impregnated with a saturating resin on site. This method is also sometimes referred to as manual layup (ML). The concrete substrate is primed and puttied, and then the saturating resin binds the fibers to the surface. A wet layup system is similar to cast-in-place concrete, in that they are saturated in place, and cured in place. (ACI Committee 440, 2008)

2.1.1.2. Prepreg systems. Prepreg FRP systems consist of partially cured unidirectional or multidirectional fiber sheets or fabrics that are preimpregnated with a saturating resin in the manufacturer's facility. Once on site, they typically do not require additional resin to bond the system to the concrete surface. Prepreg systems are saturated off-site, then similar to wet layup systems, they are cured on site. A typical prepreg system requires additional heating for curing. The manufacturer of a prepreg system should be consulted for storage and shelf-life recommendations and curing procedures. (ACI Committee 440, 2008)

2.1.1.3. Precured systems. Precured FRP systems consist of various composite shapes manufactured in a plant off-site. Common types of precured systems include unidirectional plates, multidirectional grids, and curved shells. Typically, an adhesive, along with primer and putty, is used to bond the precured shapes to the concrete surface. Another technique is to mechanically fasten (MF) precured plates to the concrete with bolts. Precured systems are similar to precast concrete, as they are saturated and cured off site. (ACI Committee 440, 2008; Holdener, Myers, & Nanni, 2004)

2.1.1.4. Near-surface-mounted (NSM) systems. NSM systems consist of surface-embedded circular or rectangular bars or plates, which are installed and bonded into grooves made on the concrete surface. An adhesive recommended by the NSM manufacturer is used to bond the FRP bar into the groove, and is cured in place. Bars and plates used in NSM are typically manufactured using the pultrusion process, which creates long, straight, constant cross-section parts. (ACI Committee 440, 2008)

2.1.2. Constituent Materials and Properties. The physical and mechanical properties of FRP composites need to be understood to properly use them for concrete strengthening. Properties are dependent on several factors, such as loading history and duration, temperature, and moisture (ACI Committee 440, 2008; Arboleda, 2014).

2.1.2.1. Constituent materials. The constituent materials chosen have a great impact on the composite properties, as various materials can fill a wide range of desired properties. The correct choice of fiber type, resin type, and, when applicable, protective coating are important in dictating performance of the composite. Additionally, changing the volume fraction of these constituents can have a big impact on composite properties (ACI Committee 440, 2008).

A wide range of Polymeric resins are available for use in FRP systems. The most common types are epoxy, vinyl esters, and polyesters and they have been formulated for use in a wide range of environments. The main qualities of resins that manufacturers desire are (ACI Committee 440, 2008):

- Development of appropriate mechanical properties for the FRP composite
- Compatibility with and adhesion to both the concrete and reinforcing fibers
- Resistance to environmental effects such as moisture, salt water, extreme temperature, and chemicals associated with concrete
- Filling ability
- Workability
- Pot life consistent with the application

Fibers are relied on to give the FRP system its strength and stiffness. The most common fiber materials are carbon, glass, and aramid. The fiber tensile properties can

vary based on manufacturing process. Table 2.1 shows typical ranges of properties for different fibers.

Table 2.1. Typical Tensile Properties of Fibers Used in FRP Systems (ACI Committee 440, 2008)

Fiber type	Elastic modulus		Ultimate strength		Rupture strain, minimum, %
	10 ³ ksi	GPa	ksi	MPa	
Carbon					
General purpose	32 to 34	220 to 240	300 to 550	2050 to 3790	1.2
High-strength	32 to 34	220 to 240	550 to 700	3790 to 4820	1.4
Ultra-high-strength	32 to 34	220 to 240	700 to 900	4820 to 6200	1.5
High-modulus	50 to 75	340 to 520	250 to 450	1720 to 3100	0.5
Ultra-high-modulus	75 to 100	520 to 690	200 to 350	1380 to 2400	0.2
Glass					
E-glass	10 to 10.5	69 to 72	270 to 390	1860 to 2680	4.5
S-glass	12.5 to 13	86 to 90	500 to 700	3440 to 4140	5.4
Aramid					
General purpose	10 to 12	69 to 83	500 to 600	3440 to 4140	2.5
High-performance	16 to 18	110 to 124	500 to 600	3440 to 4140	1.6

Protective coatings are also sometimes used to help minimize potential environmental or mechanical damage to the composite. Coatings are typically applied after the saturating resin has cured. There are a variety of forms of protecting systems including: polymer coatings, acrylic coatings, cementitious systems, and intumescent coatings. Ultraviolet light protection, fire protection, vandalism protection, impact or abrasion resistance, improve aesthetics, chemical resistance, and to prevent chemicals from leaving the system if submerged in potable water are all viable reasons why

protective systems may be desired for FRP strengthened concrete (ACI Committee 440, 2008).

2.1.2.2. Physical properties. The physical properties of FRP's are much different than steel, and in most cases this is advantageous. The density of FRP materials ranges from 75 to 130 lb/ft³ (1.2 to 2.1 g/cm³), which is four to six times lower than steel. This makes FRP easier to transport, reduces dead load on the structure, and makes them easier to handle on the project location. Table 2.2 shows the density ranges for various types of FRP and includes steel for comparison (ACI Committee 440, 2008).

Table 2.2. Typical Densities of FRP Materials (ACI Committee 440, 2008)

Steel	GFRP	CFRP	AFRP
490 (7.9)	75 to 130 (1.2 to 2.1)	90 to 100 (1.5 to 1.6)	75 to 90 (1.2 to 1.5)

Units: lb/ft³ (g/cm³)

Thermal properties must be considered for many FRP applications. The coefficient of thermal expansion of composites differs in the longitudinal and transverse directions for a unidirectional laminate. The design of the laminate can be altered to get desired thermal properties in a given direction by changing the types of fiber, resin, and volume fraction of fiber. If the application of a composite system will experience substantial temperature fluctuations, then caution should be taken to choose an FRP system that has similar thermal properties to the concrete it is strengthening. (ACI Committee 440, 2008).

Another important thermal property of FRP composites is their glass transition temperature (T_g). The value of T_g depends on the type of resin but is normally in the region of 140 to 180 °F (60 to 82.2 °C). Beyond the T_g , the molecular structure changes, and the elastic modulus of the polymer is significantly reduced. At this point, the fibers can continue to support some load in the longitudinal direction, but the system is significantly less stiff in the transverse direction, and in shear. This effect of high temperature reduces shear transfer, so other properties such as flexure strength are also affected. (ACI Committee 440, 2008)

2.1.2.3. Mechanical properties. The mechanical properties of all FRP systems, regardless of form, should be based on the testing of laminate samples with known fiber content. The properties of an FRP system should be characterized as a composite, recognizing not just the material properties of the individual fibers, but also the efficiency of the fiber-resin system, the fabric architecture, and the method used to create the composite. (ACI Committee 440, 2008)

When unidirectional FRP materials are loaded in tension, they do not exhibit any plastic behavior (yielding) like observed in steel. The stress-strain behavior of FRP is linear elastic up until failure, which is sudden and brittle. The tensile properties of a composite depend on many factors, most of which are fiber related. The type of fiber, the orientation of fibers, the quantity of fibers, and the method and conditions in which the composite is produced affect the tensile properties of the FRP material. The tensile properties can be reported in two ways: gross-laminate area (using total composite area with relatively lower strength and modulus) or net-fiber area (using known area of fiber and relatively higher strength and stiffness). Regardless of the basis for the reported

values, the load-carrying strength ($f_{tu} \cdot A_f$) and axial stiffness ($A_f \cdot E_f$) of the composite remain constant. A commercial FRP should have an ultimate tensile strength and ultimate rupture strain reported by the manufacturer. These guaranteed properties are defined by the mean of a sample of test specimens minus three times the standard deviation. This approach gives a 99.87% probability that the actual properties will exceed the reported values. (ACI Committee 440, 2008)

Coupon tests on FRP laminates have shown that the compressive strength of FRP is lower than the tensile strength. Depending on the materials composing the specimen, FRP in longitudinal compression can fail in many ways, including transverse tensile failure, fiber microbuckling, or shear failure. Externally bonded systems with FRP should not be used as compression reinforcement. (ACI Committee 440, 2008)

2.1.2.4. Time-dependent properties. As most structures are intended to last decades, it is important to consider time dependent properties such as creep and fatigue. While research in labs has simulated long term effects, more studies are needed to verify the long term effects of FRP when exposed to field conditions, with different environmental factors. (ACI Committee 440, 2008)

Creep rupture is a sudden failure of a material subject to a constant load after a period of time known as the endurance time. In general, carbon fibers are the least susceptible to creep rupture, followed by aramid, and lastly glass. Fatigue in composites has had more research than creep rupture, because it is critical for aerospace industry applications. Similar to creep, carbon fibers perform the best in fatigue loading. ACI provides recommended sustained stress limits for each fiber type, shown in Table 2.3. (ACI Committee 440, 2008)

Table 2.3. FRP Service Load Stress Limits (ACI Committee 440, 2008)

Stress type	Fiber type		
	GFRP	AFRP	CFRP
Sustained plus cyclic stress limit	$0.20f_{fu}$	$0.30f_{fu}$	$0.55f_{fu}$

2.1.3. FRP Failure Modes. While FRP materials generally have a high tensile strength, their ultimate rupture strength is rarely achieved. Instead, failure is most commonly due to a loss of strengthening action due to various types of fiber debonding. In FRP strengthened RC, it is most common that the strengthening system delaminates due to a fracture within the concrete cover (area between reinforcing steel and concrete surface). The initial debonding may occur at a crack, or at the termination of the reinforcement. Figure 2.1 shows the locations that debonding is most likely to occur at and how the failure propagates. The main method for preventing debonding is to limit the design strain in the fibers or to limit the bond shear. Aram et al. recommend limiting the fiber strain to .008, as well as limiting the shear stress to the tensile strength of the concrete. (ACI Committee 440, 2008; Aram, Czaderski, & Motavalli, 2008; Hind, Özakçab, & Ekmekyaparc, 2016)

2.1.4. Research on FRP Strengthening Systems. Various studies have been conducted around the world, using FRP to strengthen bridges, buildings, or components of structures. Included in this section are studies most relevant to the work done for this thesis.

2.1.4.1. Holdener, Myers, & Nanni, (2004). From 2003 to 2008, a research team from the University of Missouri-Rolla (UMR, now Missouri S&T) undertook a project to field strengthen bridges in order to validate FRP composite technology. The study is referred to as the five-bridge project, and officially titled: “Preservation of Missouri Transportation Infrastructure: Validation of FRP Composite Technology through Field Testing”.

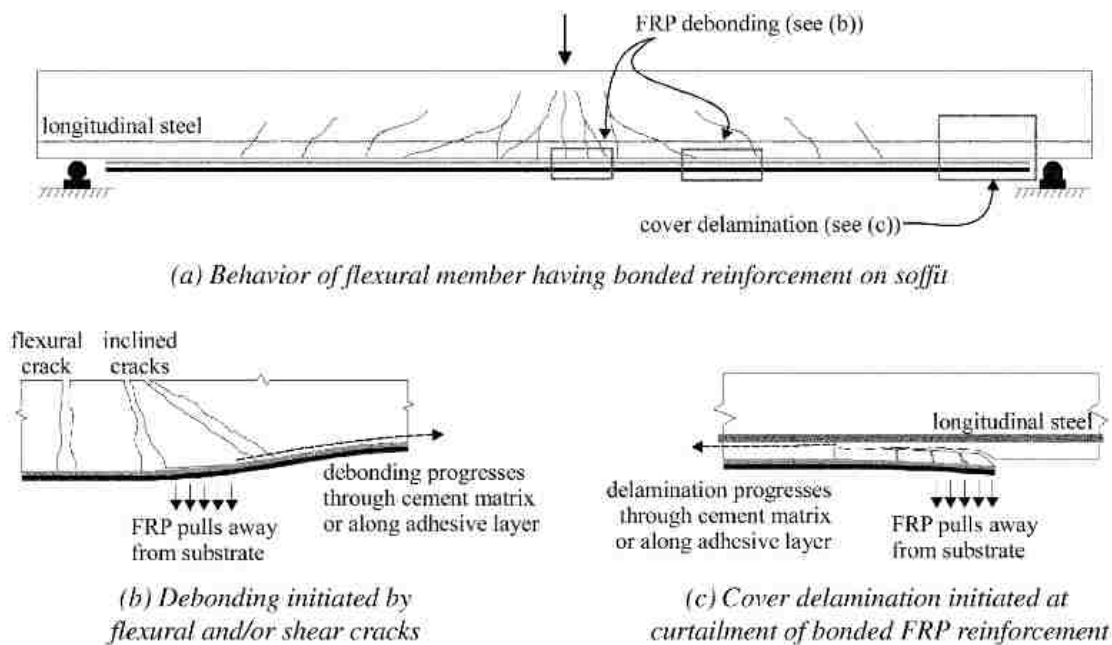


Figure 2.1. FRP Debonding Modes (ACI Committee 440, 2008)

Five structurally deficient bridges around Missouri were chosen and retrofitted with various FRP systems on their girders and slabs. Figure 2.2 shows the location of the bridges within Missouri’s DOT districts. The types of strengthening systems used are manual layup, NSM, steel-reinforced polymer (SRP), and precured laminates attached

with epoxy or mechanically fastened (MF). Table 2.4 breaks down the system types used on each bridge, and provides additional bridge details and geometry.



Figure 2.2. Location of Bridges Strengthened (Holdener et al., 2004)

Table 2.4. Details of Five Bridges Strengthened

Name	Location	Style	# Girders	Girder Spacing	Length Span Lengths	Age	Strengthening
T-0530	Crawford county	T-beam	4 (23ft wide)	6.5ft	237ft 5x 47.5ft spans	1937	CFRP wet layup, pre-cured cfrp laminates
X-0495	Iron County	T-beam	3 (24 ft wide)	9ft	137.5ft 42.5/ 52.5/ 42.5 ft	1948	CFRP wet layup, NSM bars
X-0596	Morgan County	T-beam	3 (20ft wide)	9ft	137.5ft 42.5/ 52.5/ 42.5 ft	1946	CFRP wet layup, NSM bars
P-0962	Dallas County	T-beam	3 (23 ft wide)	9ft	127.5ft 3x 42.5ft	1956	CFRP wet layup, NSM bars, SRP manual layup
Y-0298	Pulaski County	Solid slab	n/a (27ft wide)	n/a	30ft 2x 15ft spans	1937	CFRP wet layup, MF FRP laminates

The five-bridge project upgraded each bridge to meet the ultimate factored loading considering three loading conditions: HS20-44 truck load, 3S2 truck load, and lane load. These load cases satisfy both AASHTO and MoDOT requests.

Table 2.5 presents a detailed reference for the type and amount of strengthening applied to each girder and the analytical capacity increase in flexure gained by adding the composites. Holdener, Myers, and Nanni also presented details for slab flexural strengthening and girder shear strengthening, with their respective analytical capacity increase.

Table 2.5. Girder Strengthening Schedule and Analytical Capacity Increase (Holdener et al., 2004)

Bridge ID	Span #	Girder	Flexural Reinforcing Description (Girder)	Capacity Increase
X-596 ^g	2	Interior	ML: 4 Plies 20" Wide; NSM Bars: 4 Total	42%
X-596 ^g	2	Exterior	None	NA
X-596 ^g	1, 3	Interior	ML: 4 Plies 20" Wide; NSM Bars: 4 Total	44%
X-596 ^g	1, 3	Exterior	ML: 2 Plies 16" Wide	16%
T-530 ^g	1, 3, 5	Interior	ML: 4 Plies 16" Wide	29%
T-530 ^g	1, 3, 5	Exterior	ML: 2 Plies 16" Wide	15%
T-530 ^g	2, 4	Interior	1 Laminate Plate: 12" Wide	29%
T-530 ^g	2, 4	Exterior	1 Laminate Plate: 12" Wide	15%
X-495 ^g	2	Interior	ML: 5 Plies 20" Wide	40%
X-495 ^g	2	Exterior	None	NA
X-495 ^g	1, 3	Interior	ML: 5 Plies 16" Wide; NSM Bars: 2 total	44%
X-495 ^g	1, 3	Exterior	ML: 2 Plies 16" Wide	16%
P-962 ^g	1, 2	Interior	ML: 5 Plies 16" Wide plus 4 NSM Bars	56%
P-962 ^g	1, 2	Exterior	ML: 3 Plies 16" Wide	25%
P-962 ^g	3	Interior	SRP 3X2: 3 Plies 16" Wide	54%
P-962 ^g	3	Exterior	SRP 3X2: 3 Plies 16" Wide	49%

After strengthening, Holdener et al. conducted several nondestructive tests (NDT) in order to monitor the performance of the FRP systems without damaging the system or

the RC structural elements. Load testing was a vital step in validating the effectiveness of the strengthening. The bridge sites made it difficult for traditional deflection monitoring equipment, such as linear variable differential transformers (LVDT), to be used. Instead, optical laser surveying equipment was determined to be the best measure of deflection. NDT results conducted thus far on the five bridges project have shown satisfactory results with no growth in intentional or unintentional defects

Holdener, Myers, and Nanni's study is a valuable comparison, as most of the bridges strengthened are similar in geometry to bridge P0058 in this thesis. Additionally, the five bridges are other examples of composite strengthening in the field, whereas most research available was conducted in lab settings.

2.1.4.2. Rahman, Kingsley, & Kobayashi (2000). This study investigated a full-scale model of a bridge deck slab isotopically reinforced with FRP. The slab studied was 7.28 in (185mm) thick and 19.69 ft (6 m) wide. The total length of the slab was 19.69 ft (6 m) with three girders used to create two 6.56 ft (2 m) spans and a 3.28 ft (1 m) cantilever on each end. The slab was loaded in the midpoint of the two spans simultaneously, and loaded at three separate points along the width of the slab as shown in Figure 2.3. The strengthening material used was a two-dimensional carbon fiber grid. The slab was loaded monotonically to crack the concrete, then loaded cyclically to simulate 50 years of service loading, and finally loaded monotonically to failure. Strain gauges and LVDT were used to monitor the response through each load phase.

Rahman et al. found that the ultimate load of their slab was 120 kip (534 kN), more than five times the design service load. The dominant failure mode observed was punching shear. The exception was under the north jack when loaded at the west end,

where a flexural crack developed and crushing of the concrete occurred. This study showed that FRP has satisfactory constructability, and its behavior in service conditions is also satisfactory. Rahman et al. concluded that the carbon FRP grid system is suitable for use in strengthening, but advised for more research to be conducted considering other factors such as more extreme environmental changes and fatigue paired with chemical exposure.

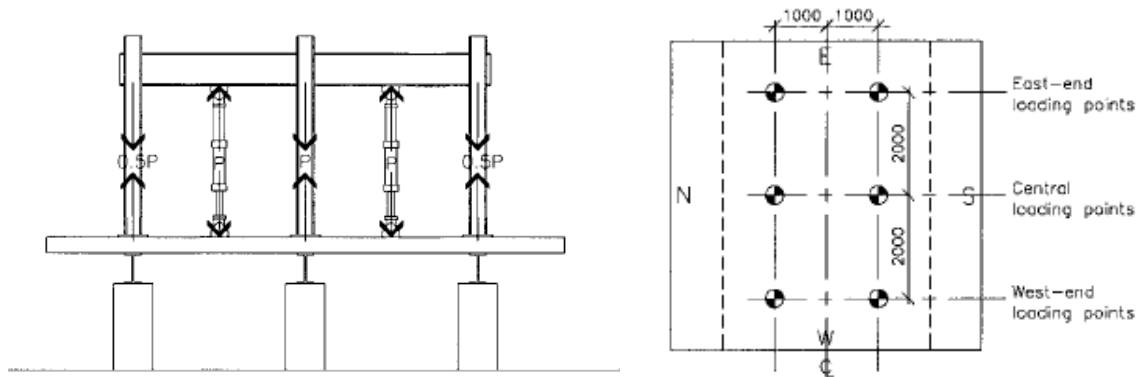


Figure 2.3. Loading Scheme (Rahman et al., 2000) (Dimensions shown are mm.
Conversion: 25.4 mm = 1 in)

2.1.4.3. Petrou, Parler, Harries, & Rizos (2008). This study investigated the monotonic and fatigue behavior of one-way and two-way reinforced concrete slabs strengthened with carbon fiber-reinforced polymer (CFRP) materials. Five one-way reinforced concrete (RC) slab specimens were removed from a decommissioned bridge in South Carolina. Additionally six half-scale, two-way RC slab specimens were

constructed to represent a bridge deck designed using the requirements of AASHTO LRFD Bridge Design Manual.

The one-way specimens were 8.5 inch (215.9 mm) thick rectangles, 14 feet (4.27 m) long and 5 feet (1.52 m) wide. Three specimens were retrofitted using CFRP strips, and two were left unstrengthened for comparison. For both monotonic and fatigue tests, the slabs were simply supported over a 13 foot (3.96 m) span, and subjected to three point bending with the load applied at midspan.

The two-way specimens were 3.75 inch (95.25 mm) thick squares, with 52 inch (1320.8 mm) sides. Two different retrofit techniques were carried out on the two-way specimens: a CFRP grid, and CFRP strips. Two slabs were strengthened with each technique, and two were left unstrengthened for comparison. For both monotonic and fatigue tests, the slabs were simply supported on all sides, resulting in a 48 inch (1219.2 mm) square test region.

The results of the monotonic testing are most relevant to this thesis. Petrou, Parler, Harries, & Rizos made the following conclusions from the monotonic tests:

- Monotonically tested one-way retrofit specimens achieved an increase in ultimate strength of 14.8% and 18.1%, over that of the unretrofit control specimen.
- The failure of the two monotonically tested retrofit one-way slabs was due to debonding of the CFRP that propagated outward from the midspan region as the applied load increased.
- For the monotonically tested two-way slabs, the CFRP strip retrofitted slab and the CFRP grid retrofitted slab achieved ultimate strength increases of 13.8% and 10.7%, respectively.

- The CFRP strip retrofitted two-way slab and the CFRP grid retrofitted two-way slab experienced increases in general cracking load of 8.7% and 34.8%, respectively.
- Punching signified the ultimate failure of all three monotonically tested two-way slabs.

2.2. FABRIC-REINFORCED CEMENTICIOUS MATRIX STRENGTHENING

FRCM systems share some of the advantageous properties of FRP, and overcome some of its limitations. In comparison, FRCM has superior heat resistance and compatibility with concrete substrate. Advantageous features of FRCM as noted by ACI 549 include (ACI Committee 549, 2013):

- a) Compatibility with chemical, physical, and mechanical properties of the concrete or masonry substrate
- b) Ease of installation due to the use of traditional plastering or trowel
- c) Porous matrix structure that allows air and moisture transport both into and out of the substrate
- d) Good performance at elevated temperatures in addition to partial fire resistance
- e) Ease of reversibility (that is, the ability to undo the repair without harming the original structure)

There are also a few limitations when using of FRCM composites for strengthening. Since the systems are based on inorganic matrixes, it is not possible to fully impregnate individual fibers. For this reason, the fiber sheets typically used in FRP that are installed by manual layup are replaced in FRCM with a structural reinforcing

mesh (fabric). The strands of the FRCM reinforcing mesh are typically made of fibers that are individually coated, but are not bonded together by a polymeric resin. If a polymer is used to either cover or bond the strands, such polymer does not fully penetrate and impregnate the fibers as it would in FRP. For these reasons, the term “dry fiber” is used to characterize an FRCM mesh (ACI Committee 549, 2013). Due to the lack of penetration, the bond cannot be assumed as perfect, which affects the theoretical behavior of FRCM (Arboleda, 2014).

Throughout its development, FRCM has been referred to by several different names or acronyms. The technology was first introduced in Europe as textile-reinforced concrete (TRC). The emphasis on textile was to signify that dry fibers are arranged in the direction of tension, rather than randomly distributed short fibers. A report by RILEM Technical Committee was one of the first to include information on strengthening with TRC (Brameshuber, 2006). Additionally, FRCM has been referred to as textile-reinforced mortar (TRM), fiber-reinforced concrete (FRC), and mineral based composites (MBC). (ACI Committee 549, 2013; Gonzalez-Libreros, Sabau, Sneed, Pellegrino, & Sas, 2017)

2.2.1. Tensile Characterization. Various researchers have studied the mechanical properties of FRCM materials. FRCM tensile properties are determined according to the test procedure specified in Annex A of AC434 (2013), in which tensile coupons are used to observe stress-strain behavior. Figure 2.4 adapted from Loreto et al. 2013 shows the behavior of a hydraulically gripped tensile coupon. The stress-strain behavior is broken down into three states: I, IIa, and IIb. State I is labeled as the uncracked zone because the strain is below the cracking strain of the matrix and the composite stiffness is governed by the reinforcement stiffness. Once the first crack

develops, load is transferred through the fabric back to the matrix and a multiple cracking pattern develops. This is shown in state IIa. At the end of this state is state IIb, where the load is carried completely by the fabric until its tensile strength is reached. In this state, the composite stiffness is governed by the reinforcement stiffness. The insert on the right of Figure 2.4 shows the reduction to an idealized tensile stress-strain curve for FRCM. The idealized curve is bilinear with a bend-over point corresponding to the intersection point obtained by continuing the initial and secondary linear segments of the response curve. The initial linear segment is uncracked linear elastic behavior and is characterized by the uncracked modulus of elasticity (E_f^*). The second linear segment is cracked behavior, and is characterized by the cracked modulus of elasticity (E_f). (ACI Committee 549, 2013; Arboleda, 2014; Loreto, Babaeidarabad, Leardini, & Nanni, 2015; Loreto, Leardini, Arboleda, & Nanni, 2013)

2.2.2. FRCM Failure Modes. Similarly to FRP, it has been observed that FRCM fibers lose strength due to various forms of debonding before the fibers reach their ultimate rupture strength. Figure 2.5 shows the four types of debonding failure modes that can occur, which are:

- a) Sudden detaching with fracture surface within concrete
- b) Gradual fiber slippage within the matrix
- c) Sudden detaching with fracture at matrix/ concrete interface
- d) Sudden detaching with fracture within matrix on a fiber plane.

In most cases, the debonding occurs within the matrix, which is different than FRP which tends to debond within the concrete cover (D'Ambrisi & Focacci, 2011; Di Tommaso, Focacci, & Mantegazza, 2008).

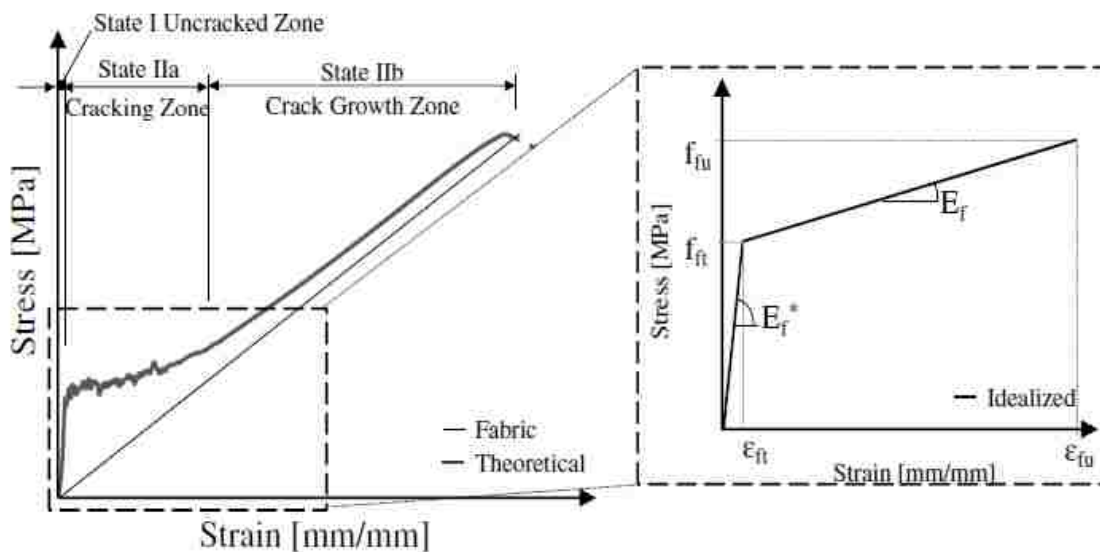


Figure 2.4. Stress-Strain Curve for Fully-Clamped FRCM in Tension (Loreto et al. 2013)

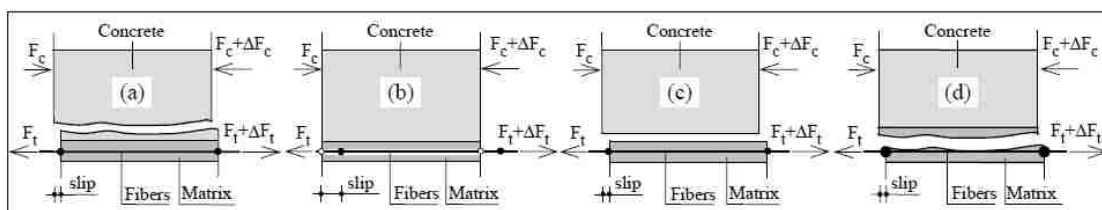


Figure 2.5. Debonding Failure Modes (Di Tommaso et al. 2008)

2.2.3. Research on FRCM Strengthening Systems. Several studies have been conducted on the effectiveness of FRCM systems for strengthening. Some of the most relevant studies to this thesis have been included.

2.2.3.1. Di Tommaso, Focacci, & Mantegazza (2008). This early study looked at the mechanics of adhesion and efficiency of strengthening RC beams with PBO-FRCM. Ten beams were tested under four point bending, with a clear span of 86.6 inches (2200 mm). The specimens had a rectangular cross section 9.84 inches (250 mm) deep

and 15.75 inches (400mm) wide. Specimens were strengthened with up to three layers of flexural strengthening and with either continuous U wrapping or a single wrap at each end.

Di Tommaso et al. found that FRCM materials are an effective way to strengthen RC beams, achieving up to 55% enhancement. They observed that failure was always caused by a loss of strengthening actions due to one of the types of fiber debonding, which typically includes slippage between fibers and matrix.

2.2.3.2. D'Ambrisi & Focacci (2011). In this study, externally bonded FRCM systems were used to strengthen reinforced concrete beams. Systems made using carbon fiber nets and PBO fiber nets were used, varying the net shape, cementitious matrices, and number of layers of reinforcement. Additionally some specimens were strengthened with carbon FRP in order to compare the performance of the FRCM systems. Specimens also had two different span lengths, and were tested in both three and four point bending. The long beams [86.6 in. (2200 mm) span] were expected to fail in shear, and tested in four-point bending configuration. The short beams [63 in. (1600 mm) span] were tested in three-point bending configuration. All beams tested had a depth of 9.84 in. (250 mm) and a width of 15.75 in. (400 mm). A total of 25 long beams and 10 short beams were tested throughout three experimental programs.

D'Ambrisi and Focacci found that for the considered cross sections, beams strengthened with PBO-FRCM materials had a flexural capacity increase (up to 54.3%) in the same order of magnitude as beams strengthened with FRP materials. The PBO FRCM systems performed better than carbon FRCM systems (up to 17.8% increase for carbon).

They also found that the failure of FRCM strengthened beams is typically caused by a loss of strengthening action as a result of one of four modes of debonding. For most cases, the debonding happens within the matrix or at the concrete-matrix interface rather than within the concrete as is common with FRP, proving that the matrix type, as well as its interface with the concrete and fibers are important factors in FRCM systems. As the number of FRCM plies increases, the debonding strain decreases, but as not as rapidly as observed in FRP. This is likely due to the difference in debonding mechanisms.

2.2.3.3. Loreto, Leardini, Arboleda, and Nanni (2013). This project studied the performance of FRCM systems used to strengthen RC slab-type elements. The specimens strengthened in this study simulated a unit slab strip 72 inches (1828.8 mm) long and had a rectangular cross section 12 inches (304.8 mm) wide and 6 inches (152.4 mm) deep. PBO FRCM was used to strengthen the slabs, with the number of plies as a test variable (0, 1, or 4 plies). Another test variable was the concrete compressive strength, as specimens with both high [5800 psi (39.99 MPa)] and low [4000psi (27.58 MPa)] strength concrete were tested. A total of 18 specimens (three of each condition) were tested in three point bending with a clear span of 60 inches (1524 mm). The loading pattern consisted of two cycles up to concrete cracking, two cycles up to steel yielding, two cycles within the plastic range of the slab, and finally loading to failure.

Loreto et al. found that FRCM with PBO is a viable technology for strengthening RC slabs. For low strength concrete, they found that the average flexural capacity increase was 141% and 205% for one and four plies respectively. For high strength concrete, the average flexural capacity increase was 135% and 212% for one and four plies respectively. The study also showed that while adding plies increases the strength,

there is a loss in ductility as a result. They also observed that the failure mode is related to the number of plies of strengthening. Specimens strengthened with one ply failed by fabric slippage within the matrix, whereas four ply specimens failed due to delamination from the substrate.

Loreto et al also performed an analysis based on the (at the time only proposed) ACI 549 (2013) design guide. They found that “the prediction [by ACI 549, 2013] is satisfactory and underestimates the enhancement attributable to FRCM strengthening because the tensile properties used in the analysis do not depend on fiber rupture but are based on the performance of the FRCM tensile coupon during the crack formation zone.” As ACI 549 2013 was used in this thesis for strengthening design, it is safe to assume the calculations for strength increase are conservative.

2.2.3.4. Babaeidarabad, Loreto, and Nanni (2014). This project studied RC beams strengthened in flexure with PBO-FRCM systems. For the study, 18 beams were tested in three point bending, with a clear span of 60 inches (1524 mm). The specimens were 72 inches (1828.8 mm) long with a rectangular cross-section 12 inches (304.8 mm) deep and 6 inches (152.4 mm) wide. Variables studied in this project are the influence of concrete strength [4200 psi or 6200 psi (28.96 MPa or 42.75 MPa)], and number of layers (0, 1, or 4) of FRCM reinforcement. Babaeidarabad et al. investigated the flexural capacity, pseudoductility, and failure mechanisms of the specimens.

Babaeidarabad et al observed that the strengthening produced average enhancements of 32% and 92% for the low strength concrete with one and four plies respectively. Similarly they observed average enhancements of 13% and 73% for the high strength concrete with one and four plies respectively when compared to the control

sets. ACI 549 limits the capacity increase to 50% of the unstrengthened capacity, so the reported design capacities in this study would be limited in field use. The researchers also observed that the failure mode is governed by the number of plies of FRCM reinforcement, with one ply specimens failing by slippage of the fabric within the matrix, and four ply specimens failing by FRCM delamination from the substrate. Babaeidarabad et al. created load-deflection diagrams, and observed that FRCM is effective in increasing the flexural capacity, but also decreases pseudoductility. As expected, pseudoductility is higher for the lower FRCM amount.

Babaeidarabad et al. also conducted sectional analysis following methodology according to ACI 318 (2011) and ACI 549 (2013). Their analysis showed that predicted flexural strength underestimates the experimental results, but with a reasonable accuracy and the design values become more conservative after applying the appropriate strength reduction factor and the 50% limit on strength increase.

2.2.3.5. Ombres (2015). Ombres studied the structural performance of RC beams strengthened in shear with PBO-FRCM. A total of 9 beams were tested in two series. All beams were 9.84 ft (3000 mm) long and had rectangular sections 9.84 inches (250 mm) deep and 5.91 inches (150 mm) wide. All tests were simply supported with a clear span of 8.86 ft (2700 mm). The first series aimed to evaluate the compatibility and effectiveness of PBO-FRCM and estimate the influence of strengthening configuration on structural performance. They did so by comparing one unstrengthened beam to two strengthened beams with different U-wrap configuration (continuous and discontinuous). For this series, both three point and four point bending schemes were used with a shear span-to-depth ratio (a/d) of 3.0 for each scheme.

The second series consisted of six beams, all of which were strengthened in flexure with three plies of PBO, in order to force failure by shear. Five of these specimens were also strengthened in shear with configurations attempting to observe the effects of reinforcement ratio (number of plies) and strengthening configuration (continuous vs discontinuous wraps). For this series, only the three point bending scheme was used with with a shear span-to-depth ratio (a/d) of 2.78.

After completion of the experimental program, Ombres drew the following conclusions:

- PBO-FRCM systems allow for significant improvement of shear capacity of RC beams if an adequate strengthening configuration is used.
- When using a discontinuous U-wrap scheme, a proper ratio of strip width to strip spacing must be chosen to permit correct activation of the strips, and better allow them to contribute to the shear capacity.
- There is a clear interaction between the externally bonded FRCM strips and the internal steel stirrups.

2.2.3.6. Loreto, Babaeidarabad, Leardini, and Nanni (2015). This project studied RC beams that were strengthened in shear with FRCM. This study used 18 beams that were heavily reinforced in flexure to ensure a shear failure. The beams were strengthened in shear with PBO-FRCM and tested under three point bending. Parameters considered were concrete compressive strength [low 4060psi and high 5800psi (27.99 MPa and 39.99 MPa)] and number of plies (0, 1, or 4) with three replications made for each combination. The specimens were 72 inches (1828.8 mm) long and had a

rectangular cross section 12 inches (304.8 mm) deep and 6 inches (152.4 mm) wide. The specimens were tested with a shear span-to-depth ratio of 3.0 for all beams.

Loreto et al. found that FRCM increases shear strength, but not proportionally to the number of plies. The average strength enhancement for low strength concrete compared to the control beam was 121% and 151% for one and four plies respectively. For the high strength concrete specimens the increases were 126% and 161% for one and four plies respectively. They also found that the failure mode differed based on the number of plies of strengthening. Specimens with one ply failed due to fiber slippage within the matrix, whereas the four ply specimens failed by delamination from the substrate.

This study also included analysis of the ultimate shear capacity based on the procedures in ACI 318 (2011) and ACI 549.4R (2013) in order to compare with the experimental results. Loreto et al. found that the analysis underestimates the enhancement due to FRCM strengthening. This demonstrates that ACI549 is conservative for both flexure and shear design.

2.3. STEEL REINFORCED GROUT

Steel reinforced grout (SRG) is another type of strengthening system being studied for applications in strengthening RC. Similarly to FRCM, the SRG systems use an inorganic, cementitious matrix, but high-strength steel cords are used as the fibers. These cords are made into a fabric that is much more cost efficient than carbon or PBO. The cords used in SRG systems are manufactured by the same process used for making reinforcement of automobile tires. (Huang et al. 2005)

The performance of SRG systems depend heavily on the stress transfer between the wires and the matrix. For this reason, various configurations of twisted wires are used, which provides a mechanical interlock performing much better than a single wire. These twisted cords are often made into a unidirectional fabric using a backing to keep the cords in line. The most common cords and fabrics used are manufactured by Hardwire LLC. Figure 2.6 shows a fabric and two types of cords used. (Barton et al., 2005; Huang et al., 2003)

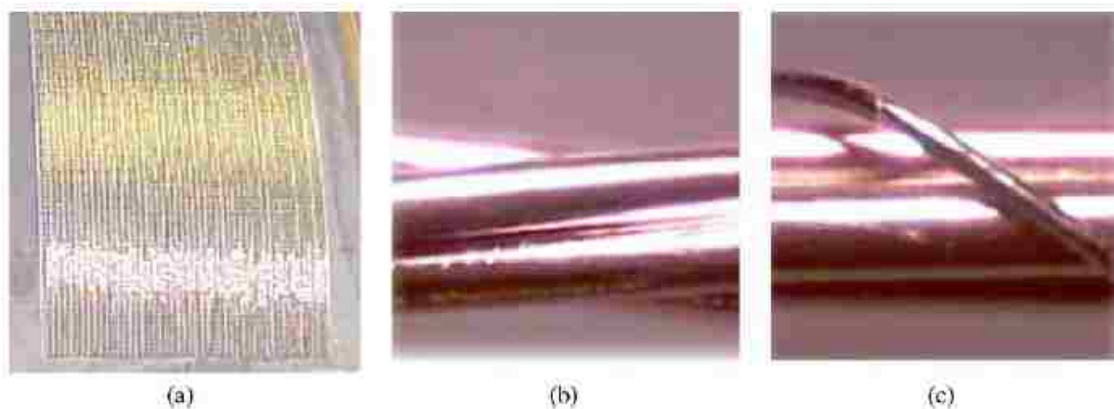


Figure 2.6. Steel Reinforcement: (a) steel fabric, (b) 3X2 cord and (c) 3SX cord. (Barton et al. 2005)

2.3.1. Research on SRG Strengthening. Research is ongoing in the field of strengthening RC with SRG systems. Some of the most relevant studies to this thesis have been included.

2.3.1.1. Huang et al. (2003). Huang et al. studied the properties and potential application of SRG and steel reinforced polymer (SRP). Their experimental work included testing of SRG and SRP strengthened beams, with an unstrengthened beam for comparison. The three beams had a tee shaped cross section, with a flange width of 15 inches (381 mm) and a web width of 6 inches (152.4 mm). The flange depth was 4 inches (101.6 mm) and the overall depth of the beams was 16 inches (406.4 mm). The 10 foot (3.05 m) long beams were tested in four point bending with a simply supported clear span of 8 feet (2.44 m). Huang et al. observed a 30% and 20% ultimate capacity increase for the SRP and SRG strengthened specimens respectively when compared to the control. Both beams failed at midspan by debonding of the system. They concluded that both systems have potential for structural applications.

2.3.1.2. Wobbe et al. (2004). This team studied the flexural capacity of RC beams externally strengthened with SRP and SRG. The unidirectional cords used were 3x2 and 3SX, both manufactured by Hardwire and shown above in Figure 2.6. The 3x2 cord type consists of 5 wires; three straight with two wrapped around. The 3SX chord consists of three identical wires twisted and then overwrapped with a single smaller wire. Sheets with 3SX cords have a lower density of cords, allowing better penetration of matrix which makes them better for use with SRG. Four 8 foot (2.44 m) long beams were cast with rectangular cross section 12 inches (304.8 mm) deep and 8 inches (203.2 mm) wide. One beam was left unstrengthened as a control. Two specimens were strengthened with SRP using 3x2 cords, using one ply on one beam and two plies on the other. The final specimen was strengthened with two plies of SRG using 3SX cords.

The beams were tested in four point bending with a simply supported span length of 80 inches (2.03 m). Each beam was monotonically loaded to failure with midspan deflection and strain at several points being monitored. Compared to the control beam, the specimen strengthened with one ply of SRP had an ultimate strength increase of 42% and the specimen with two plies of SRG had an increase of 33%. These two beams had a similar total number of strands, since the density of the two types of cord differ, which explains their similar behavior. The beam strengthened with two plies of SRP had an ultimate strength increase of 67% compared to the control. All three retrofitted beams failed due to concrete cover delamination. Wobbe et al. concluded that both SRP and SRG have great potential for flexural strengthening of RC structures.

2.4. NON DESTRUCTIVE TESTING

Nondestructive testing (NDT) techniques are a valuable way to get feedback on the quality of installation of externally bonded composite systems. NDT allows for gathering information without damaging the structural element or strengthening system. The following tests have been researched previously and were considered for use in this strengthening project.

2.4.1. Load Testing. Load testing is a valuable way to validate the effectiveness of a composite strengthening system in the field. An initial load test should be conducted before the installation of a system, in order to have base values for comparison. Ideally, after the strengthening system is installed, a series of load tests should be conducted in order to observe the increased stiffness from strengthening and monitor any changes in stiffness over time. (Holdener et al., 2004; Merkle, 2004; Missouri Department of Transportation, 2005; J J Myers, Holdener, Merkle, & Hernandez, 2008)

The most common method for load tests involves using loaded dump trucks, which move to predetermined stop locations along the bridge. These stops are locations that cause maximum shear or moment for the spans. At each stop, the bridge is given time to settle, with deflection readings taken periodically. (Holdener et al., 2004)

Deflection measurements can be taken by either contact, or non-contact monitoring. Contact methods such as LVDT's and String Transducers are the traditional methods. These devices can be tedious to set up, and depending on the terrain, may be unusable for some applications. The devices were designed for laboratory use, and their adaptations for field use produce complications and sources for error. Once set up and calibrated, they can take continuous data readings. The non-contact alternative is optical laser surveying equipment, consisting of prisms installed and a total station to take the readings. This method takes much less time to set up, but readings can only be taken about every one minute. Merkle and Myers showed that the Leica TCA 2003 Total Station is accurate to .005 inches (0.127 mm) at distances of 200 ft (60.96 m) to the target or less (Merkle and Myers, 2004). This accuracy is comparable to the accuracy of contact monitoring methods. (Holdener et al., 2004; Merkle, 2004)

2.4.2. Surface Roughness. Having the optimum surface roughness is critical for FRP and FRCM systems because the bond will be poor if the surface is too rough or too smooth. For use in the five bridge project, a new technology was developed at UMR to measure the surface roughness. The optimum surface roughness was identified with a profilometer utilizing image analysis techniques, which is the first existing roughness measuring device for use in the field. Holdner et al. described how the device works as follows: "The laser profilometer projects thin strips of laser light at an angle of 45

degrees onto concrete surfaces. A high resolution camera perpendicular to the concrete surface then records a video that is digitized and sent to a computer for analysis. The roughness can then be quantified based upon the average pixel to pixel angles; this is called an average inclination angle.” Figure 2.7 shows the device in use. (Holdener et al., 2004; Missouri Department of Transportation, 2005)



Figure 2.7. Laser Profilometer (Holdener et al. 2004)

2.4.3. Fiber Alignment. Proper fiber alignment is critical to the performance of an FRP or FRCM system because the fibers are strongest along their length. Both ACI 440.2R and ACI 549.4R design guides state that variations as little as 5 degrees can have a large impact on system performance. In order to monitor the variance, FRP is installed

with a tracer woven into the fiber that can be seen through the matrix. A chord can then be stretched across the installed system in the desired alignment, and imaging software is used to determine the angle differences. (Holdener et al., 2004; ACI Committee 440, 2008; ACI Committee 549, 2013)

2.4.4. FRP Delamination. Surface delaminations or voids between either the system and the concrete surface or between layers of reinforcement can drastically reduce the strength of an FRP or FRCM system. Causes of such delaminations include moisture (in FRP), fluctuating temperatures, and improper installment. According to ACI 440.2R and ACI 549.4R, delaminations over 25 square inches (16129 square mm) should be repaired by cutting away and patching. The system should then be reevaluated to ensure repairs were properly installed. NDT methods used to detect delaminations include acoustic sounding (hammer sounding), impact-echo, impulse response, ultrasonics, infrared thermography, and near-field microwave techniques. (Holdener et al., 2004; ACI Committee 440, 2008; ACI Committee 549, 2013)

3. DESIGN OF STRENGTHENING SYSTEMS

This section contains the analysis and design procedures used in the strengthening of Missouri Bridge P-0058 located in south central Missouri near Lanton, Missouri. A description of the bridge and materials are included. For this project, spans 1 and 4 were strengthened and spans 2 and 3 were left unstrengthened. The middle spans had very poor access, making it difficult to strengthen them. In addition, having unstrengthened spans for comparison can provide valuable information for the study's future intended work.

3.1. BRIDGE DESCRIPTION

Missouri Bridge P-0058 was selected from a list of candidate bridges in Missouri. The candidates were all considered structurally deficient according to MoDOT. Missouri bridges receive condition ratings periodically for their deck, superstructure (sup), and substructure (sub). In the most recent inspection report, bridge P-0058 received deck/sup/sub ratings of 4/4/6, with 4 meaning poor, and 6 meaning satisfactory. Due to the age and condition, bridge P-0058 is currently load posted as shown in Figure 3.1.

Bridge P-0058 is located on Highway 142 and spans the Myatt Creek in Howell County, Missouri. This bridge was originally constructed in 1951 and consists of four simply supported reinforced concrete spans. For this study, the spans were numbered 1 through 4 from west to east. The two spans farthest west (1 & 2) are 37.5 feet (11.43 m) long and the two to the east (3 & 4) are 27.5 feet (8.38 m), for a total bridge length of 130 feet (39.62 m). The deck is six inches thick and is supported by three tee beams spaced 7.0833 ft. (2.16 m) on center. For this project, the three beams are referred to as beam 1 through 3, with 1 being the northern most, and 3 farthest south. The total deck width is

17.1667 ft. (5.232 m) with a curb to curb roadway of 14 ft (4.267 m). Due to the narrow roadway, the bridge is limited to one lane of traffic with yield to oncoming traffic signs in each direction. Figure 3.2 shows the bridge's approach, and a profile view.

The longer spans have slightly different geometry from the shorter spans. Cross sections with dimensions for each span length can be found in Section 3.4.



Figure 3.1. Bridge P-0058 Load Posting



Figure 3.2. Bridge P-00585 Approach and Profile View

3.2. MATERIALS USED

The four different strengthening systems used are described in this section. Properties for each material are given by the manufacturer, or obtained through tests performed in a lab setting.

3.2.1. Fiber-Reinforced Polymer. Carbon FRP manufactured by Structural Technologies was chosen for use in this strengthening project. The product used is V-Wrap™ C200HM High Modulus Carbon Fiber Fabric (Structural Technologies, 2016b). The resin used is V-Wrap™770 Epoxy Adhesive which is also manufactured by Structural Technologies. It is a two-part epoxy that is designed to be used in wet-layup composite strengthening (Structural Technologies, 2016a). As stated in ACI 440.2R-08 account for long term exposure to the environment and must be reduced based on the exposure of the application. Bridges are in the exterior exposure category, so the ultimate strain and ultimate strength of the carbon shown in Table 3.1 were reduced to 85% of the given values for design properties.

Table 3.1. CFRP Properties from Manufacturer

System	Eq. Thickness [in ² /in]	Ultimate Strain [%]	Garunteed Ultimate Strength [ksi]	Modulus of Elasticity [ksi]
Carbon FRP	0.00650	1.67	550.00	33000.00

Conversion: 1 in²/in = 25.4 mm²/mm; 1 ksi = 6.895 MPa

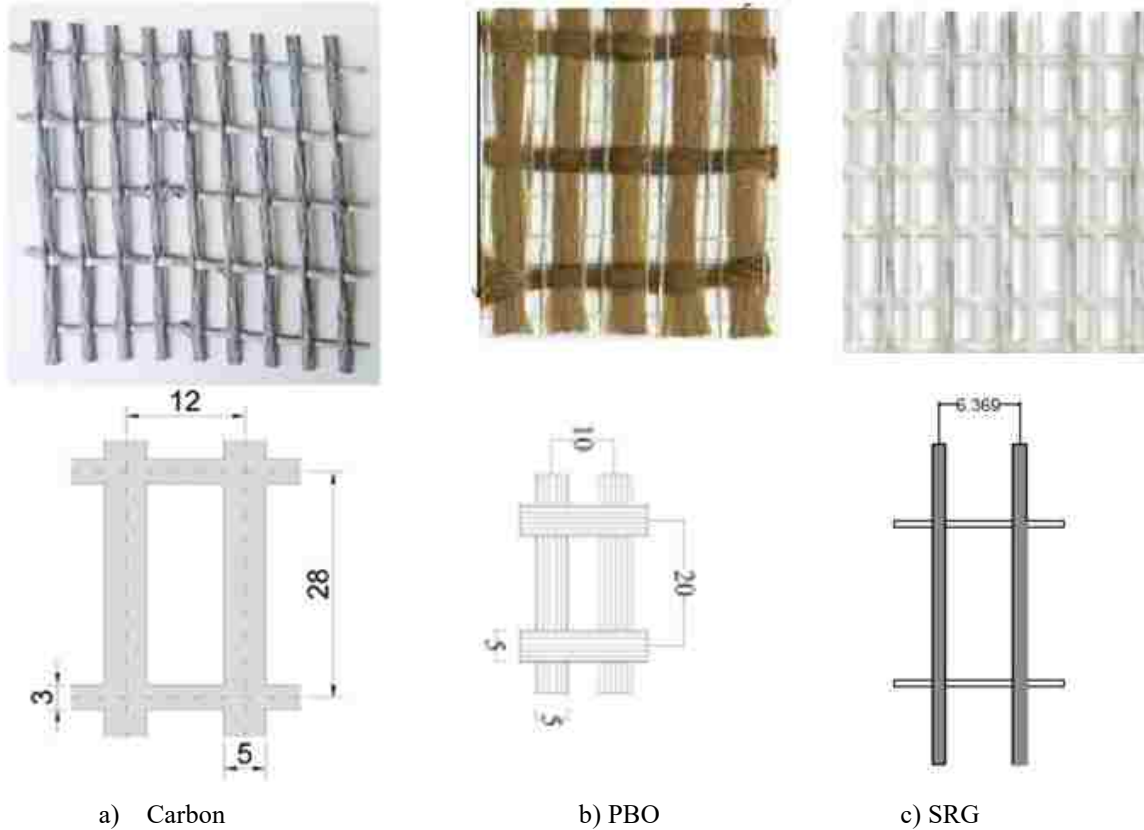
3.2.2. Fabric-Reinforced Cementitious Matrix. Three different systems with cementitious matrix were used in this study. The fiber types used were carbon (C-FRCM), PBO, and steel cords. As described in Section 2.2.2, when designing with FRCM, the properties should come from an idealized bilinear stress strain curve, but the contribution of FRCM before cracking is neglected. The idealized curve should come from statistic data from a series of coupon tests. The properties used in this study were provided by a research team at the University of Miami, and are displayed in Table 3.2. (Babaeidarabad et al. 2014)

The carbon FRCM system used is CSS-UCG Unidirectional Carbon Grid which is manufactured by Simpson Strong-Tie. It is designed to be field installed with CSS-CM cementitious matrix also manufactured by Simpson Strong-Tie. (Simpson Strong-Tie, 2017, 2018) The PBO FRCM system used consists of fibers and inorganic matrix both manufactured by Ruredil (Ruredil, 2012). The SRG system chosen uses GeoSteel G600® mesh with either GeoCalce® Fino or GeoLite® cementitious matrix, all of which are manufactured by Kerakoll S.p.A. (Kerakoll S.p.A., 2014) Figure 3.3 shows each fabric, and their layout of fibers.

Table 3.2. FRCM Statistical Properties

System		Eq. Thickness [in ² /in]	Ultimate Strain [%]	Ultimate Strength [ksi]	Cracked Modulus of Elasticity [ksi]
Carbon FRCM	mean	0.00618	1.64	202.20	9209.94
	St. dv		0.43	2.03	1902.88
PBO FRCM	mean	0.00180	1.76	241.34	18564.83
	St. dv		0.13	11.17	2175.57
SRG	mean	0.00333	1.40	196.40	13478.36
	St. dv		0.30	14.70	2487.40

Conversion: 1 in²/in = 25.4 mm²/mm; 1 ksi = 6.895 MPa



(Dimensions in mm. 1in.=25.4mm.)

Figure 3.3. Fibers Used in FRCM (Nanni, 2018)

3.3. ANALYSIS OF EXISTING CAPACITY

Analysis was performed according to ACI 318-14 (ACI Committee 318, 2014).

ACI analysis was chosen over AASHTO because it is referenced by the composite strengthening design guides. The analysis was based on the following assumptions:

- Plane sections remain plane after loading
- Maximum strain at the extreme concrete compression fiber shall be assumed equal to 0.003

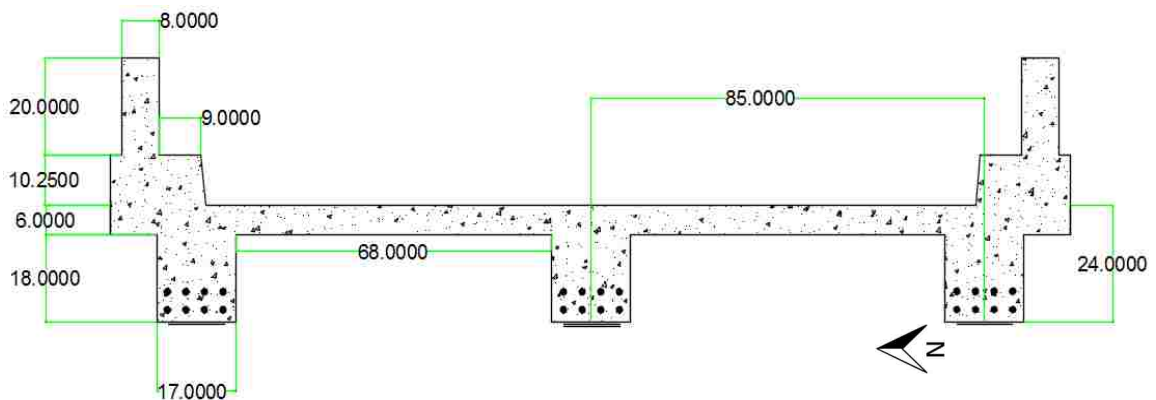
- Tensile strength of concrete shall be neglected in flexural and axial strength calculations

Original design drawings were referenced for dimensions and design material properties and are found in Appendix A. The flexural steel reinforcement in the bridge has a yield strength of 33 ksi (227.5 MPa) according to MoDOT drawings. This value was used in the analysis of the existing capacity as well as the design of strengthening systems. The concrete compressive strength was reported by MoDOT as 3 ksi (20.7 MPa), however, field tests showed that it is much higher. Schmidt hammer tests on each beam of spans 1 and 4 gave equivalent compressive strength readings ranging from 5800 psi (40.0 MPa) to 8500 psi (58.6 MPa), with an average of 7289 psi (50.26 MPa). 6000 psi (41.4 MPa) was used in analysis and design of strengthening, which exceeds two standard deviations below the average test value.

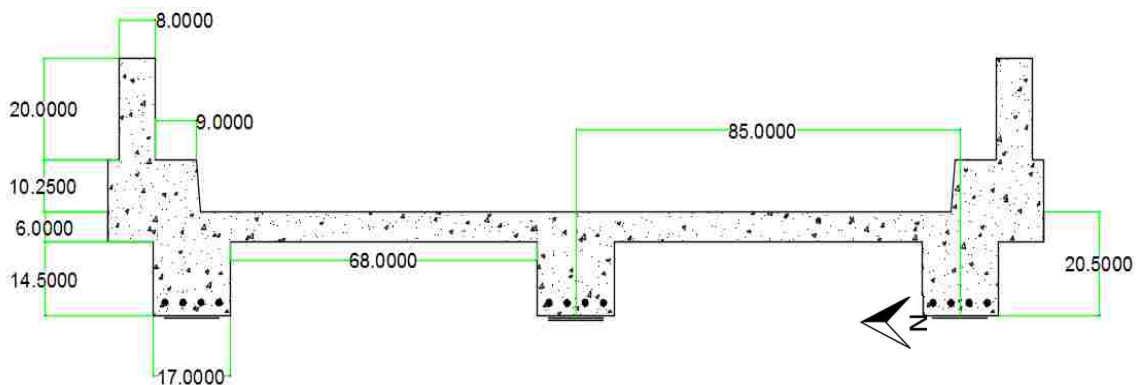
3.3.1. Flexure. Since the bridge has simply supported spans, each girder type was analyzed individually as simply supported with positive moment only. Girder geometrical properties, shown in Figure 3.4 and Table 3.3, were found in MoDOT's design drawings and then verified by measurements in the field. The effective flange width was calculated as per ACI 318 with the equations shown in Figure 3.5.

The tee beams were analyzed using the Whitney stress-block model, first assuming that the compression block fell within the flange. This assumption was verified for each case. It was also assumed, and later verified, that the steel yields at nominal capacity. Table 3.4 shows the amount of internal flexural steel reinforcement for each girder type, as shown in MoDOT design drawings.

Table 3.5 shows the moment capacity for each girder type before strengthening. Full calculations can be found in Appendix A. The flexural strength reduction factor (Φ) for the nominal capacity is .9 for each beam, as per ACI 318 for beams that are tension controlled.



a) Spans 1 and 2 (units shown in inches) Conversion: 1 in. = 25.4 mm



b) Spans 3 and 4 (units shown in inches) Conversion: 1 in. = 25.4 mm

Figure 3.4. Cross Sections of Spans

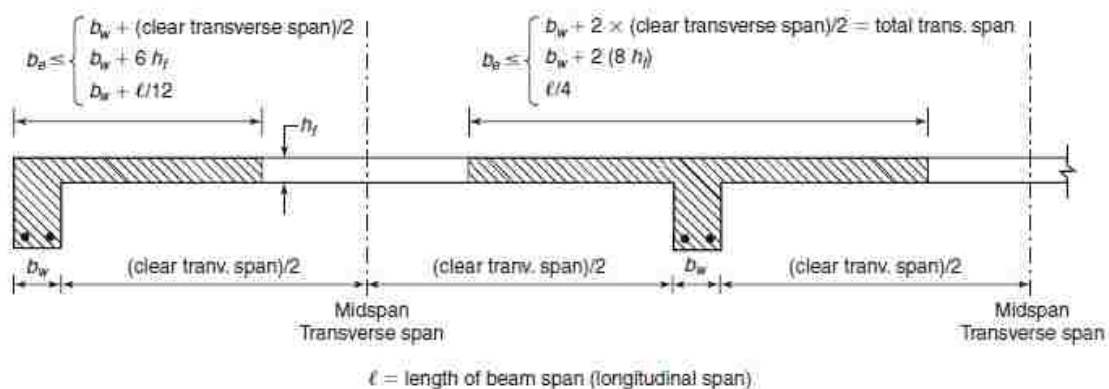


Figure 3.5. Effective Flange Width (Wight & Macgregor, 2012)

Table 3.3. Geometrical Properties

Span	Girder Type	Overall Height h, (in)	Width of the Web b, (in)	Width of the Flange b _e , (in)	Slab Thickness h _f , (in)
1 & 2	Interior	24	17	85	6
	Exterior	24	17	61	6
3 & 4	Interior	20.5	17	79	6
	Exterior	20.5	17	58	6

Conversion: 1 in. = 25.4 mm

Table 3.4. Flexural Internal Steel Reinforcement at Midspan

Span	Girder Type	Tensile Steel Area A _s , (in ²)	Effective Depth d, (in)
1 & 2	All	11.32	19.82
3 & 4	All	6.24	18

Conversion: 1 in. = 25.4 mm

Table 3.5. Existing Nominal Moment Capacity

Span	Girder Type	Nominal Moment Capacity Mn (kip-ft)
1 & 2	Interior	603.49
	Exterior	598.22
3 & 4	Interior	304.50
	Exterior	302.91

Conversion: 1 kip-ft = 1355.8 N-m

3.3.2. Shear. Each girder type was analyzed for shear capacity as per ACI 318.

Table 3.6 shows the internal steel shear reinforcement as originally constructed. This information was gathered from MoDOT design drawings.

Table 3.6. Shear Internal Steel Reinforcement

Span	Girder Type	Shear Steel Area A_v , (in ²)	Stirrup Spacing s , (in)
1 & 2	All	0.4	15
3 & 4	All	0.4	12

Conversion: 1 in. = 25.4 mm

The total shear capacity of a beam type member is taken as the combination of the contributions from the concrete and the reinforcing steel. Both of the shear contributions were calculated in accordance with ACI 318, and are shown in Table 3.7. The shear

strength reduction factor (Φ) for the nominal capacity is .75 as per ACI 318. Full calculations can be found in Appendix B.

Table 3.7. Existing Nominal Shear Capacity

Span	Girder Type	Shear Contribution from Steel V_s (kip)	Shear Contribution from Concrete V_c (kip)	Nominal Shear Capacity V_n (kip)
1 & 2	All	17.44	52.19	69.63
3 & 4	All	19.80	47.41	67.21

Conversion: 1 kip = 4.448 kN

3.4. GIRDER STRENGTHENING DESIGN

With six girders to be strengthened using four different systems, decisions were made in an attempt to get the best information possible in the long term. Research field applications and data is presently not available on FRCM and SRG, so cementitious systems were chosen to be the main focus. Each girder type is controlled by flexure, so the focus of the strengthening is for flexure.

A parametric study was completed, varying the different span lengths (which have different section depths and areas of steel reinforcement), the different strengthening systems (Carbon FRCM, PBO FRCM, CFRP and SRG), the width of the plies, and different numbers of plies of strengthening up to four plies. This study showed which systems performed better than others on the long spans. It also made clear the expected result of multiple layers of each system. After consideration, it was decided to use two

plies of each system, which will give valuable information with lower labor and material costs.

Table 3.8 shows a section of the data for the moment capacity parametric using 17 in. (43.2 cm) wide plies. This table also includes the percent difference of the percent increase in capacity for the same amount of strengthening applied to the long vs. short spans. A lower percentage here shows that the system is less effected by which span length they are installed on. While carbon FRP and Carbon FRCM were most impacted by the span length, their higher efficiency overall made them the best choice for strengthening the long spans. The full parametric study results with example calculations is given in Appendix C.

Table 3.8. Moment Capacity Parametric Data

Moment Capacity Parametric (17 inch width)	Long Span % increase	Short Span % increase	Long vs Short span % difference	Average % difference
FRCM-PBO	1 Ply	1.84%	2.98%	61.9%
	2 Ply	4.45%	7.10%	59.4%
	3 Ply	7.07%	11.22%	58.7%
	4 Ply	9.67%	15.33%	58.4%
FRCM-Carbon	1 Ply	2.58%	5.15%	99.5%
	2 Ply	6.29%	11.43%	81.6%
	3 Ply	10.00%	17.70%	77.0%
	4 Ply	13.71%	23.96%	74.8%
SRG	1 Ply	0.99%	1.06%	6.5%
	2 Ply	3.24%	3.88%	19.5%
	3 Ply	5.50%	6.69%	21.8%
	4 Ply	7.75%	9.51%	22.7%
CFRP	1 Ply	11.46%	18.92%	65.1%
	2 Ply	17.72%	31.31%	76.7%
	3 Ply	21.62%	38.24%	76.9%
	4 Ply	24.91%	44.07%	76.9%

The focus of this study is flexural strengthening, but some shear strengthening was also provided. The effects of MoDOT posting vehicles H20 Legal and 3S2 were considered. Strengthening in shear to accommodate these trucks maintains that the girders are expected to fail in flexure after strengthening. The long spans are controlled by the Missouri 3S2 truck. The maximum shear exceeds the pre strengthening capacity by about 5 kips (22.2 kN) for the 2 feet (.61 m) closest to supports in the shear envelope. For the short spans, the H20 Legal truck controls. The short spans have adequate shear strength without strengthening. U-wraps, which are generally used for shear strengthening, also help anchor the flexural reinforcement and reduce the failure by debonding and also aid field installation by reducing ability of the flexural strengthening to sag, so they will be used on each span. The exact wrapping configuration was decided after consulting with the design teams of each manufacturer. The chosen wrapping scheme for each beam can be found in Appendix D.

3.4.1. Fiber Reinforced Polymer. Design and analysis was performed according to ACI 318 (ACI, 2014) and ACI 440 (ACI Committee 440, 2008), based on the following assumptions:

- Design calculations are based on the dimensions, internal reinforcing steel, and material properties of existing member being strengthened
- Plane sections remain plane after loading, so strains are proportional to distance from the neutral axis
- The bond between FRP and concrete substrate as well as that of the fabric to the matrix is perfect
- Shear deformation within the adhesive is very small and is neglected

- The maximum usable compressive strain in the concrete (ϵ_{cu}) is 0.003 in/in
- Tensile strength of concrete is neglected
- The FRP has a linear elastic stress-strain relationship to failure

3.4.1.1. Flexure design. ACI 440 imposes strengthening limits in order to guard against structure collapse should bond or other failure of the system occur due to damage, vandalism, or other causes. To make the structure able to still resist a reasonable level of load should a failure occur, Equation 3.1 must be satisfied. R_n is the nominal strength of a member and S_{DL} and S_{LL} are the dead load and live load effects.

$$(\Phi R_n)_{existing} \geq (1.1S_{DL} + 0.75S_{LL})_{new} \quad (3.1)$$

In order to reduce the failure by debonding, ACI 440 limits the effective strain in the FRP to a level in which debonding may occur (ϵ_{fd}), which is defined by Equation 3.2. The limit is based on the compressive strength of the concrete (f'_c), the number of layers of fabric (n_f), the modulus of elasticity of the FRP (E_f), and the effective thickness of the fabric (t_f). This equation also limits the debonding strain to 90 percent of the ultimate strain (ϵ_{fu}). This equation was developed based on statistical analysis of a database of flexural test beams that failed by debonding (ACI Committee 440, 2008).

$$\epsilon_{fd} = 0.083 \sqrt{\frac{f'_c}{n_f E_f t_f}} \leq .9 \epsilon_{fu} \quad (3.2)$$

The ultimate strength of a section is found based on the internal strain and stress distribution under flexure at the ultimate limit state. The procedure for obtaining the

ultimate strength must satisfy strain compatibility and force equilibrium, as well as consider the governing mode of failure. The procedure chosen uses a trial-and-error method to find a solution. Figure 3.6 illustrates steps in the procedure described in the following.

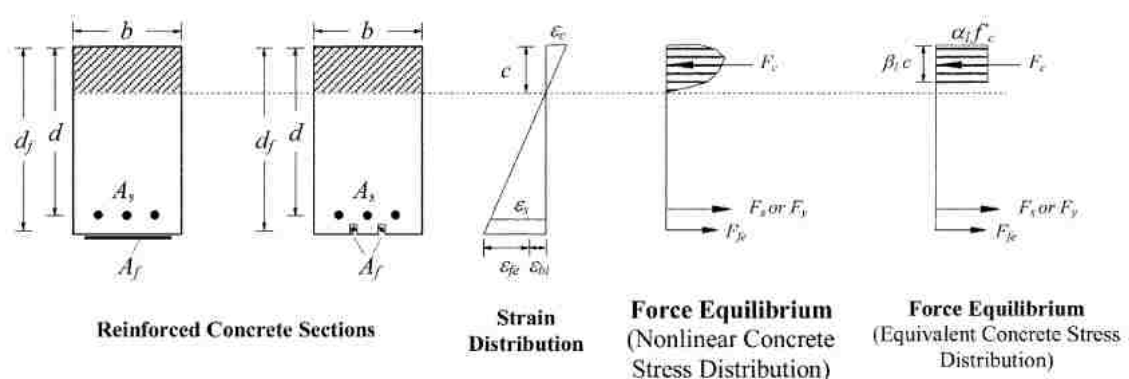


Figure 3.6. Internal Stress and Strain Distribution in Flexure (ACI Committee 440, 2008)

The procedure for obtaining the ultimate strength begins by assuming a value of c , or the depth to the neutral axis. With this assumption, the strain level in the FRP (ϵ_{fe}) can be calculated using Equation 3.3. This equation considers the failure mode for the assumed neutral axis. If the left side of the inequality governs, then concrete crushing controls the flexural failure, and if the right side governs, then FRP failure by either debonding or rupture controls the section failure. In the equation, d_f is the depth of the fibers from the extreme compression face, which is taken as the height of the beam being strengthened. The strain level in the concrete surface at the time of FRP strengthening

(ε_{bi}) is considered in the equation, and it is calculated based on the properties and dimensions of the RC section and the moment caused by the dead load.

$$\varepsilon_{fe} = \varepsilon_{cu} * \left(\frac{(d_f - c)}{c} \right) - \varepsilon_{bi} \leq \varepsilon_{fd} \quad (3.3)$$

With the effective strain in the FRP known, the effective stress level (f_{fe}) can be calculated using Hooke's law, assuming perfectly elastic behavior. Based on the strain level in the FRP, the strain in the steel (ε_s) can also be found using the linear strain distribution. Then, the stress in the steel (f_s) is determined using its stress-strain curve. This method uses a rectangular equivalent compressive stress block as shown in Figure 3.6, where the distribution factors α_1 and β_1 are defined by Equations 3.7 and 3.6. With the strain and stress levels in the FRP and steel known for the assumed neutral axis depth, the internal equilibrium can be checked using Equations 3.4 through 3.8

$$E_c = 57000\sqrt{f'_c} \quad (3.4)$$

$$\varepsilon'_c = \frac{1.7f'_c}{E_c} \quad (3.5)$$

$$\beta_1 = \frac{4\varepsilon'_c - \varepsilon_c}{6\varepsilon'_c - 2\varepsilon_c} \quad (3.6)$$

$$\alpha_1 = \frac{3\varepsilon'_c \varepsilon_c - (\varepsilon_c)^2}{3\beta_1 (\varepsilon'_c)^2} \quad (3.7)$$

$$c' = \frac{(A_s f_s + A_f f_{fe})}{\alpha_1 f'_c \beta_1 b} \quad (3.8)$$

where E_c is the modulus of elasticity of the concrete, ε_c is the compressive strain level in concrete, ε'_c is the compressive strain corresponding to f'_c , A_s is the area of flexural steel reinforcement, and A_f is the area of flexural FRP fibers.

If the assumption of the neutral axis depth was correct, then the value for c assumed will be in agreement with c' calculated from Equation 3.8, which shows that the tension and compression in the section are equal. If the assumption was incorrect, then iterations are done by changing the value of c and repeating the process of calculating strains and stresses. The correct value for the neutral axis depth is found when convergence occurs and the neutral axis depth is returned as c' .

The nominal flexural strength of the section is computed using the force equivalent forces and the moment arm between them. Equation 3.9 shows the moment capacity provided by both the original RC section, and the added external FRP strengthening. For FRP contribution, an additional reduction factor, Ψ_f , is applied. For flexure, the value used is .85, which is based on reliability analysis and the inherent uncertainties of FRP compared to more widely used materials (ACI Committee 440, 2008).

$$M_n = A_s f_s \left(d - \frac{a}{2} \right) + \Psi_f A_f f_{fe} \left(d_f - \frac{a}{2} \right) \quad (3.9)$$

ACI 440.2R also includes limits on the service load stress in the steel and FRP. The guide has equations based on cracked-section analysis of the FRP-strengthened reinforced concrete section that were used to check the service stresses against their

limits. The stress limit for steel is 80% of the yield strength, and for carbon, the limit is 55% of the ultimate fiber strength.

3.4.1.2. Shear design. Three different wrapping schemes are discussed in ACI 440 for shear strengthening of RC members: complete wrapping, 3-sided “U-wrap”, and 2-sided. Complete wrapping is the most efficient technique, but it is rarely possible for girders, because the integral slab prevents access to the top side. U-wraps are the next efficient method, and were chosen for this project. Shear strengthening systems can also be installed continuously along the span, or placed as discrete strips, however, complete encasement is discouraged, as it prevents migration of moisture (ACI Committee 440, 2008). Figure 3.7 illustrates a cross sectional view of a girder strengthened with U-wraps (a), as well as side views of beams strengthened with discrete strips both vertical (b) and inclined (c). The figure also shows the dimensional variables used in strengthening calculations.

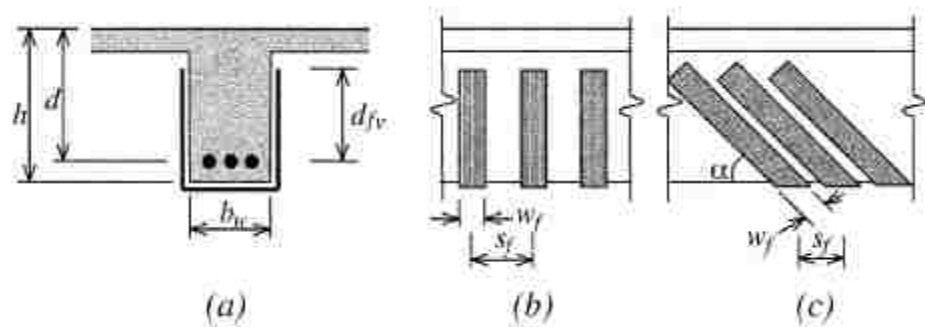


Figure 3.7. Shear Strengthening with FRP Nomenclature (ACI Committee 440, 2008)

The nominal shear capacity of an FRP strengthened reinforced concrete member is calculated with Equation 3.10. For shear reinforcement, Ψ_f has a value of .85 for U-wrapped members. As typical for shear design, Φ is taken as .75.

$$\Phi V_n = \Phi(V_c + V_s + \Psi_f V_f) \quad (3.10)$$

In Equation 3.10, the shear contributions from the concrete (V_c) and steel (V_s) are calculated as per ACI 318. The contribution from FRP is calculated based on fiber quantity and orientation, as well as an assumed crack pattern. Equation 3.11 gives the shear contribution of the FRP reinforcement based on the tensile stress in the FRP across the assumed crack.

$$V_f = \frac{(A_{fv} f_{fe} (\sin\alpha + \cos\alpha) d_{fv})}{s_f} \quad (3.11)$$

A_{fv} and f_{fe} are defined by Equations 3.12 and 3.13. Figure 3.7 shows the definition of the terms α (orientation of the strips), s_f (center to center spacing of strips), and d_{fv} (depth of flexural reinforcement from top of shear reinforcing fibers). The figure also shows the variables used in calculating the area of shear reinforcing fibers: n (number of plies), t_f (effective thickness of one ply), and w_f (width of a strip).

$$A_{fv} = 2nt_f w_f \quad (3.12)$$

$$f_{fe} = \varepsilon_{fe} E_f \quad (3.13)$$

ACI 440 has different limitations on the effective strain in the FRP for shear than for flexure. There are also different limitations for completely wrapped beams than 2 or 3-sided since delamination is more likely to occur for the latter. For U-wrapped beams, Equation 3.14, which uses a bond reduction coefficient (κ_v), is used. This equation also limits the strain to 0.4%, which helps avoid the loss of aggregate interlock of the concrete.

$$\varepsilon_{fe} = \kappa_v \varepsilon_{fu} \leq 0.004 \quad (3.14)$$

Shear design with FRP also has limits to how much strength enhancement can be added. In in-lb units, the limit for the contribution of steel and FRP combined is given by Equation 3.15.

$$V_s + V_f \leq 8\sqrt{f'c}b_wd \quad (3.15)$$

3.4.2. Fiber Reinforced Cementitious Matrix. Design and analysis was performed according to ACI 318-14 and ACI 549 (2013) based on the following assumptions:

- Plane sections remain plane after loading
- The bond between FRCM and concrete substrate as well as that of the fabric to the matrix is perfect
- The maximum usable compressive strain in the concrete is 0.003 in/in

- FRCM has a bilinear-elastic behavior up to failure, however, the contribution of FRCM before cracking is neglected

3.4.2.1. Flexure design. The procedure for FRCM design laid out in ACI 549 is similar to the FRP design in ACI 440. The initial step is to get material properties from coupon tests. Rather than using Equation 3.2 to limit strain to prevent debonding, ACI 549 uses statistics from coupon tests and defines the ultimate strain, ϵ_{fd} , as the average ϵ_{fu} minus one standard deviation. This ultimate tensile strain is then multiplied by the cracked modulus of elasticity (E_f) to get the ultimate tensile strength of the FRCM. In order to prevent slippage of fibers within the matrix, the design tensile strain (ϵ_{fe}) is further limited to the smaller of ϵ_{fd} and 0.012.

The ultimate moment capacity is calculated based on the internal strain and stress distribution under flexure at the ultimate limit state. A trial-and-error method is used for obtaining the ultimate strength, which satisfies strain compatibility and force equilibrium and considers the governing mode of failure. Figure 3.6 illustrates steps in the procedure. Once iterations of Equations 3.4 through 3.8 are done to find the neutral axis depth, and internal stresses are found, the ultimate moment capacity is found using Equation 3.16.

$$M_n = A_s f_s \left(d - \frac{a}{2} \right) + A_f f_{fe} \left(d_f - \frac{a}{2} \right) \quad (3.16)$$

ACI 549.4R also has limitations on the amount of enhancement provided. The increase in flexural capacity strength provided by FRCM reinforcement should not exceed 50 percent of the existing flexural capacity. Additionally, the stresses in steel under service loads should be limited to 80 percent of the yield strength. In order to

prevent concerns over creep rupture and fatigue, the service level tensile stress in the FRCM is limited to a percentage of the design tensile strength based on the fiber type as shown in Table 3.9.

Table 3.9. Creep and Fatigue Stress Limits (ACI Committee 549, 2013)

	Fiber type				
	AR glass	Aramid	Basalt	Carbon	PBO
Creep rupture and fatigue	$0.20f_{fa}$	$0.30f_{fa}$	$0.20f_{fa}$	$0.55f_{fa}$	$0.30f_{fa}$

3.4.2.2. Shear design. For shear strengthening with FRCM, the procedure based on ACI 549 is very similar to what was used for FRP. The statistical properties from coupon tests that were used in flexure design are again used in shear design. ACI 549 limits the design tensile strain in the FRCM for shear to the smaller of 0.004 and the ultimate strain from tests. Equations 3.12 through 3.14 are used to determine the shear contribution from the FRCM strengthening. The total shear strength of the RC section with added FRCM is then calculated using equation 3.17. As typical for shear design, a strength reduction factor, Φ , of .75 is applied to the nominal shear strength, V_n .

$$V_n = V_c + V_s + V_f \quad (3.17)$$

The total shear strength provided by the FRCM and steel is limited by equation 3.18. Additionally, the increase in shear strength after adding FRCM should not exceed 50 percent of the existing capacity.

$$V_s + V_f \leq 8\sqrt{f'c}b_wd \quad (3.18)$$

3.4.3. Summary of Design. Table 3.10 gives a summary of both flexural and shear strengthening added to bridge P-0058. All strips used for strengthening are 12 inches wide. Details of the shear strengthening wrapping scheme are located in Appendix D. Appendix E contains a detailed bill of materials as built.

Table 3.10. Summary of Strengthening System Design

	Span 1	Span 2
	Carbon FRCM/ CFRP	
	36.1875ft	36.1875ft
Girder 1	CFRP: Flexure: 2 ply Shear: one ply 17in spacing, 18 strips total	No Strengthening
Girder 2	Carbon FRCM: Flexure: 2 ply Shear: one ply 12in spacing, 20 strips total	No Strengthening
Girder 3	Carbon FRCM: Flexure: 2 ply Shear: one ply 12in spacing, 20 strips total	No Strengthening
	Span 3	Span 4
		PBO FRCM/ SRG
	26.375ft	26.375ft
Girder 1	No Strengthening	SRG: Flexure: 2 ply Shear: two ply 18in spacing, 13 strips total
Girder 2	No Strengthening	SRG: Flexure: 2 ply Shear: two ply 18in spacing, 13 strips total
Girder 3	No Strengthening	PBO FRCM: Flexure: 2 ply Shear: two ply 18in spacing, 13 strips total

4. INSTALLATION OF STRENGTHENING SYSTEMS

The installation of strengthening systems requires an emphasis on attention to detail. The procedures used should agree with ACI 440, ACI 549, and the suggestions of the material manufacturers. This section describes the planned procedure for installing strengthening on Bridge P-0058. The installation of the strengthening systems follows the completion of this thesis.

4.1. PRE INSTALLATION

Composite strengthening systems require some preparatory work before manual layup. The preinstallation helps with the performance of the system in the future.

4.1.1. Substrate Repair. The quality and strength of the substrate is important for performance of externally bonded strengthening systems. Areas that were damaged by concrete spalling were addressed to avoid compromising the integrity of the strengthening system. Figure 4.1 shows spalling on a girder. As shown in the figure, much of the damaged areas were below drop drains and were exposed to water regularly and salt concentrations in the winter. Cement mortars that are compatible with both the concrete substrate and the systems used for strengthening were used for the patching. For the carbon FRCM system, the cementitious matrix (CSS-CM) can be used to patch voids and defects that are no deeper than 2 in. (51 mm) (Simpson Strong-Tie, 2017).

4.1.2. Surface Preparation. The surface of the substrate must be prepared accordingly to allow optimal bonding conditions for load transfer to the strengthening systems. Strengthening for both flexure and shear are bond critical, and thus require an adhesive bond between the system and the substrate. Sand blasting, shown in Figure 4.2,

was used to remove all laitance, dust, dirt, oils, and other matter that could interfere with the bond of the system. This surface preparation also provides a rough surface that is



Figure 4.1. Spalling on Girder

critical for the resin or cementitious matrix to bond to. ACI 440 requires “a minimum concrete surface profile (CSP) 3 as defined by the ICRI (International Concrete Repair Institute) surface- profile chips.” For the Simpson FRCM system, it is recommended to achieve a minimum $\frac{1}{4}$ in. (6 mm) amplitude which is a CSP-6-9 (Simpson Strong-Tie, 2017). Surface irregularities such as fins and form lines were also removed or taken down to $\frac{1}{32}$ inch as per ACI 440.

Surface preparation also includes rounding of corners that the fabric will wrap around in order to prevent stress concentrations in the fibers. ACI 440 requires a

minimum radius of .5 inches (12.7 mm) for FRP, whereas ACI 549 states a radius not less than 0.75 inch (19.1 mm) before FRCM shear strengthening. The guidelines of each manufacturer were in agreement with these corner radius limits. A radius of 0.75 inch (19.1 mm) was used for each girder that was rounded and was achieved by grinding with a special bit as shown in Figure 4.3. The exception were girders strengthened with SRG, which were left unrounded.



Figure 4.2. Surface Preparation by Sand Blasting



Figure 4.3. Rounding Corners

On the days selected for installation, attention was also given to the environmental conditions such as wetness of the surface and temperature. For FRP systems, the surface must be dry, as water in the pores can prevent resin penetration and reduce mechanical interlock. Moisture vapor can also cause bubbles in the resin before curing which hurt bond performance. For FRCM and SRG systems, however, a saturated surface-dry condition is acceptable. FRCM and SRG can typically be applied to surfaces subject to moisture vapor transition, as the bond to substrate is not compromised.

For all three types of systems, there are limitations to the temperature at which the installation can take place, however temperature is much more critical to FRP systems. ACI 440 discusses problems with resin penetration if the surface is too cold, and suggests following the guidelines of the manufacturer. Structural Technologies gives the approximate pot life of V-Wrap 770 epoxy as 3 to 6 hours at 68°F (20°C), and the system should only be applied when the ambient temperature is between 40°F and 100°F (4°C to 38°C) (Structural Technologies, 2016a). ACI 549 recommends limits to the temperature on the day of installation. Temperatures above 95 degrees Fahrenheit (35°C) may reduce the workability of the mortar, and temperature below 43 degrees Fahrenheit (6°C) can slow down setting considerably. Simpson Strong-Tie has stricter limits for their mortar, allowing a range of 41°F (5°C) to 86°F (30°C) (Simpson Strong-Tie, 2017, 2018). Ruredil states that there are essentially no differences in workability time between 41°F (5 °C) and 104°F (40 °C) for their inorganic matrix, but recommends installation between 41°F (5°C) and 95°F (35°C) (Ruredil, 2012).

4.2. INSTALLATION

The fiend installation of strengthening systems requires a good plan to be made before the day of installation. Attention to detail is crucial to adhere to the guidelines of ACI design guides as well as the suggestions of each manufacturer. The plan for installing strengthening on Bridge P-0058 follows.

4.2.1. Mixing of Resin or Matrix. Mixing of the resin was done in accordance with the manufacturer's recommendations. The suggested mixing ratio was followed, and complete mixing (based on mix time and visual inspection) was achieved before use. Electric paddle mixing was used to prepare the batches as shown in Figure 4.4, and batch size was kept small so that the resin could be used up in the recommended pot life for ideal viscosity. V-Wrap 770 comes in two parts referred to as A and B. Part A was premixed for 2 minutes, then the full contents of Part B pail were added to the full contents of Part A pail. Part A and Part B were then blended with a mechanical mixer for 3 minutes until uniformly blended. (Structural Technologies, 2016a)

Mortars were also mixed as specified by the manufacturer's recommended batch size, mix ratio, method, and time. Figure 4.4 shows the mixing process. Batch sizes were small so that the mortar could be used within its plastic state. This allows for the best viscosity for the matrix to penetrate the fabric.

The recommended procedure for mixing both Ruredil's and Simpson Strong-Tie's mortars is as follows. To start, 90% of the total mixing water recommendation depending on the desired consistency of the mortar was added. The batch was then mixed with a mechanical mixer at least 3 minutes adding the remaining 10% of the recommended total water if necessary until a homogeneous mixture with the desired consistency is formed.

The mixture was allowed to rest 1 minute and then remixed another 10 seconds before applying. No additional water was added after the setting process is started. (Simpson Strong-Tie, 2017; Ruredil, 2012)



Figure 4.4. Mixing Resin and Cementitious Matrix

4.2.2. Manual Layup. For each system, the sheets of fabric were pre measured and cut in the Missouri S&T labs in order to reduce prep work in the field prior to installation. Figure 4.5 shows materials being cut in the lab. The carbon FRP sheets were applied by wet layup as shown in Figure 4.6. The sheets were properly aligned, avoiding deviations of more than 5 degrees in either direction of the girder line as given as the acceptable tolerance in ACI 440. The sheets were set into the surface saturant, and rollers

were used to smooth the fabric and remove bubbles. After about 10 minutes of setting, another layer of resin was rolled over to complete impregnation.



Figure 4.5. Preparing Sheets in Lab Setting

For the FRCM and SRG systems, trowels were used to apply an even, $\frac{1}{4}$ to $\frac{1}{2}$ inch (6–13 mm) thick layer of matrix over the surface. The fabric was then gently pressed into the matrix, and another $\frac{1}{4}$ to $\frac{1}{2}$ inch (6–13 mm) thick layer of additional matrix was smoothed over the top. Figure 4.6 shows this process. For each system, two plies of flexural reinforcement were used, and the second layer was applied before complete curing of the first layer. The SRG system presented other issues due to its rigidity in comparison to the other fabrics. For u-wraps, a machine is needed to aid bending before the system can be installed.

For each system, flexural reinforcement was fully installed before shear reinforcement. This allowed for the flattest surface possible for the flexural sheets.

Additionally, having the U-wraps on the exterior created the best anchorage qualities to aid the flexural system.



Figure 4.6. Manual Layup

4.2.3. Curing. For FRCM systems, it is important to properly cure the system to achieve the desired strength. Installation shall be kept humid and protected against heat and wind for 3 to 5 days by wet curing or using an ASTM C309 compliant water-based curing compound. The use of curing compounds may affect adhesion of subsequent surface treatments. SSD surface conditions and proper curing procedures are critical to prevent premature drying or cracking. (Ruredil, 2012; Simpson Strong-Tie, 2017)

4.2.4. Durability Study. For each system, additional strips were installed in areas other than the girders to serve as a durability study area. The strips are intended to be used for pull-off testing at different times in the future. Different types of testing will be done to monitor performance in pure tension as well as shear to observe different

failure modes. These strips will be exposed to the same environmental conditions as the girder strengthening such as freeze and thaw cycles, and ultraviolet light. These conditions can cause durability concerns and effect the bond performance of the strengthening systems in the long term.

5. LOAD TESTING

For this project, load testing was performed to record baseline serviceability behavior prior to strengthening and is expected to be repeated post-strengthening on spans 1 and 4 (furthest east and west). Load testing is observing and measuring the response of a structure subjected to controlled loads in the elastic range. Both static and dynamic tests were conducted. The pre-strengthening load test was performed on July 3rd 2018, and the static test is described in this section. Deflection data of the girders was collected with both LVDTs and surveying equipment. Repetition of load testing over the years following strengthening will allow for monitoring of the system's performance. Any major loss of the systems' strength or stiffness may be observed through load testing. (John J. Myers, Holdener, & Merkle, 2012)

5.1. INSTRUMENTATION

Field visits were taken prior to the first load test in order to install instrumentation for monitoring during the load tests. An epoxy was used to attach steel plates to the underside of the beams in spans 1 and 4. These plates were placed at locations where optical surveying prisms were later magnetically attached to be used to monitor deflection. Even at the highest points, the prisms were quickly and easily installed using a range pole. The deck was not to be monitored. A Leica TCA 2003 Automatic Total Station was used to save and read the coordinates. Research on total station use for load testing has shown that this total station can measure deformation accurate to 0.005 inches (.127 mm) or better at close range, which is comparable to LVDT's (Hernandez & Myers, 2018; Myers et al., 2008). The layout of the prisms is shown in Figure 5.1 and

Figure 5.2. A total of 22 prisms were used between the two spans, with 2 additional per span used as reference prisms.

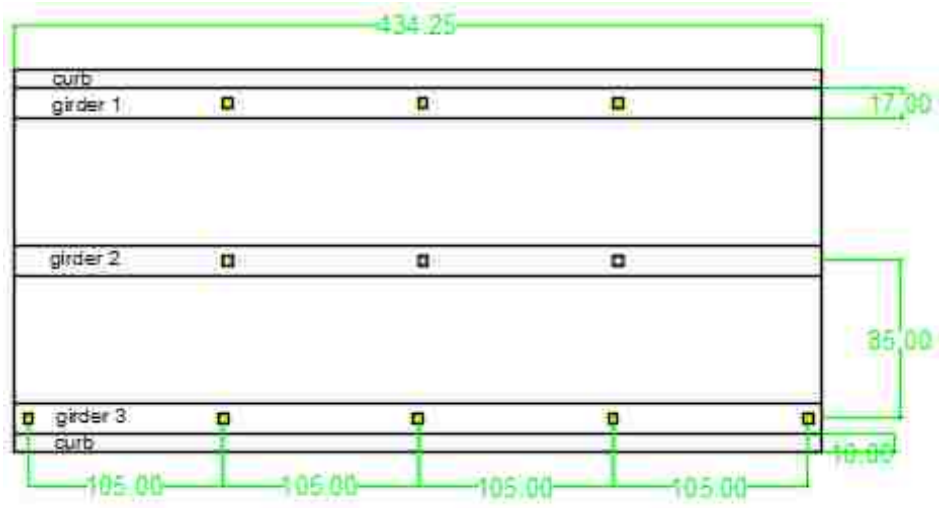


Figure 5.1. Span 1 Prism Layout (Dimensions shown in inches, 1 in. = 25.4 mm)

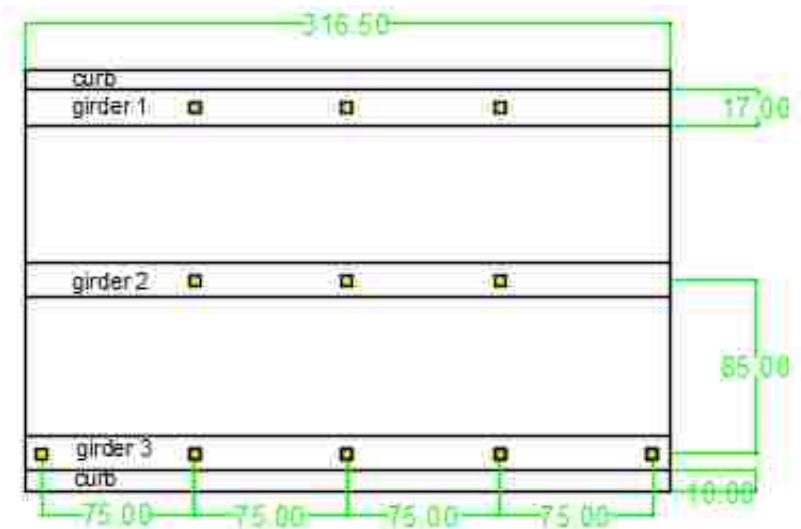


Figure 5.2. Span 4 Prism Layout (Dimensions shown in inches, 1 in. = 25.4 mm)

5.2. SETUP

On the day of the test, equipment was set up and checked for functionality prior to starting the load test. LVDTs on stands were set up as another way to monitor deflection throughout the testing. They allowed for much more frequent readings than the total station. The LVDTs were used at midspan of each beam. Figure 5.3 shows the midspan setup, including LVDTs and the data acquisition system (DAS) employed during the test. In addition, Figure 5.3 shows three prisms at midspan, and the total station is in the background. Figure 5.4 shows the setup for the total station test. Once prisms were installed and the total station was setup on a secure tripod with a clear view of the targets, the device was programmed to mark the locations of each prism with respect to reference prisms. The reference prisms were also used to check if the total station had moved between readings. Each prism was named sequentially, and the names were documented in a field book. The total station was programmed to take three readings at each point, and an average value was used, neglecting any large variances.

Pre-test setup also included marking the physical truck stops to be used. These stops differed between the two spans due to the different geometry. The length and capacity of span 1 allowed for two loaded trucks to be used. In order to observe the maximum moment, the trucks were placed back to back, centered about the midspan. Span 4's smaller girders and shorter span length made a one truck setup necessary. Using the axle weights and distances between axles, the proper location of the truck for maximum moment was determined and marked.



Figure 5.3. Data Acquisition System Setup



Figure 5.4. Total Station Setup

5.3. PROCEDURE

For each test described in the following, traffic control was used to ensure the results were due to the test trucks. Three H20 dump trucks were provided by MoDOT, and labeled as trucks A, B, and C. Trucks A and B were loaded with gravel to be about 38 kips (169 kN) each, and were used for the static load tests. Truck C was empty, and was only used for the dynamic load tests. Figure 5.5 shows the axle configuration of the trucks. The exact truck and axle weights were recorded so that variances in the weights on future load tests will be known for normalization and comparison.

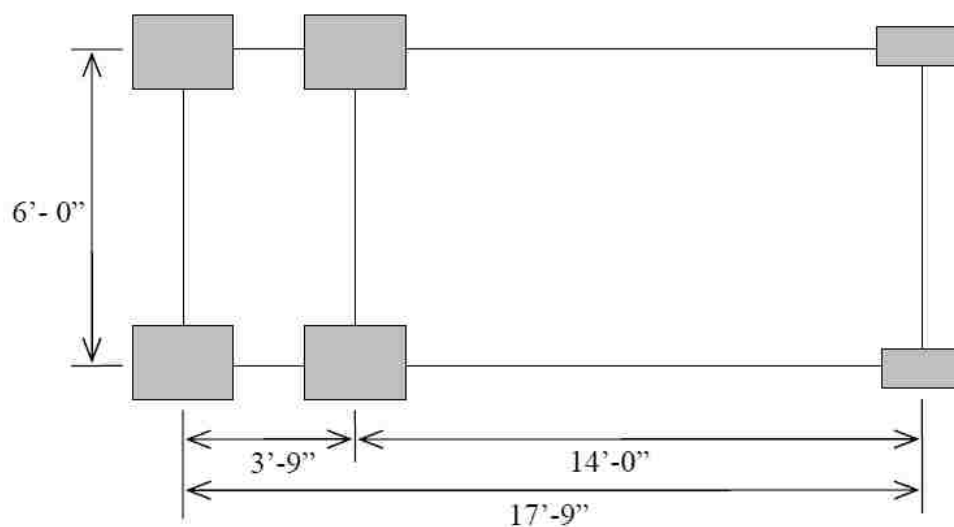
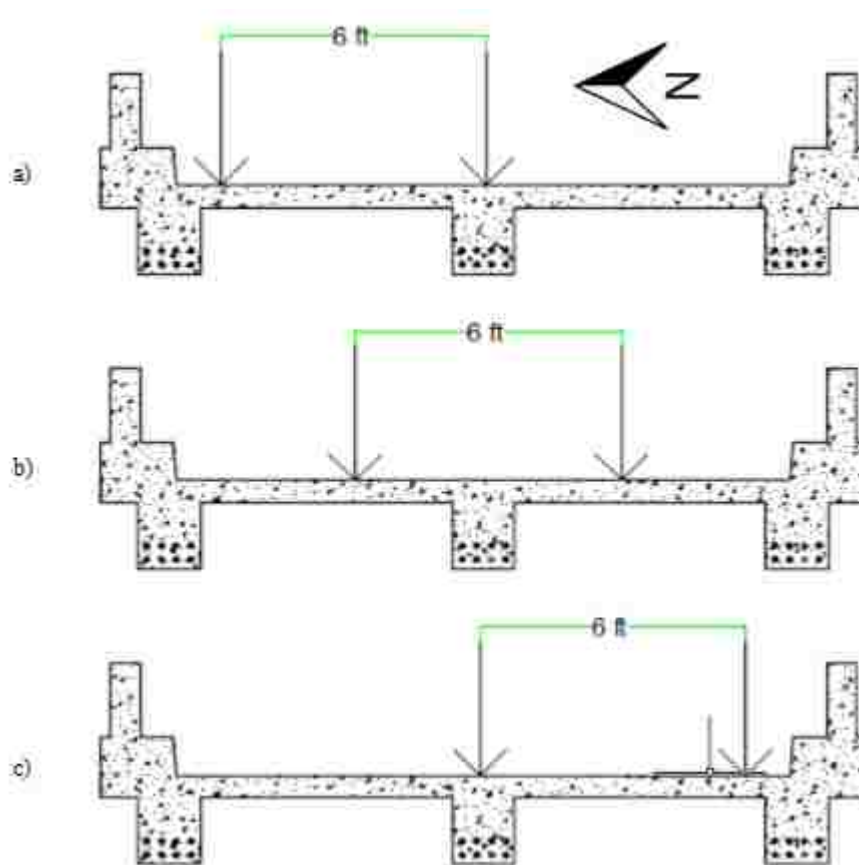


Figure 5.5. H20 Dump Truck Axle Configuration (Merkle, 2004) (Conversion: 1 ft. = 0.305 m, 1 in = 25.4 mm)

For both spans, three different static tests were done, moving the trucks across the bridge from north to south. This allowed for observing the effect of different load

distributions to each girder. Setups 1 and 3 produced an overload condition on the two exterior girders, while setup two was symmetrically centered. All of the stops tested had the truck weight centered longitudinally on the span, to produce the maximum positive moment. The three positions are shown in Figure 5.6.



Conversion: 1 ft. = 0.305 m

Figure 5.6. Load Test Truck Placements. a) Setup 1; b) Setup 2; c) Setup 3

The testing began with span 1. An initial reading was taken with the total station, and the strain gauge and LVDT data began being collected at a rate of 1Hz. The total

station was programmed to take three readings at each point, and an average value was used, neglecting any large variances. Next the trucks were positioned as close to the northern safety barrier as possible, as shown as position 1.

Figure 5.7 shows the trucks in position. Measurements were taken to know the exact location of the trucks, and the bridge was given time to respond to the load. After about 5 minutes, the total station was used to take readings of all the prisms on the span. This same procedure was repeated for placements 2 (centered on the span) and three (close to the south barrier). After these three static tests, the bridge was given time to relax, and final total station readings were taken.



Figure 5.7. Trucks on Span 1 for Load Test

The DAS and other equipment were then moved across the river to span 4, and a similar setup was completed. Initial total station readings were taken and LVDT data

began collecting. Three stops were used on span 4, locating the single truck close to the north barrier, centered, and close to the south barrier. Figure 5.8 shows the loaded truck on span 4.



Figure 5.8. Truck on Span 4 for Load Test

5.4. RESULTS AND DISCUSSION

Upon completion of load testing, the data must be processed and condensed down to extract the useful information. Theoretical modeling was also done to compare the load test results to.

5.4.1. Data Analysis. The total station data was uploaded to a computer for farther analysis. Each measurement was taken in sets of three readings, and these values were averaged, with any outliers removed. For each point, there was a control set from

before loading and sets for each truck stop. Deflection was found by subtracting the control reading average from each truck stop reading average. A second control set was intended to be taken after the stops were concluded, but the total station was moved before the reading could happen. This additional control set would have helped verify that nothing moved undesirably and the set would be used in adjusting for thermal effects. However, consistency of the reference points, and points where zero deflection was expected showed that total station settling wasn't an issue. While the temperature was rising throughout the tests, the total time for span one tests was only an hour and a half, and the increase in temperature was low over this time. An increase in temperature is known to cause an increase in camber, (upward deflection at midspan) however very minimal thermal adjustments were required for these load tests (Merkle, 2004). Once these adjustments were complete, deflections were plotted as a function of distance from the west support.

Table 5.1. Pre Strengthening Load Test Axle Loads

	Weight (kips)		
	Front Axle	Rear Axles	Total
Truck A	13900	24280	38180
Truck B	14180	24020	38200

5.4.2. Theoretical Modeling. Individual Tee-Beam analysis was performed for each girder, breaking the full cross section into three individual tee-beams. This model was to find the theoretical pre-strengthening deflection from the load test. The loads used

were from the truck weight tickets collected during the load tests. The truck geometry was verified in the field, and this geometry along with the truck stop diagrams were used to locate the wheel loads, which were assumed to act as point loads. The loads are shown in Table 5.1.

Two Tee-Beam models were made, first ignoring any contribution from the barrier walls and then adding their influence by estimating their stiffness contribution to the interior and exterior girders. MoDOT distribution factors were used to distribute the wheel loads to each girder, and calculate the maximum influence each girder may see from the trucks. The Tee-Beams were analyzed as simply supported structures. Assumptions were required for beam stiffness properties. It was assumed that each beam was uncracked and the gross moment of inertia was used. The modulus of elasticity was approximated based on the field-measured compressive strength of the concrete, as per ACI 318.

Bridge P-0058 has a tight girder spacing relative to many other RC bridges. Additionally, span 1 has a transverse diaphragm at midspan. Both of these factors increase the transfer of load between the girders, and help the span act as a unit. This transfer can allow girders in better condition (therefore more stiff) to attract more load and compensate for weaker girders. The degree at which the load is transferred is difficult to estimate without full knowledge of cracking, corrosion, and other deterioration. For the model considering the barriers, it was estimated that 25% of the stiffness of a barrier was transferred to the interior girder while the remaining 75% of the stiffness influenced the exterior girder closest to the barrier. Since there are barriers on each side, the interior

girder was given 50% of a barrier added stiffness, with 25% coming from each side. The excel spreadsheets used to calculate theoretical deflections are included in Appendix G.

5.4.3. Results. Figure 5.9 through 5.11 show the plotted deflections along the length of each girder for the pre strengthening load tests on span 1. These deflection data points are all from the total station readings during testing. The values at midspan were compared to LVDT deflection readings to verify the accuracy of the readings.

Figure 5.9 shows the results of stop 1, which overloaded the north side, placing the wheel lines very close to directly over girders 1 and 2. The span behaved as expected and girders 1 and 2 saw most of the influence. This stop had the highest deflection seen of any stop at 0.077 inches (2.0 mm). Based on visual inspection, girder 1 is in the worst condition due to spawling. The load test also suggests that girder 1 is in the worst condition of the three based on the highest observed deflection being from stop 1.

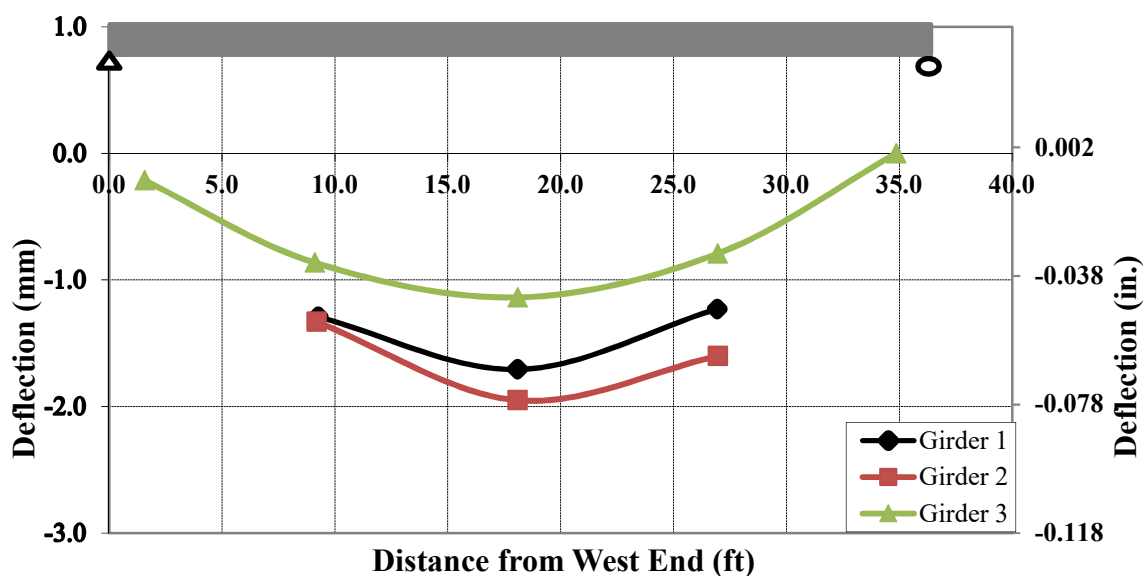


Figure 5.9. Span 1 Stop 1 Vertical Deflection

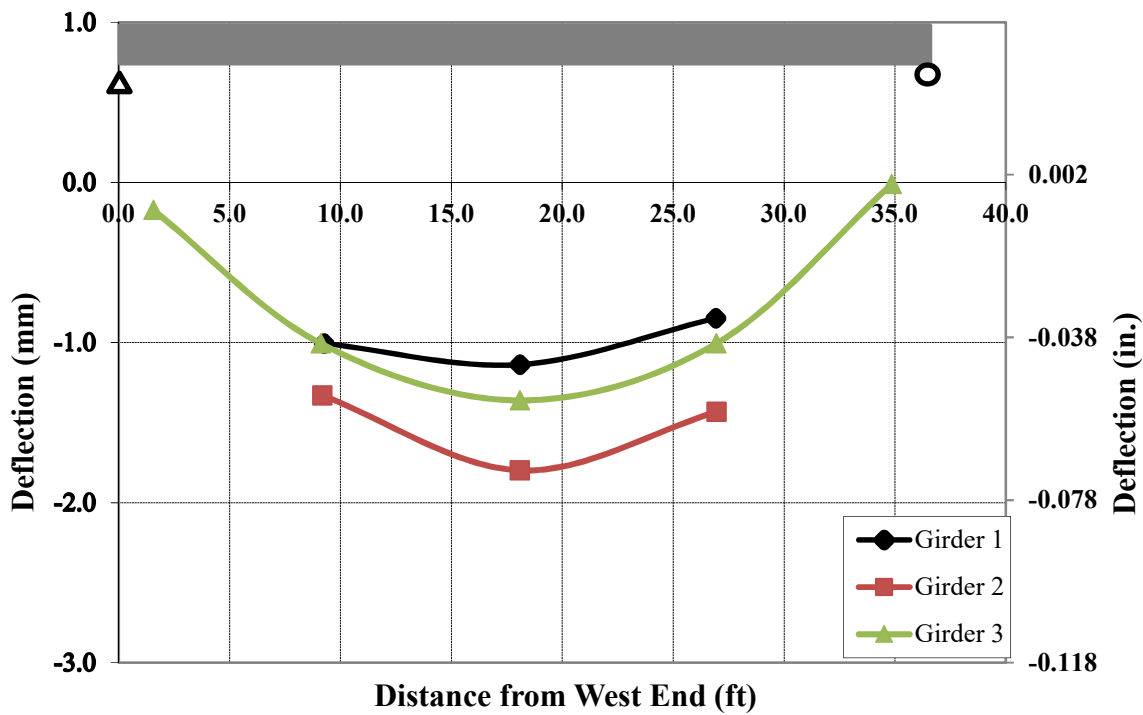


Figure 5.10. Span 1 Stop 2 Vertical Deflection

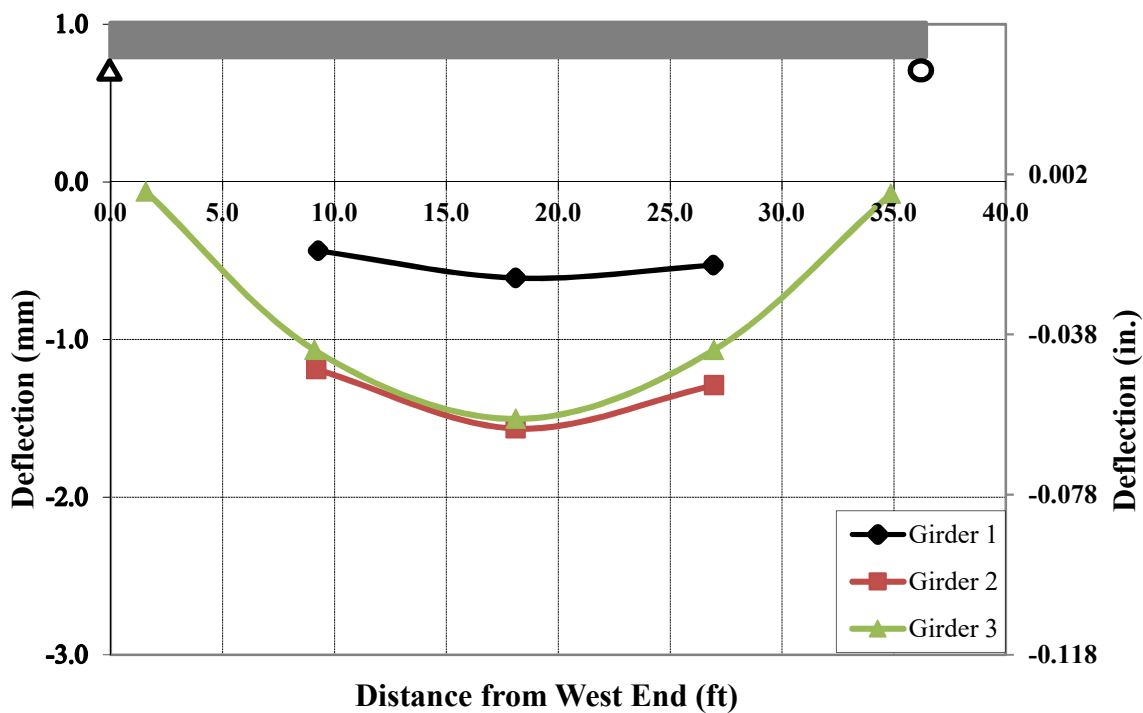


Figure 5.11. Span 1 Stop 3 Vertical Deflection

The results of stop two are shown in Figure 5.10. This stop had the trucks centered, straddling girder two. As expected, girder two deflected slightly more than the other two girders for this loading. Based on field measurements, the trucks were placed 4 inches (101.6 mm) south of being perfectly centered. This lack of symmetry could have caused error in the results, and could explain why girder 3 deflected more than girder 1 for this stop. Additionally, if girder 3 is in better condition than girder 1, then girder 3 would attract more load as the load is transferred transversely through the span. Stop 3, shown in Figure 5.11, overloaded the south of the bridge, with most of the weight over girders two and three. The results were as expected, with these overloaded girders having the highest deflection. Girder 1 had very little deflection from stop 3, which suggests that little load was transferred to it, as the other stiffer girders took the load.

Figures 5.12 through 5.17 show a comparison of the theoretical deflection models to the deflection values measured with the total station in the field. The plots are broken up by load test stop, as well as by interior and exterior girders.

The Tee-Beam analysis not considering the barriers predicted the maximum midspan deflection to be about 0.25 in. (6.3 mm) for the interior girder and about 0.28 in. (7.2 mm) for the exterior girders for each stop. These values are over 300% higher than any observed deflections. This model was overly conservative which suggests that the barrier walls and diaphragm have a large impact on the rigidity of the bridge working as a full unit.

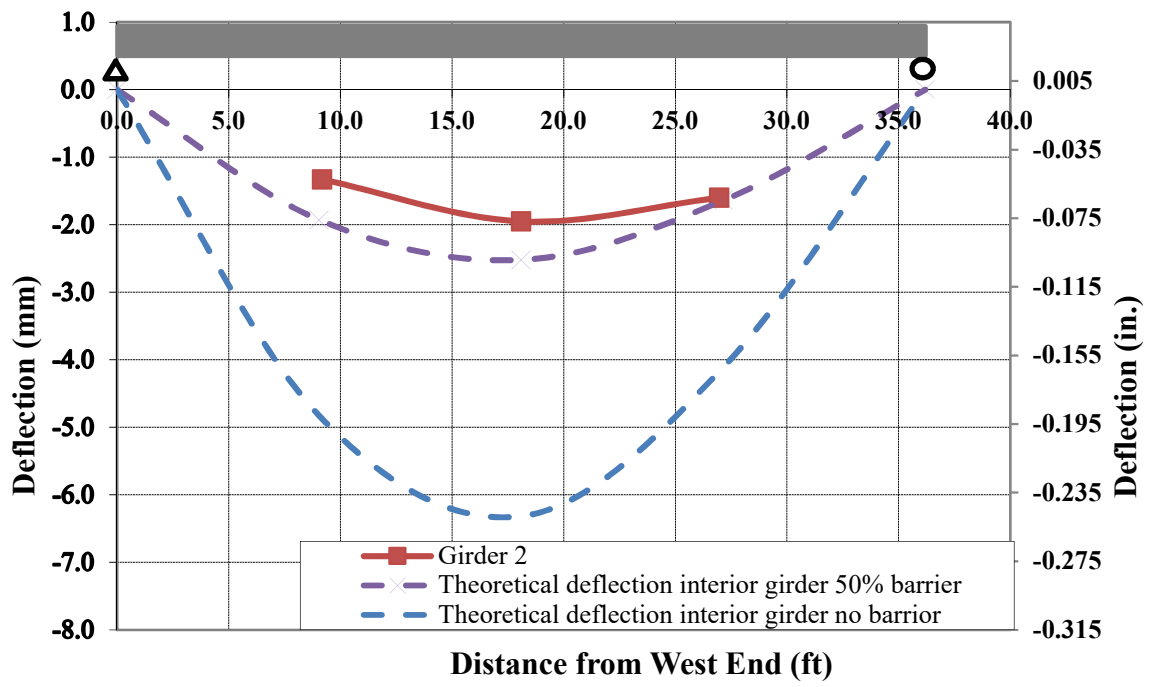


Figure 5.12. Span 1 Stop 1 Interior Girder Deflection Comparison

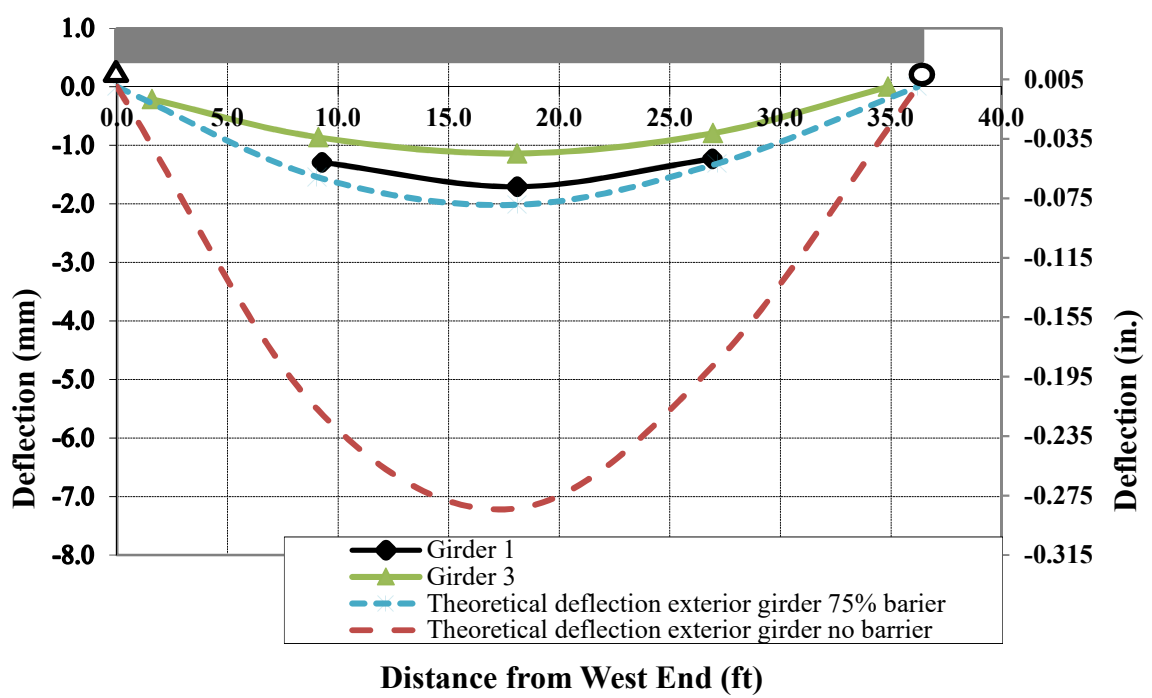


Figure 5.13. Span 1 Stop 1 Exterior Girder Deflection Comparison

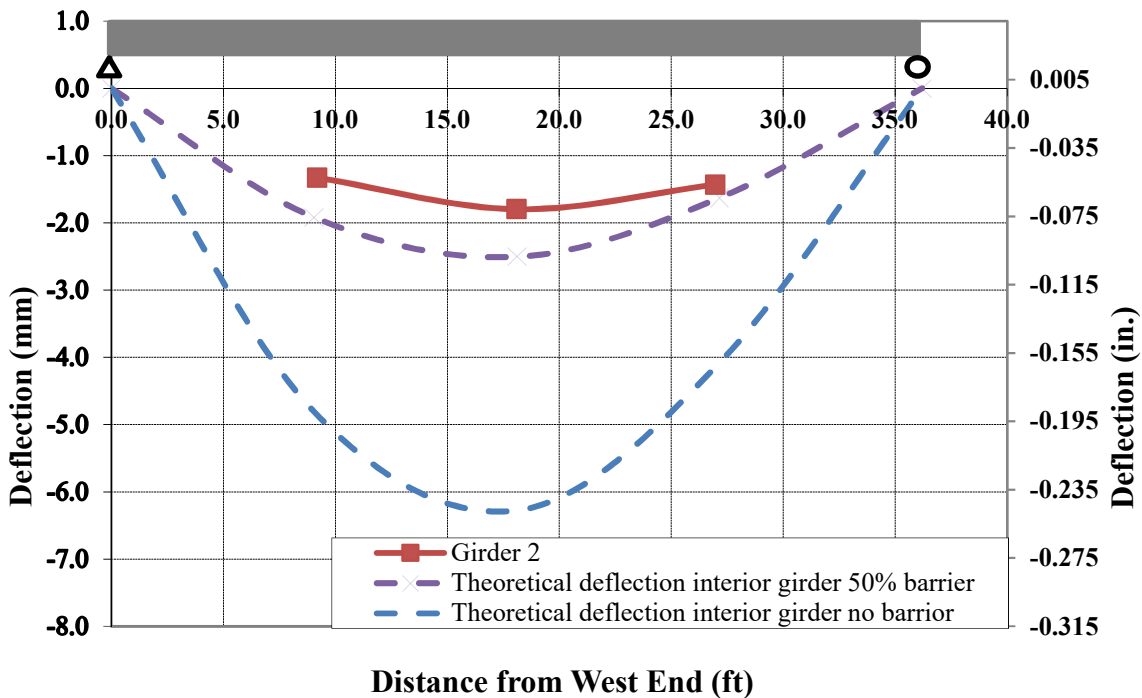


Figure 5.14. Span 1 Stop 2 Interior Girder Deflection Comparison

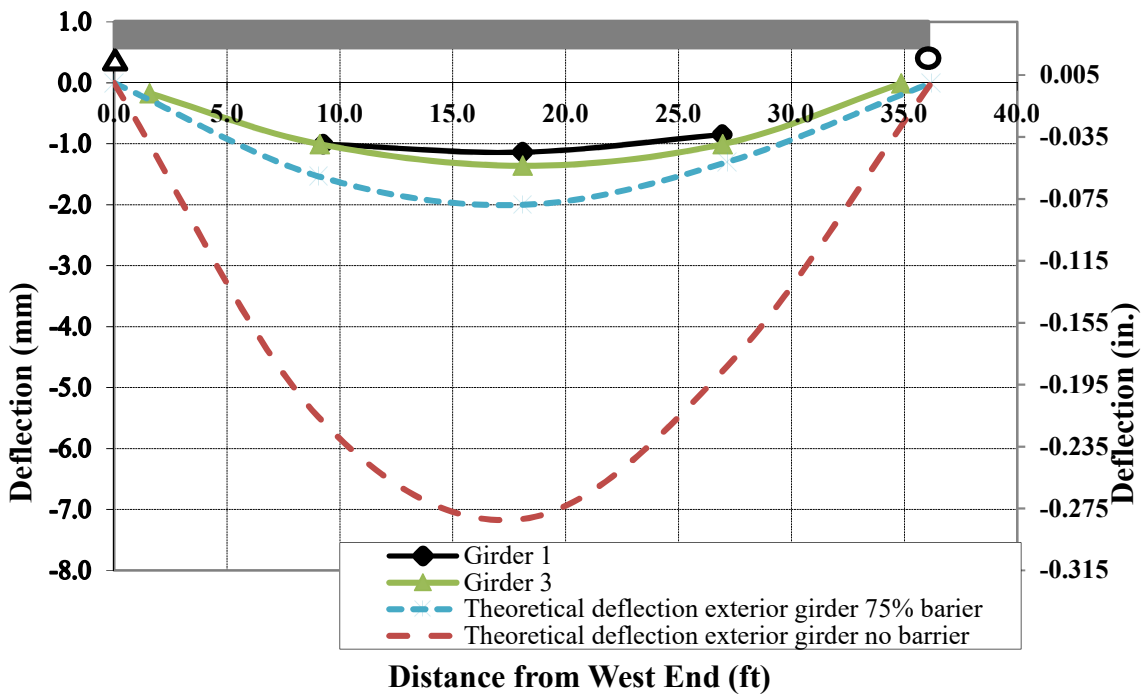


Figure 5.15. Span 1 Stop 2 Exterior Girder Deflection Comparison

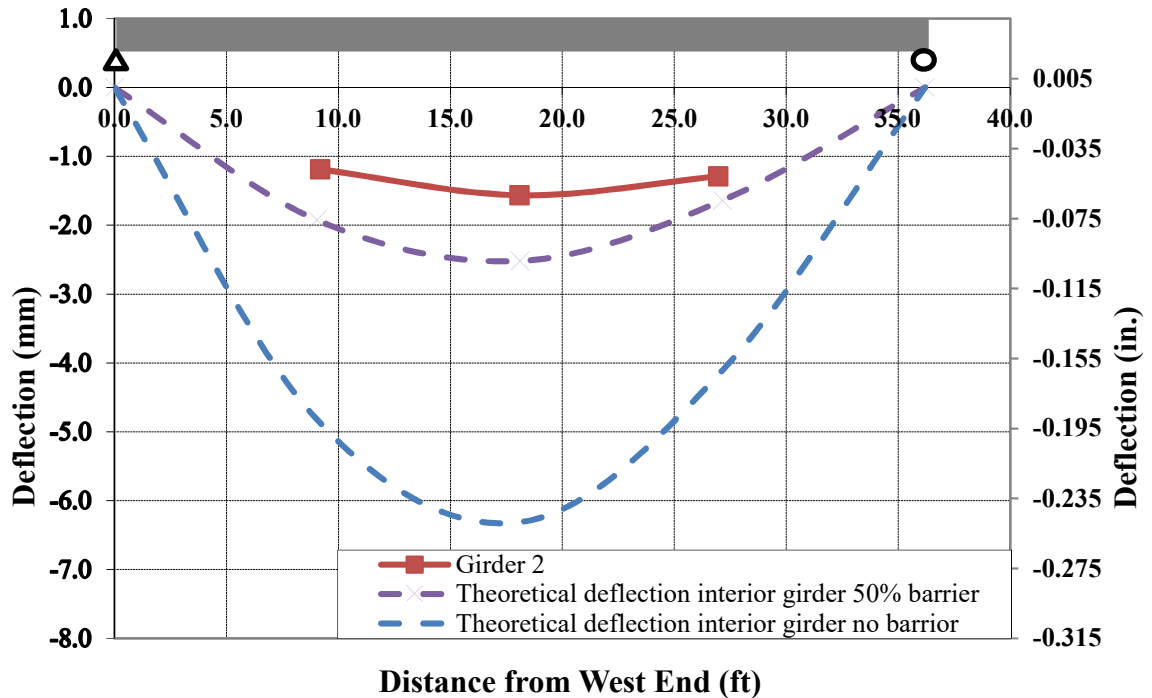


Figure 5.16. Span 1 Stop 3 Interior Girder Deflection Comparison

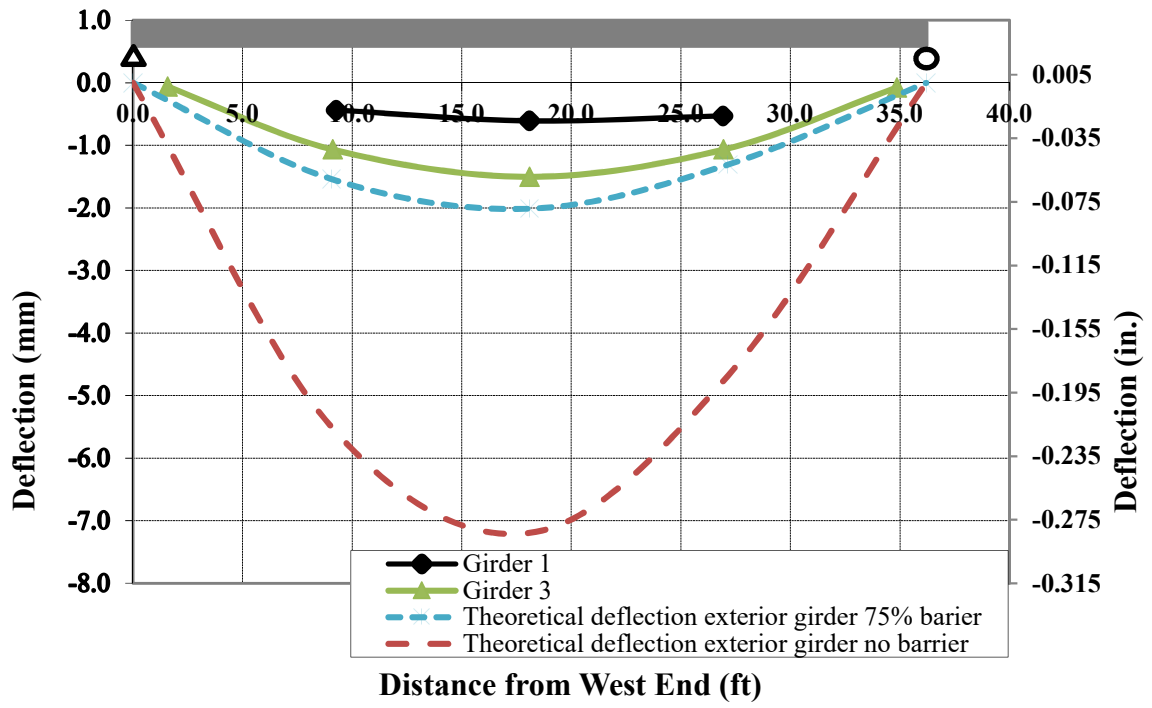


Figure 5.17. Span 1 Stop 3 Exterior Girder Deflection Comparison

The Tee-Beam analysis considering the barrier walls predicted the maximum deflection at midspan to be about 0.10 in. (2.5 mm) for the interior girder and about 0.08 in. (2.0 mm) for the exterior girders for each stop, which range from 18% to 80% higher than the observed midspan deflections. With the estimated barrier wall stiffness contributions added, the model was still conservative. One potential contributing factor to the model being conservative is that the modulus of elasticity of the concrete was calculated based off of a conservative estimate of the concrete compressive strength, whereas these in situ properties may be higher. Regardless of how conservative the Tee-Beam analysis estimates were, the deflection results of the pre-strengthening load test showed that the girders are in good condition.

6. SUMMARY AND CONCLUSIONS

6.1. SUMMARY

The objective of this study was to validate cementitious composite systems for strengthening of RC in the field. Bridge P0058 in Howell County, Missouri was chosen from a list of structurally deficient candidate bridges to be the site for the demonstration of four composite strengthening systems. The systems used are FRP with carbon fibers, FRCM with carbon, FRCM with PBO, and SRG.

The original bridge design was reviewed, and geometry was verified in the field. Field measurements of the concrete compressive strength showed a significant increase. Each cross section was reanalyzed with this increase in compressive strength to obtain the pre-strengthening capacity.

A parametric study was completed to see which systems performed most efficiently on longer spans, and to observe the effect of adding additional plies of each system. From this study, a final design was chosen with each strengthened beam being enhanced by a minimum of 4% in flexure and 11% in shear. Each design followed the guidelines of ACI 440.2R-08 and ACI 549.4R-13 as applicable.

A pre-strengthening load test was completed to obtain a baseline of the responses for comparison later on. Deflection data from static test stops were presented and will be used for comparison with future load tests.

The strengthening systems were successfully installed in summer 2018. This project showed that cement based composite strengthening systems are a viable technology for future use.

6.2. FINDINGS AND CONCLUSIONS

The design and installation process lead to several conclusions regarding field strengthening of bridge girders. The parametric study included in the design phase gave valuable comparisons in the theoretical performance of the four systems.

- If one equal width ply of each system is installed on four identical girders, Carbon FRP has the highest theoretical moment capacity increase, followed by carbon FRCM, then PBO FRCM, and finally SRG.
- All four systems are more efficient on the shorter spans, which have a shallower section containing less steel reinforcement.
- When comparing the capacity gained by adding the same area of fibers added to the deeper and shallower cross sections, the average added capacity was 18% higher on the shallow than the deep section for SRG. This is low compared to the other systems, which had increases of 60% for PBO, 83% for C-FRCM, and 74% for CFRP. While carbon FRP and Carbon FRCM were most impacted by the span length, their higher efficiency overall made them the best choice for strengthening the long spans.

The load tests also gave valuable information about the condition of the bridge. The girders are in good condition overall, especially when compared to the theoretical maximum midspan deflection values calculated using Tee-Beam Analysis. The load tests also suggested that girder 1 is the most damaged of the span 1 girders, which agreed with the visual inspection done during site visits.

It is anticipated that field installation will produce comparisons in the feasibility of each type of system for strengthening existing bridges. These expected findings are

based on the specific strengthening systems chosen, and the conditions in which they were installed.

- Field application was successful for all four systems. This project is the first documented field implementation of cement based strengthening systems for research. The study demonstrated that cementitious systems are easier to work with in the field than systems using epoxy or other resins. When installation takes place in late summer, the cementitious matrix is much less effected by, and easier to work with in the high heat.
- A durability study area was created, so that pull off tests can later show how the bonding of the systems have held up over time exposed to field conditions.
- A long term study of the performance of these systems was created. The Missouri Department of Transportation has agreed to allow the bridge girders to be brought to Missouri S&T once the bridge is decommissioned in approximately 5 to 8 years. This will allow for future studies discussed farther in Section 6.4.
- A long term load testing study was also started by this project. Future load tests intended to be conducted about twice a year will show the increase in stiffness from the strengthening. The repeated tests will also capture potential loss of stiffness over time exposed to the environment.

6.3. RECOMMENDATIONS

This study showed that FRCM and SRG systems are a viable alternative to FRP and externally bonded steel systems, but taught some factors that are important for consideration. When deciding if strengthening is the best choice for a bridge, it is

important to check for access for lifts. With the naturally rough, rocky surface of a creek bed, it can be difficult to get equipment under the girders and it is labor intensive to set up scaffolding.

This study also showed the importance of preparatory work before starting the installation. Field cuts are difficult to make accurately, so precise measurement and cutting should be done before bringing materials on site. This is extra critical for SRG systems, since bends for U-wraps requires equipment that cannot be easily transported to the field.

It is important to note that field installation by manual layup is a labor-intensive task. While other strengthening techniques using steel plates or precured FRP laminate can be installed with as few as two people, it is not recommended to attempt manual layup installation without more manpower.

6.4. FUTURE WORK

The Missouri Department of Transportation has indicated that bridge P0058 is likely to be up for replacement in the coming years. The strengthening systems have been designed with the hopes of being able to do destructive testing once the bridge is out of service. The intent is to saw cut the deck of each span to create three large Tee beams that could be transported to the Missouri S&T SERL. Once on campus, the six strengthened girders can be tested to failure to show the actual ultimate strength after field installation and several years of field exposure. This is expected to show that the predictions of ultimate strength of ACI 440 and ACI 549 are conservative. This project will be a unique and valuable study of girders that are strengthened in the field, and then exposed to actual service conditions.

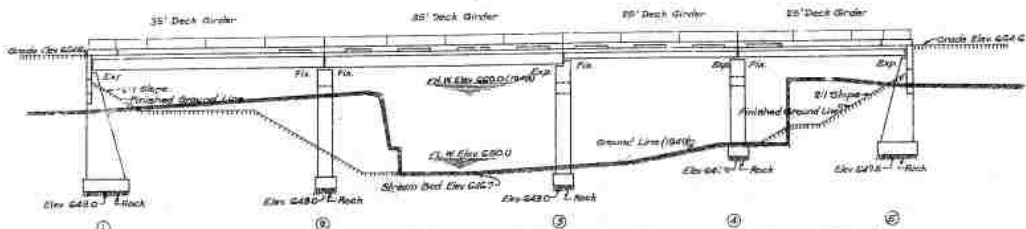
The six unstrengthened girders will provide control for comparison, as well as give the ability to strengthen some in the lab to gain additional data. Potential studies include:

1. Using more plies of reinforcement.
2. Different shear wrapping schemes, including changing the angle of orientation.
3. Strengthening systems that use mechanical anchorage.
4. Using new emerging strengthening systems.

APPENDIX A.
MODOT DESIGN DRAWINGS

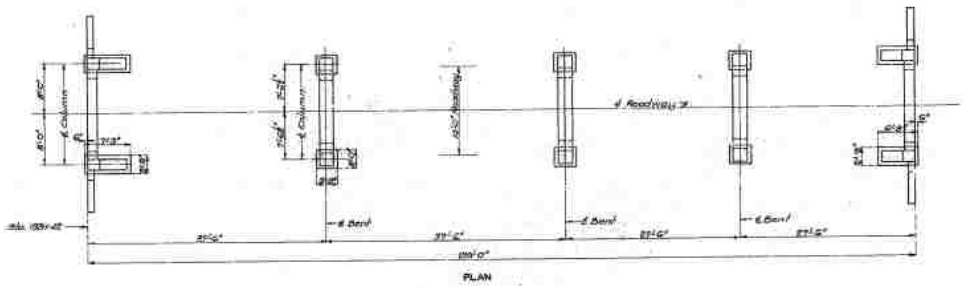
MISSOURI STATE HIGHWAY DEPARTMENT

PRO. NO.	STATE	FED. AID PROJ. NO.	THIS YEAR	SECT. NO.	SHEET NO.	TOTAL SHEETS
106	MO.			19		

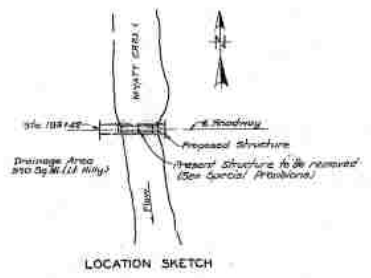


Note: All loose, shaly or disintegrated rock shall be removed and the footing placed on fairly well undisturbed rock. If well rock is encountered the footing shall be carried at least 4' into good rock against vertical faces of same. In no case shall footings of Bents A, B, C and D be placed higher than elevations shown.

Note: All existing fill under grade of bridge shall be removed to natural ground line. Payment for this excavation outside limits of excavation for structure will be made at unit contract price for Roadway Excavation.



106



Item	Unit	Quantity	Total
Class 1 Excavation for Structures	Cu. Yds.	60	60
Class 2 Excavation for Structures	Cu. Yds.	100	100
Class 3 Excavation (Handwall)	Cu. Yds.	115	115
Class 3 Excavation (Except Handwall)	Cu. Yds.	83.3	83.3
Reinforcing Steel	Lbs.	6350	32080
Structural Steel Reinforcing Plates	Lbs.	1650	1650

Note: Excavation for bridge made above Elev 521.0 will be paid for as Class 1 Excavation for Structures. Excavation for bridge made below Elev 521.0 will be paid for as Class 2 Excavation for Structures.

COMPLETE BILL OF SUBSTRUCTURE REINFORCING STEEL

No.	Size	Length	No. Lumps	Reinforcing Schedules & Cutting Diagrams
1	1/2"	11.2'	21	DI
2	1/2"	11.2'	21	DI
3	1/2"	11.2'	21	DI
4	1/2"	11.2'	21	DI
5	1/2"	11.2'	21	DI
6	1/2"	11.2'	21	DI
7	1/2"	11.2'	21	DI
8	1/2"	11.2'	21	DI
9	1/2"	11.2'	21	DI
10	1/2"	11.2'	21	DI
11	1/2"	11.2'	21	DI
12	1/2"	11.2'	21	DI
13	1/2"	11.2'	21	DI
14	1/2"	11.2'	21	DI
15	1/2"	11.2'	21	DI
16	1/2"	11.2'	21	DI
17	1/2"	11.2'	21	DI
18	1/2"	11.2'	21	DI
19	1/2"	11.2'	21	DI
20	1/2"	11.2'	21	DI
21	1/2"	11.2'	21	DI
22	1/2"	11.2'	21	DI
23	1/2"	11.2'	21	DI
24	1/2"	11.2'	21	DI
25	1/2"	11.2'	21	DI
26	1/2"	11.2'	21	DI
27	1/2"	11.2'	21	DI
28	1/2"	11.2'	21	DI
29	1/2"	11.2'	21	DI
30	1/2"	11.2'	21	DI
31	1/2"	11.2'	21	DI
32	1/2"	11.2'	21	DI
33	1/2"	11.2'	21	DI
34	1/2"	11.2'	21	DI
35	1/2"	11.2'	21	DI
36	1/2"	11.2'	21	DI
37	1/2"	11.2'	21	DI
38	1/2"	11.2'	21	DI
39	1/2"	11.2'	21	DI
40	1/2"	11.2'	21	DI
41	1/2"	11.2'	21	DI
42	1/2"	11.2'	21	DI
43	1/2"	11.2'	21	DI
44	1/2"	11.2'	21	DI
45	1/2"	11.2'	21	DI
46	1/2"	11.2'	21	DI
47	1/2"	11.2'	21	DI
48	1/2"	11.2'	21	DI
49	1/2"	11.2'	21	DI
50	1/2"	11.2'	21	DI
51	1/2"	11.2'	21	DI
52	1/2"	11.2'	21	DI
53	1/2"	11.2'	21	DI
54	1/2"	11.2'	21	DI
55	1/2"	11.2'	21	DI
56	1/2"	11.2'	21	DI
57	1/2"	11.2'	21	DI
58	1/2"	11.2'	21	DI
59	1/2"	11.2'	21	DI
60	1/2"	11.2'	21	DI
61	1/2"	11.2'	21	DI
62	1/2"	11.2'	21	DI
63	1/2"	11.2'	21	DI
64	1/2"	11.2'	21	DI
65	1/2"	11.2'	21	DI
66	1/2"	11.2'	21	DI
67	1/2"	11.2'	21	DI
68	1/2"	11.2'	21	DI
69	1/2"	11.2'	21	DI
70	1/2"	11.2'	21	DI
71	1/2"	11.2'	21	DI
72	1/2"	11.2'	21	DI
73	1/2"	11.2'	21	DI
74	1/2"	11.2'	21	DI
75	1/2"	11.2'	21	DI
76	1/2"	11.2'	21	DI
77	1/2"	11.2'	21	DI
78	1/2"	11.2'	21	DI
79	1/2"	11.2'	21	DI
80	1/2"	11.2'	21	DI
81	1/2"	11.2'	21	DI
82	1/2"	11.2'	21	DI
83	1/2"	11.2'	21	DI
84	1/2"	11.2'	21	DI
85	1/2"	11.2'	21	DI
86	1/2"	11.2'	21	DI
87	1/2"	11.2'	21	DI
88	1/2"	11.2'	21	DI
89	1/2"	11.2'	21	DI
90	1/2"	11.2'	21	DI
91	1/2"	11.2'	21	DI
92	1/2"	11.2'	21	DI
93	1/2"	11.2'	21	DI
94	1/2"	11.2'	21	DI
95	1/2"	11.2'	21	DI
96	1/2"	11.2'	21	DI
97	1/2"	11.2'	21	DI
98	1/2"	11.2'	21	DI
99	1/2"	11.2'	21	DI
100	1/2"	11.2'	21	DI

GENERAL NOTES:
 Design Specifications A.A.S.H.O. 1948
 Loading R10-43
 Reinforcing Steel stress 18,000 psi
 Class 3 Concrete Strength 1,000 psi
 All concrete shall be Class 3
 Where joint filler is specified on plans it shall conform with the requirements of Section 301.04(a) of the Standard Specifications for Premixed Material for Paving.

6.6 Elev 527.45 N.W. 1/4 Sec 18 R14E
 BRIDGE OVER MYATT CREEK
 STATE ROAD FROM LANTON EAST TO OREGON CO. LINE
 ABOUT 12.3 MILES W. OF THAYER.
 PROJECT NO. S-938(2002.A) (50) STA. 183+42
 HOWELL COUNTY

Drawn by *V. W. Bonaloni* Date *6/5/1951*
 Checked by *C. W. Brown* Date *6/5/1951*
 FINISHED
 FINISHED
 STD. C-808
 STD. C-10 R3
 P-58

Shown Nov 1950 by W.L.W.
 Traced Mar 1950 by M.E.L.
 Checked Feb 1951 by C.S.A.

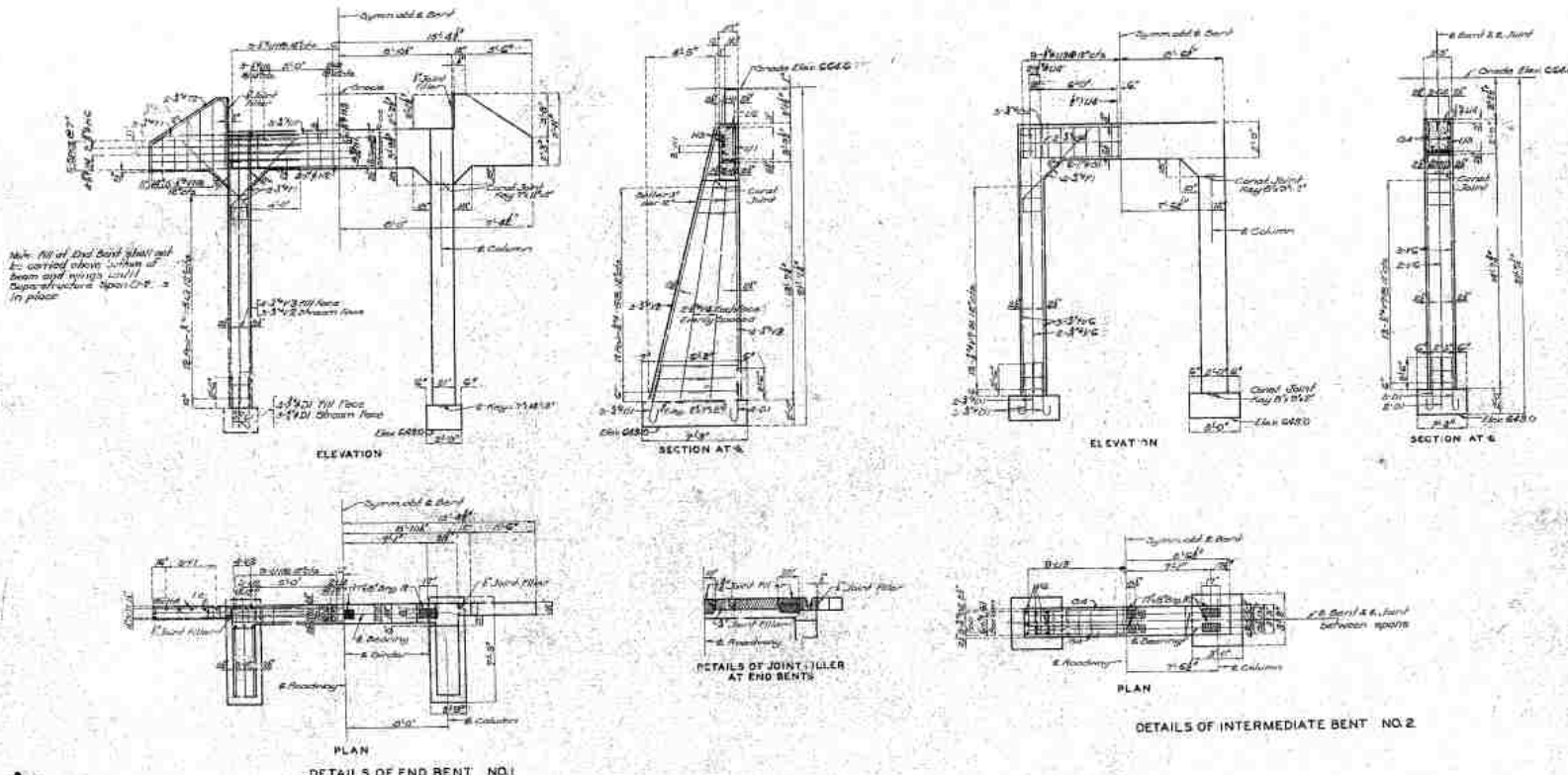
Note: This drawing is not to scale. Follow dimensions.

Sheet No. 1 of 6

SEE FULL PLANS BROWN LINES

MISSOURI STATE HIGHWAY DEPARTMENT

DESIGN NO.	DATE	DESIGNED BY	CHECKED BY	SCALE	TOTAL SHEETS
101					58



101

BRIDGE OVER MYATT CREEK
 STATE ROAD FROM LANTON EAST TO OREGON CO. LINE
 ABOUT 12.3 MILES W. OF THAYER
 PROJECT NO. 3-9323(30CA)507 STA. 95+42
 HOWELL COUNTY

FINISHED FINISHED FINISHED
 P-58

Drawn: Nov. 1890 by W.A.W.
 Revised: Nov. 1890 by M.E.L.
 Checked: Feb. 1917 by C.L.S.

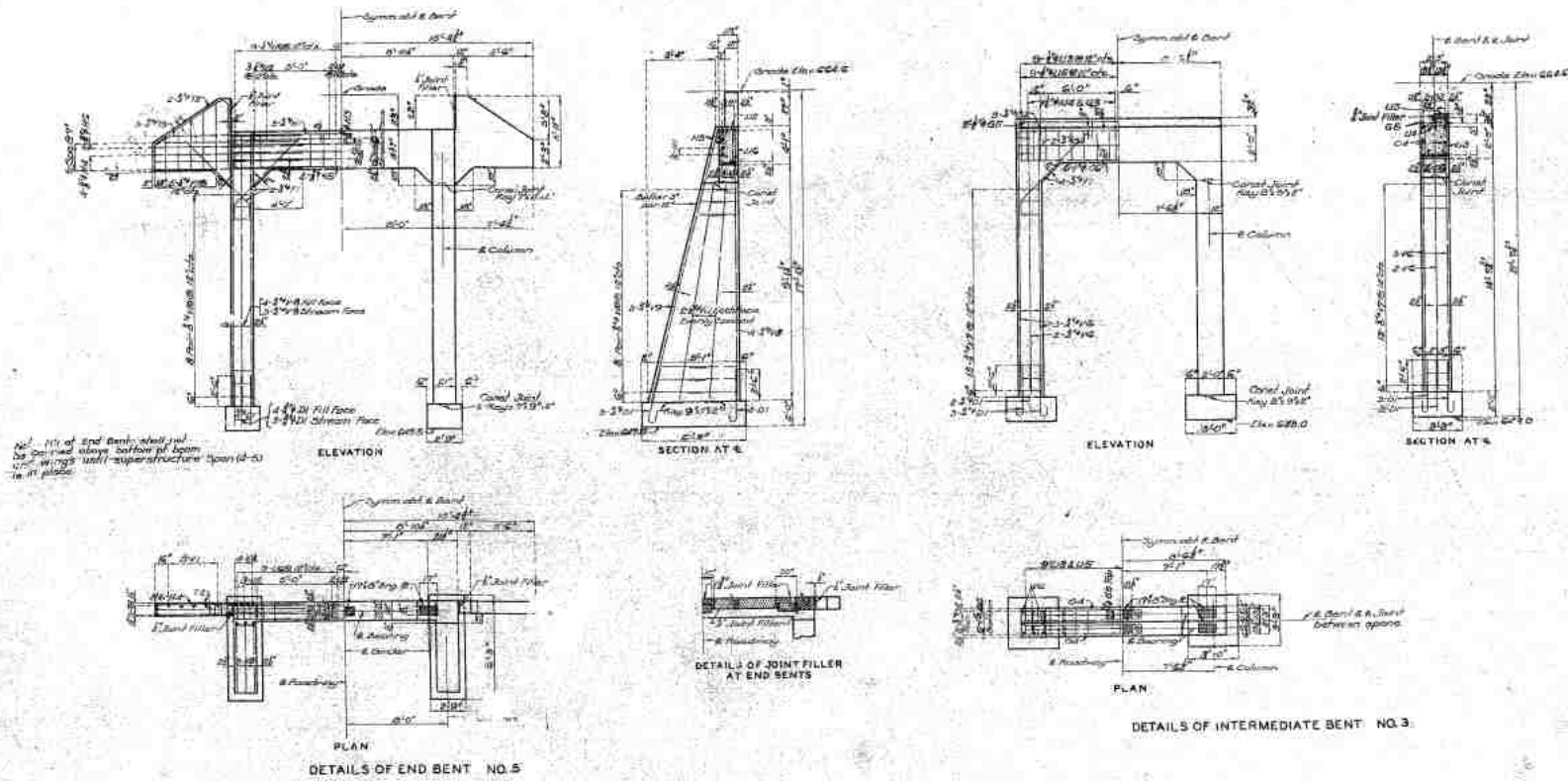
Note: This drawing is not to scale. Follow dimensions.

Sheet No. 2 of 5

SEE PLAN FOR COLUMN DIMENSIONS

MISSOURI STATE HIGHWAY DEPARTMENT

PROJECT	DATE	FILE NO.	PIECE NO.	SHEET NO.	TOTAL SHEETS
8					



Note: All of End Bent shall be of same size bottom of beam 12" wings with superstructure span (10-5) in all places.

BRIDGE OVER MYATT CREEK
 STATE ROAD FROM LANTON EAST TO OREGON CO. LINE.
 ABOUT 12.3 MILES W. OF TRAYER
 PROJECT NO. 3-938(2) BECA (50) STA. 93+42
 HOWELL COUNTY

FINISHED
 P-58

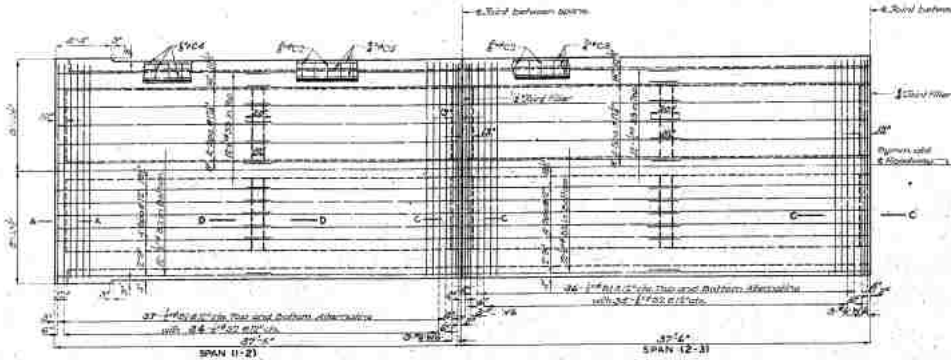
Drawn Nov. 1901 by W.L.W.
 Traced Nov. 1900 by M.L.L.
 Checked Feb. 1901 by P.A.S.

Note: All of structural steel to be of same millwork dimensions.

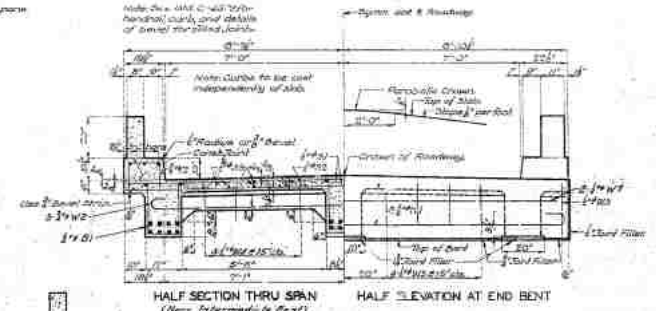
SEE FINAL PLANS FOR DIMENSIONS

MISSOURI STATE HIGHWAY DEPARTMENT

PROJ. NO.	DATE	REV. NO.	TOTAL SHEETS	SHEET NO.	TOTAL SHEETS
100	1937	1	100	100	100



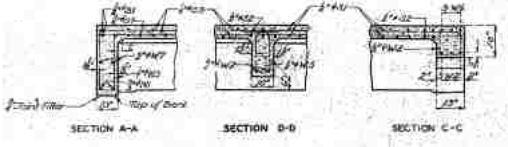
PLAN OF SLAB SHOWING REINFORCEMENT



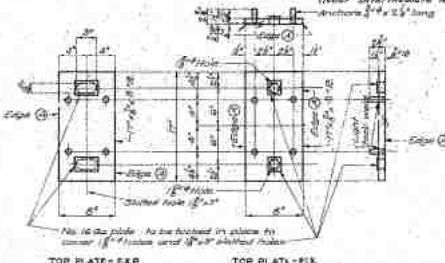
HALF SECTION THRU SPAN (Near Intermediate Bent) HALF ELEVATION AT END BENT



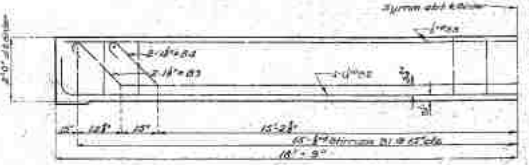
HALF SECTION THRU SPAN (Near Intermediate Bent)



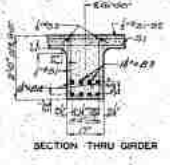
SECTION A-A SECTION B-B SECTION C-C



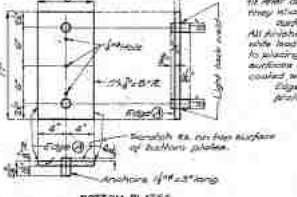
TOP PLATE - EXP. TOP PLATE - FIX.



GIRDER REINFORCEMENT



SECTION THRU GIRDER



DETAILS OF BEARING PLATES

No.	Size	Length	Mark	Location	Detailing
10	1/2" x 3/4"	31'-0"	C1	Top	[Diagram]
11	1/2" x 3/4"	31'-0"	C2	Top	
12	1/2" x 3/4"	31'-0"	C3	Top	
13	1/2" x 3/4"	31'-0"	C4	Top	[Diagram]
14	1/2" x 3/4"	31'-0"	C5	Top	
15	1/2" x 3/4"	31'-0"	C6	Top	
16	1/2" x 3/4"	31'-0"	C7	Top	[Diagram]
17	1/2" x 3/4"	31'-0"	C8	Top	
18	1/2" x 3/4"	31'-0"	C9	Top	
19	1/2" x 3/4"	31'-0"	C10	Top	[Diagram]
20	1/2" x 3/4"	31'-0"	C11	Top	
21	1/2" x 3/4"	31'-0"	C12	Top	
22	1/2" x 3/4"	31'-0"	C13	Top	[Diagram]
23	1/2" x 3/4"	31'-0"	C14	Top	
24	1/2" x 3/4"	31'-0"	C15	Top	
25	1/2" x 3/4"	31'-0"	C16	Top	[Diagram]
26	1/2" x 3/4"	31'-0"	C17	Top	
27	1/2" x 3/4"	31'-0"	C18	Top	
28	1/2" x 3/4"	31'-0"	C19	Top	[Diagram]
29	1/2" x 3/4"	31'-0"	C20	Top	
30	1/2" x 3/4"	31'-0"	C21	Top	

Note: Bars in above will be lapped and lapped separately.

BAR SIZE	CONCRETE
1/2" x 3/4"	100
3/4" x 1"	100
1" x 1 1/4"	100
1 1/4" x 1 3/4"	100
1 3/4" x 2"	100
2" x 2 1/4"	100

BRIDGE OVER MYATT CREEK
 STATE ROAD FROM LANTON EAST TO OREGON CO. LINE
 ABOUT 1/2 MILES W. OF THAYER
 PROJECT NO. S-938(2) SECA 1301 STA. 163+42
 HOWELL COUNTY

FINISHED

FINISHED P-58

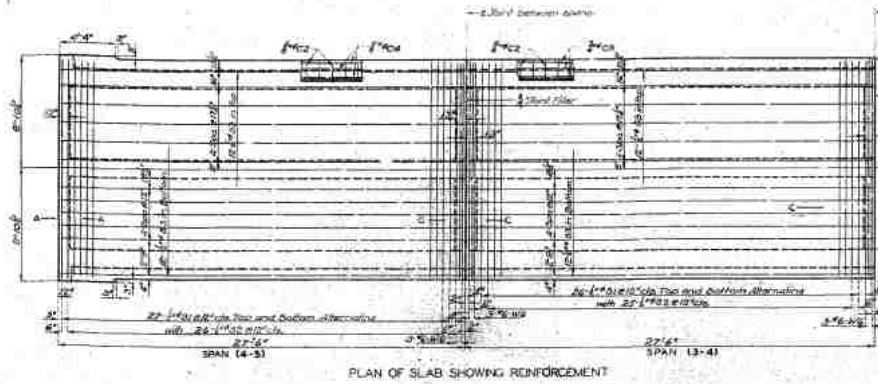
Designed by (S) by M.E. & A.L.K.
 Checked by (S) by C.E.A.
 Drawn by (S) by M.E.
 Printed April 1937 No. 100

Note: This drawing is not to scale. Follow dimensions.

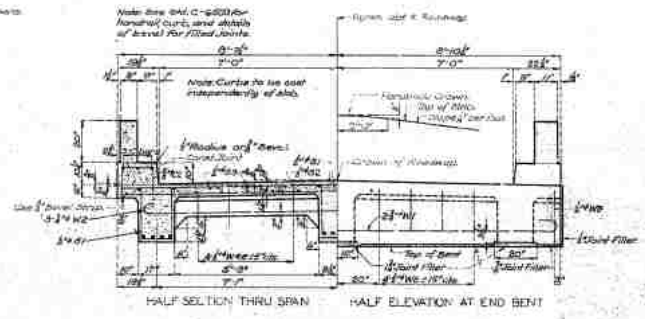
Sheet No. 100 of 100

MISSOURI STATE HIGHWAY DEPARTMENT

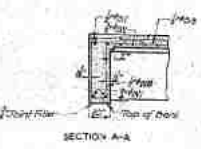
REV.	DATE	BY	CHKD.	APP'D.	DATE	REASON
1	11/10/21



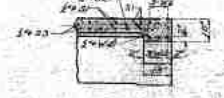
PLAN OF SLAB SHOWING REINFORCEMENT



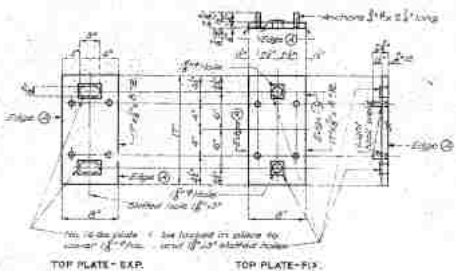
HALF SECTION THRU SPAN HALF ELEVATION AT END BENT



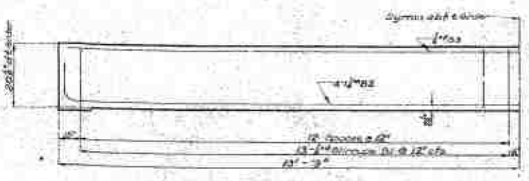
SECTION A-A



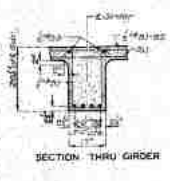
SECTION C-C



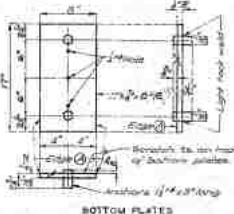
TOP PLATE - EXP. TOP PLATE - P.L.



GIRDER REINFORCEMENT



SECTION THRU GIRDER



DETAILS OF BEARING PLATES

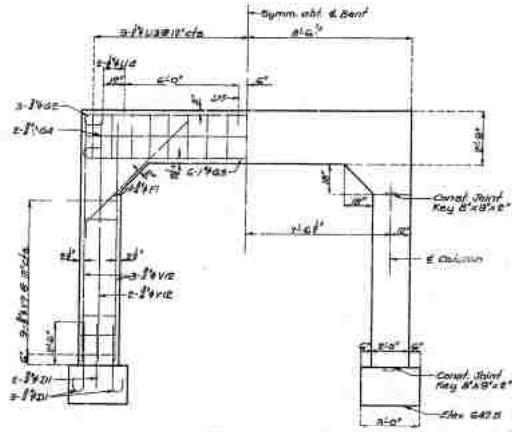
No.	Size	Length	Mark	Location	Bending schedule
10	1/2"	3'-0"	CE		
11	1/2"	3'-0"	CE		
12	1/2"	3'-0"	CE		
13	1/2"	3'-0"	CE		
14	1/2"	3'-0"	CE		
15	1/2"	3'-0"	CE		
16	1/2"	3'-0"	CE		
17	1/2"	3'-0"	CE		
18	1/2"	3'-0"	CE		
19	1/2"	3'-0"	CE		
20	1/2"	3'-0"	CE		
21	1/2"	3'-0"	CE		
22	1/2"	3'-0"	CE		
23	1/2"	3'-0"	CE		
24	1/2"	3'-0"	CE		
25	1/2"	3'-0"	CE		
26	1/2"	3'-0"	CE		
27	1/2"	3'-0"	CE		
28	1/2"	3'-0"	CE		
29	1/2"	3'-0"	CE		
30	1/2"	3'-0"	CE		
31	1/2"	3'-0"	CE		
32	1/2"	3'-0"	CE		
33	1/2"	3'-0"	CE		
34	1/2"	3'-0"	CE		
35	1/2"	3'-0"	CE		
36	1/2"	3'-0"	CE		
37	1/2"	3'-0"	CE		
38	1/2"	3'-0"	CE		
39	1/2"	3'-0"	CE		
40	1/2"	3'-0"	CE		
41	1/2"	3'-0"	CE		
42	1/2"	3'-0"	CE		
43	1/2"	3'-0"	CE		
44	1/2"	3'-0"	CE		
45	1/2"	3'-0"	CE		
46	1/2"	3'-0"	CE		
47	1/2"	3'-0"	CE		
48	1/2"	3'-0"	CE		
49	1/2"	3'-0"	CE		
50	1/2"	3'-0"	CE		
51	1/2"	3'-0"	CE		
52	1/2"	3'-0"	CE		
53	1/2"	3'-0"	CE		
54	1/2"	3'-0"	CE		
55	1/2"	3'-0"	CE		
56	1/2"	3'-0"	CE		
57	1/2"	3'-0"	CE		
58	1/2"	3'-0"	CE		
59	1/2"	3'-0"	CE		
60	1/2"	3'-0"	CE		
61	1/2"	3'-0"	CE		
62	1/2"	3'-0"	CE		
63	1/2"	3'-0"	CE		
64	1/2"	3'-0"	CE		
65	1/2"	3'-0"	CE		
66	1/2"	3'-0"	CE		
67	1/2"	3'-0"	CE		
68	1/2"	3'-0"	CE		
69	1/2"	3'-0"	CE		
70	1/2"	3'-0"	CE		
71	1/2"	3'-0"	CE		
72	1/2"	3'-0"	CE		
73	1/2"	3'-0"	CE		
74	1/2"	3'-0"	CE		
75	1/2"	3'-0"	CE		
76	1/2"	3'-0"	CE		
77	1/2"	3'-0"	CE		
78	1/2"	3'-0"	CE		
79	1/2"	3'-0"	CE		
80	1/2"	3'-0"	CE		
81	1/2"	3'-0"	CE		
82	1/2"	3'-0"	CE		
83	1/2"	3'-0"	CE		
84	1/2"	3'-0"	CE		
85	1/2"	3'-0"	CE		
86	1/2"	3'-0"	CE		
87	1/2"	3'-0"	CE		
88	1/2"	3'-0"	CE		
89	1/2"	3'-0"	CE		
90	1/2"	3'-0"	CE		
91	1/2"	3'-0"	CE		
92	1/2"	3'-0"	CE		
93	1/2"	3'-0"	CE		
94	1/2"	3'-0"	CE		
95	1/2"	3'-0"	CE		
96	1/2"	3'-0"	CE		
97	1/2"	3'-0"	CE		
98	1/2"	3'-0"	CE		
99	1/2"	3'-0"	CE		
100	1/2"	3'-0"	CE		

BRIDGE OVER MYATT CREEK
 STATE ROAD FROM LANTON EAST TO OREGON CO. LINE
 ABOUT 12.3 MILES W. OF THAYER
 PROJECT NO. S-938121 SEC. A (S) STA. 193+42
 HOWELL COUNTY

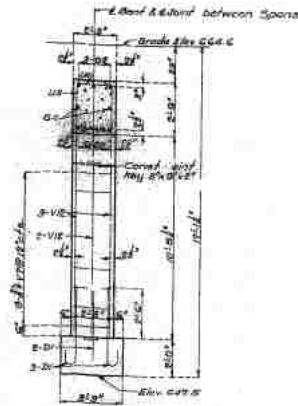
FINISHED
 P-58

MISSOURI STATE HIGHWAY DEPARTMENT

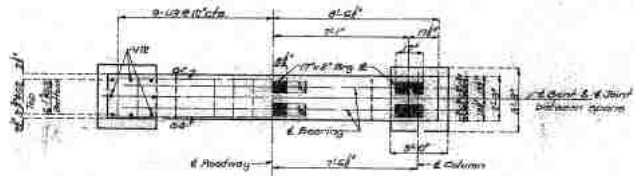
TOT. ROAD DIST. NO.	SECT.	PRO. NO.	FISCAL YEAR	SHEET NO.	TOTAL SHEETS
6	40	2-10771	19		



ELEVATION



SECTION AT E



PLAN

DETAILS OF INTERMEDIATE BENT NO. 4.

BRIDGE OVER MYATT CREEK
 STATE ROAD FROM LANTON EAST TO OREGON CO. LINE
 ABOUT 12.3 MILES W. OF THAYER
 PROJECT NO. 2-93863 SEC. A (150) STA. 193+42
 HOWELL COUNTY

FINISHED
 F-58

Drawn Nov. 1950 by W.L.W.
 Revised Dec. 1950 by W.E.L.
 Checked Feb. 1951 by C.S.E.

Note: This drawing is not to scale. Yellow dimensions.

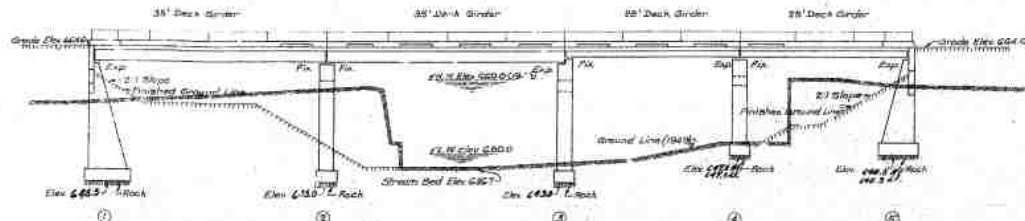
Sheet No. 6 of 6

SEE FINAL PLANS BROWN LINES

MISSOURI STATE HIGHWAY DEPARTMENT

DES. NO.	DATE	BY	CHKD.	SHEET	TOTAL
1	10/20/52	W.H.	H.W.	1	1

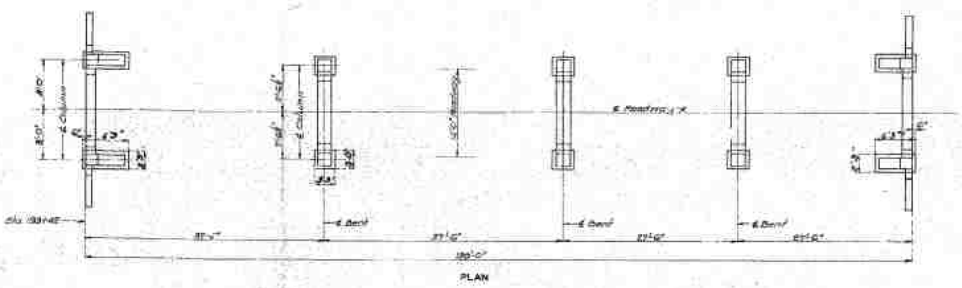
FINAL PLANS



Note: All loose, shelly, or disintegrated rock shall be removed and the surface placed on hard, solid undisturbed rock. If soil rock is not available, the bridge shall be carried on piers of masonry and cast against vertical faces of same. In no case shall piers of same be placed higher than stations shown.

GENERAL ELEVATION

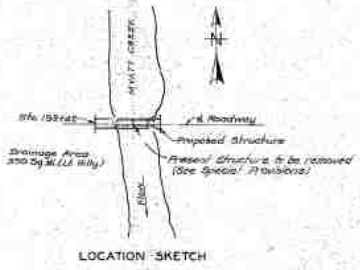
Note: Old roadway, if under water, shall be removed to natural ground line. Excavation for this structure outside limits of excavation for structure will be made of well controlled price for roadway excavation.



PLAN



112



LOCATION SKETCH

FINAL QUANTITIES				
Item	Unit	Substr.	Superstr.	Total
Class 1 Excavation for Structures	Cu. Yds.	59.2		59.2
Class 2 Excavation for Structures	Cu. Yds.	76.2		76.2
Class 2 Concrete (Manholes)	Cu. Yds.		11.0	11.0
Class 2 Concrete (Bench Markers)	Cu. Yds.	36.8	81.8	118.6
Reinforcing Steel	Lbs.	6220	2218	8438
Structural Steel Reinforcing Plates	Lbs.		1680	1680
Structural Steel Reinforcing Bars	Cu. Yds.	0.5	0.6	1.1
Final Total		196.2	208.4	404.6

Note: Excavation for bridge piers shall be to Elev 651.0. Excavation for bridge piers shall be paid for as Class 1 Excavation for Structures. Excavation for bridge piers shall be paid for as Class 2 Excavation for Structures.

COMPLETE BILL OF SUBSTRUCTURE REINFORCING STEEL			
Bar	Size	Length	Weight
1	1/2"	10.0'	1.10
2	1/2"	10.0'	1.10
3	1/2"	10.0'	1.10
4	1/2"	10.0'	1.10
5	1/2"	10.0'	1.10
6	1/2"	10.0'	1.10
7	1/2"	10.0'	1.10
8	1/2"	10.0'	1.10
9	1/2"	10.0'	1.10
10	1/2"	10.0'	1.10
11	1/2"	10.0'	1.10
12	1/2"	10.0'	1.10
13	1/2"	10.0'	1.10
14	1/2"	10.0'	1.10
15	1/2"	10.0'	1.10
16	1/2"	10.0'	1.10
17	1/2"	10.0'	1.10
18	1/2"	10.0'	1.10
19	1/2"	10.0'	1.10
20	1/2"	10.0'	1.10
21	1/2"	10.0'	1.10
22	1/2"	10.0'	1.10
23	1/2"	10.0'	1.10
24	1/2"	10.0'	1.10
25	1/2"	10.0'	1.10
26	1/2"	10.0'	1.10
27	1/2"	10.0'	1.10
28	1/2"	10.0'	1.10
29	1/2"	10.0'	1.10
30	1/2"	10.0'	1.10
31	1/2"	10.0'	1.10
32	1/2"	10.0'	1.10
33	1/2"	10.0'	1.10
34	1/2"	10.0'	1.10
35	1/2"	10.0'	1.10
36	1/2"	10.0'	1.10
37	1/2"	10.0'	1.10
38	1/2"	10.0'	1.10
39	1/2"	10.0'	1.10
40	1/2"	10.0'	1.10
41	1/2"	10.0'	1.10
42	1/2"	10.0'	1.10
43	1/2"	10.0'	1.10
44	1/2"	10.0'	1.10
45	1/2"	10.0'	1.10
46	1/2"	10.0'	1.10
47	1/2"	10.0'	1.10
48	1/2"	10.0'	1.10
49	1/2"	10.0'	1.10
50	1/2"	10.0'	1.10
51	1/2"	10.0'	1.10
52	1/2"	10.0'	1.10
53	1/2"	10.0'	1.10
54	1/2"	10.0'	1.10
55	1/2"	10.0'	1.10
56	1/2"	10.0'	1.10
57	1/2"	10.0'	1.10
58	1/2"	10.0'	1.10
59	1/2"	10.0'	1.10
60	1/2"	10.0'	1.10
61	1/2"	10.0'	1.10
62	1/2"	10.0'	1.10
63	1/2"	10.0'	1.10
64	1/2"	10.0'	1.10
65	1/2"	10.0'	1.10
66	1/2"	10.0'	1.10
67	1/2"	10.0'	1.10
68	1/2"	10.0'	1.10
69	1/2"	10.0'	1.10
70	1/2"	10.0'	1.10
71	1/2"	10.0'	1.10
72	1/2"	10.0'	1.10
73	1/2"	10.0'	1.10
74	1/2"	10.0'	1.10
75	1/2"	10.0'	1.10
76	1/2"	10.0'	1.10
77	1/2"	10.0'	1.10
78	1/2"	10.0'	1.10
79	1/2"	10.0'	1.10
80	1/2"	10.0'	1.10
81	1/2"	10.0'	1.10
82	1/2"	10.0'	1.10
83	1/2"	10.0'	1.10
84	1/2"	10.0'	1.10
85	1/2"	10.0'	1.10
86	1/2"	10.0'	1.10
87	1/2"	10.0'	1.10
88	1/2"	10.0'	1.10
89	1/2"	10.0'	1.10
90	1/2"	10.0'	1.10
91	1/2"	10.0'	1.10
92	1/2"	10.0'	1.10
93	1/2"	10.0'	1.10
94	1/2"	10.0'	1.10
95	1/2"	10.0'	1.10
96	1/2"	10.0'	1.10
97	1/2"	10.0'	1.10
98	1/2"	10.0'	1.10
99	1/2"	10.0'	1.10
100	1/2"	10.0'	1.10

GENERAL NOTES: Design Specifications A.A.C.H. 1948. Loading 110-14. Reinforcing Steel Areas 100000. Class B Concrete Areas 100000. All concrete shall be Class B. Where joint filler is specified on plans it shall conform with the requirements of Section 201.19.14 of the Standard Specifications for Preliminary Manual for Plans.

S.M. 287-48 10/20/52 15' x 14' x 14' 19140
 BRIDGE OVER MYATT CREEK
 STATE ROAD FROM LANTON EAST TO OREGON CO. L. E.
 ABOUT 1.3 MILES E. OF THAYER
 PROJECT NO. 2-236(2)S.C. A (501 STA. 193+42)
 HOWELL COUNTY

DESIGNED BY: W. W. GARDNER 10/20/52
 CHECKED BY: C. W. BROWN 10/20/52
 FINISHED

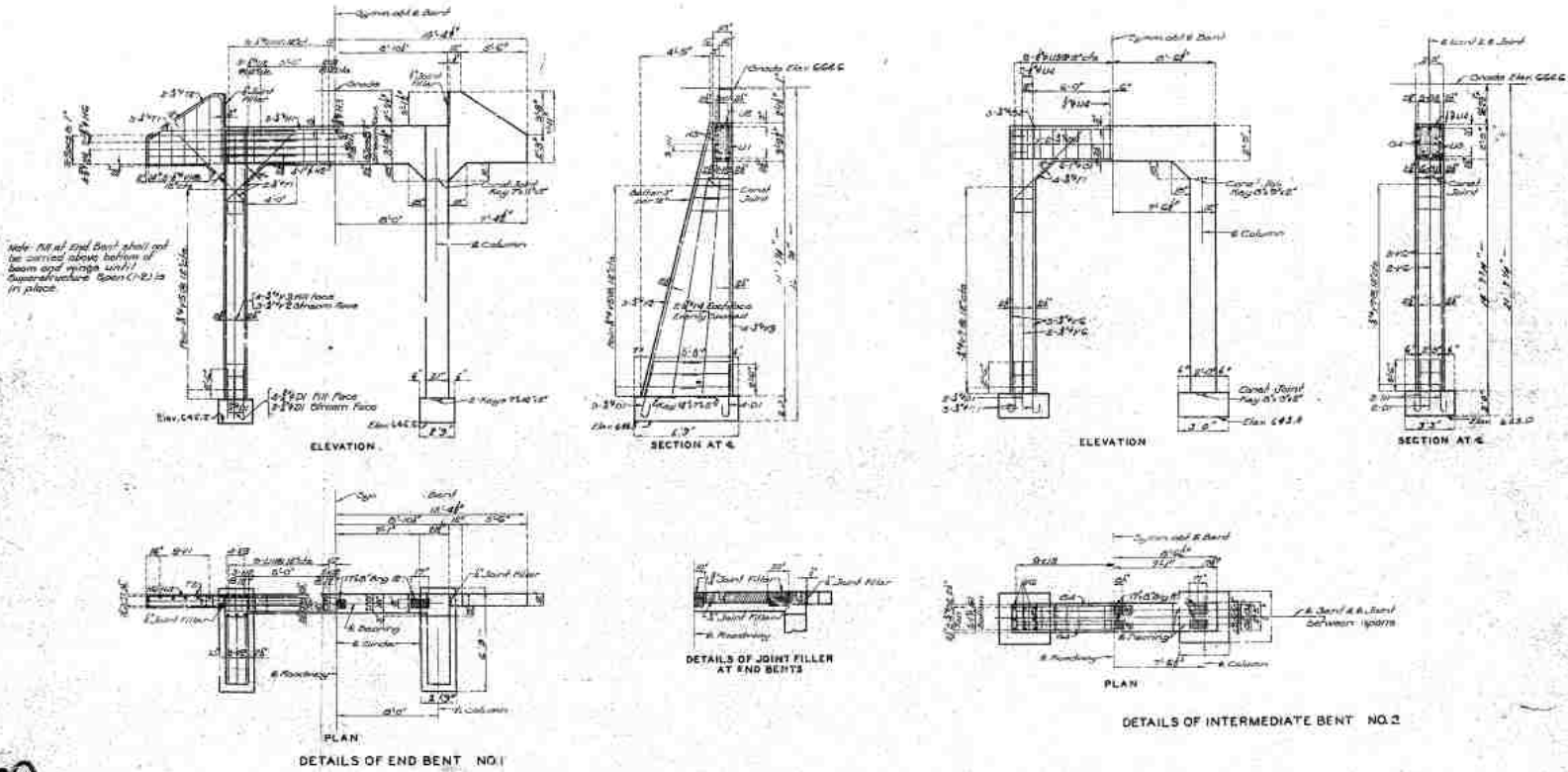
FINISHED	STD. C-2504
FINISHED	STD. C-10. R3
FINISHED	P-58

FINAL PLANS

MISSOURI STATE HIGHWAY DEPARTMENT

DESIGN NO.	DATE	REV. NO.	TOTAL SHEETS	CURRENT SHEET NO.	TOTAL SHEETS
8	8-2-27	10			

FINAL PLANS



113

NOT REV. BY K.L.W.
 DATE NOV. 1930 BY M.E.L.
 CHECKED BY J.P. & C.S.B.

Note: This drawing is not to scale. Full size dimensions.

Sheet No. 2A of 4

BRIDGE OVER MYATT CREEK
 STATE ROAD FROM LANTON EAST TO OREGON CO. LINE
 ABOUT 12.3 MILES W. OF FRAYER
 PROJECT NO. 3-938(2)32; ALSO: STA. 109+42

HOWELL COUNTY

FINISHED

FINISHED

FINISHED

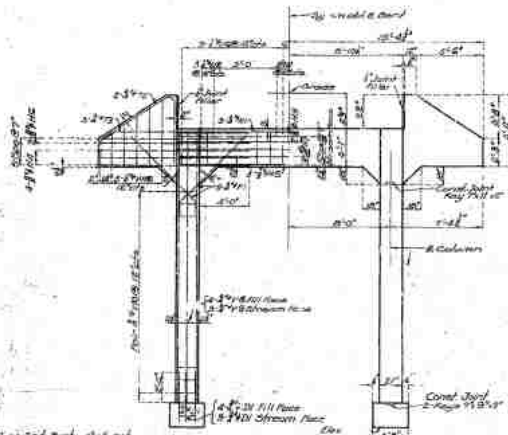
P-58

FINAL PLANS

MISSOURI STATE HIGHWAY DEPARTMENT

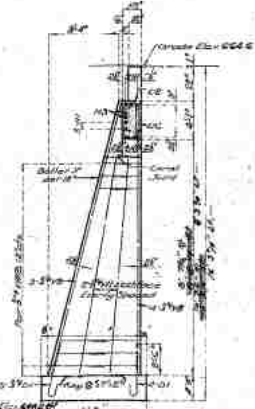
DES. APPR.	DRAWN	CHKD.	INSP.	DATE	SCALE

FINAL PLANS

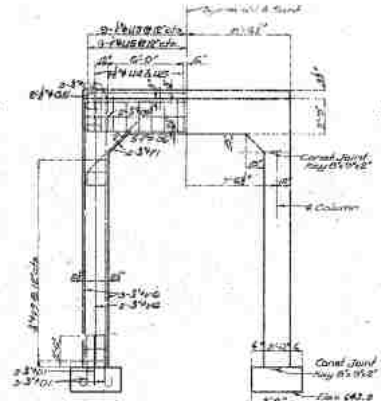


ELEVATION

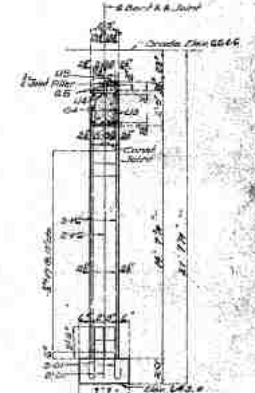
Note: All in End Bent shall not be covered unless bottom pt beam and wings MIN. superstructure spans 20-50 ft in place.



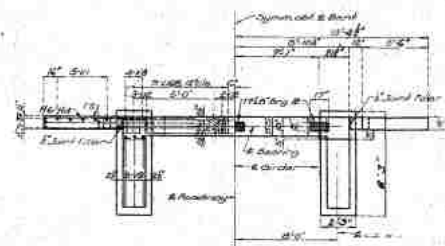
SECTION AT 3



ELEVATION



SECTION AT 4



PLAN
DETAILS OF END BENT NO. 5



DETAILS OF JOINT FILLER AT END BENTS



PLAN
DETAILS OF INTERMEDIATE BENT NO. 3

BRIDGE OVER MYATT CREEK
STATE ROAD FROM LANTON EAST TO OREGON CO. LINE
ABOUT 12.3 MILES W. OF THAYER
PROJECT NO. B-9361P-20CA (50) STA. 192+42
HOWELL COUNTY

FINISHED

FINISHED

FINISHED

P-58

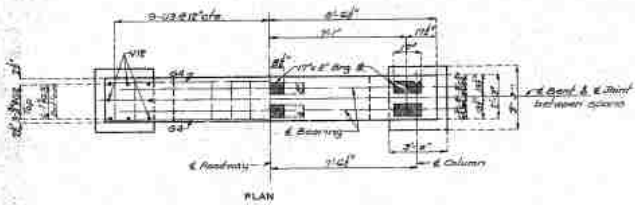
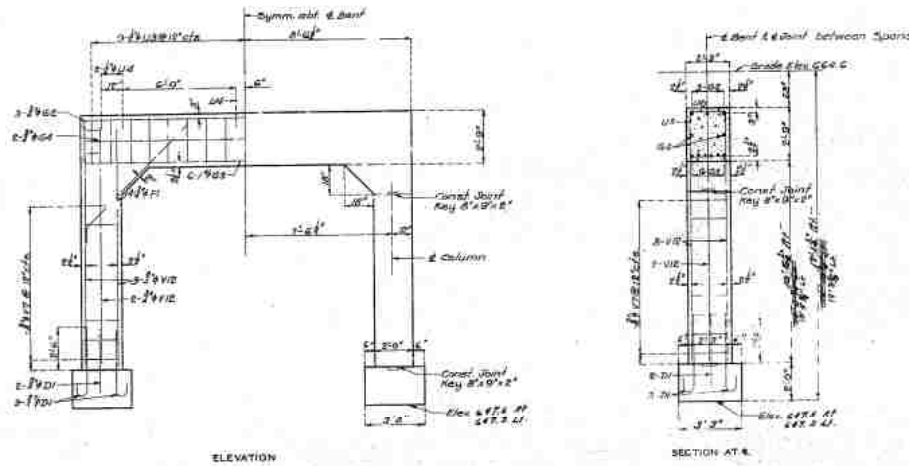
FINAL PLANS

114

MISSOURI STATE HIGHWAY DEPARTMENT

FED. ROAD DIST. NO.	STATE	FED. AID PROJ. NO.	FEDERAL FISCAL YEAR	PROJECT NO.	SHEET NO.	TOTAL SHEETS
1	MO		1954	193	14	

FINAL PLANS



DETAILS OF INTERMEDIATE BENT NO. 4.

115

Drawn Nov. 1950 by W.L.V.
 Checked Dec. 1950 by W.E.L.
 Checked Feb. 1951 by C.S.D.

Note: This drawing is not to scale. Follow dimensions.

Sheet No. C.A. of 4

FINISHED
 FINISHED
 FINISHED

BRIDGE OVER MYATT CREEK
 STATE ROAD FROM LANTON EAST TO OREGON CO. LINE
 ABOUT 12.3 MILES W. OF THAYER
 PROJECT NO. 2-95812; SEC. 1150; STA. 193+42

HOWELL COUNTY

FINISHED

P-58

FINAL PLANS

APPENDIX B.

ANALYSIS OF EXISTING CAPACITY

Bridge P0058 capacity pre-design

Michael Janke
Spring 2018

Short spans, interior girder

$$L := 26.375\text{ft}$$

$$b_w := 17\text{in}$$

$$h_f := 6\text{in}$$

$$b_c := \min\left(b_w + 2.68 \frac{\text{in}}{2} \cdot b_w + 2.8 h_f, \frac{L}{4}\right) = 79.125\text{in}$$

$$h := 20.5\text{in}$$

$$d := h - 2.5\text{in} = 18\text{in}$$

$$f_c := 6000\text{psi}$$

$$\beta_1 := .75$$

$$f_y := 33000\text{psi}$$

$$A_s := 4 \cdot 1.56\text{in}^2 = 6.24\text{in}^2$$

$$a := A_s \cdot \frac{f_y}{.85 f_c \cdot b_c} = 0.51\text{in} < hf, \text{OK}$$

Moment Capacity:

$$M_n := A_s \cdot f_y \cdot \left(d - \frac{a}{2}\right) = 304.502\text{kip}\cdot\text{ft} \quad \phi_m := .9$$

$$\phi_m \cdot M_n = 274.052\text{kip}\cdot\text{ft}$$

$$A_{s_min} := 200 \frac{b_w \cdot d \cdot \text{psi} \cdot \text{in}^2}{\text{in} \cdot f_y \cdot \text{in}} = 1.855\text{in}^2 < A_s, \text{OK}$$

Shear Capacity:

$$A_v := 2 \cdot 2\text{in}^2 = 0.4\text{in}^2$$

$$s := 12\text{in}$$

$$V_c := \frac{2}{1000} \left(\frac{f_c}{\text{psi}}\right)^2 \cdot \frac{1}{\text{in}} \cdot \frac{b_w \cdot d \cdot \text{kip}}{\text{in}} = 47.405\text{kip} \quad \phi_v := .75$$

$$V_s := A_v \cdot f_y \cdot \frac{d}{s} = 19.8\text{kip}$$

$$V_n := V_c + V_s = 67.205\text{kip}$$

$$\phi_v \cdot V_n = 50.404\text{kip}$$

Short spans, exterior girder

$$L := 26.375 \text{ ft}$$

$$b_w := 17 \text{ in}$$

$$h_f := 6 \text{ in}$$

$$b_c := 58 \text{ in}$$

$$h := 20.5 \text{ in}$$

$$d := h - 2.5 \text{ in} = 18 \text{ in}$$

$$f_c := 6000 \text{ psi}$$

$$\beta_1 := .75$$

$$f_y := 33000 \text{ psi}$$

$$A_s := 4 \cdot 1.56 \text{ in}^2 = 6.24 \text{ in}^2$$

$$a := A_s \cdot \frac{f_y}{.85 \cdot f_c \cdot b_c} = 0.696 \text{ in} \quad < h_f, \text{ OK}$$

Moment Capacity:

$$M_n := A_s \cdot f_y \cdot \left(d - \frac{a}{2} \right) = 302.907 \text{ kip} \cdot \text{ft} \quad \phi_m := .9$$

$$\phi_m \cdot M_n = 272.616 \text{ kip} \cdot \text{ft}$$

$$A_{s_min} := 200 \frac{b_w \cdot d \cdot \text{psi} \cdot \text{in}^2}{\text{in} \cdot f_y \cdot \text{in}} = 1.855 \text{ in}^2 \quad < A_s, \text{ OK}$$

Shear Capacity:

$$A_v := 2 \cdot .2 \text{ in}^2 = 0.4 \text{ in}^2$$

$$s := 12 \text{ in}$$

$$V_c := \frac{2}{1000} \cdot \left(\frac{f_c}{\text{psi}} \right)^{\frac{1}{2}} \cdot \frac{b_w \cdot d \cdot \text{kip}}{\text{in} \cdot \text{in}} = 47.405 \text{ kip} \quad \phi_v := .75$$

$$V_s := A_v \cdot f_y \cdot \frac{d}{s} = 19.8 \text{ kip}$$

$$V_n := V_c + V_s = 67.205 \text{ kip}$$

$$\phi_v \cdot V_n = 50.404 \text{ kip}$$

Long spans, interior girder

$$L := 36.1875 \text{ ft}$$

$$b_w := 17 \text{ in}$$

$$h_f := 6 \text{ in}$$

$$b_e := \min\left(b_w + 2 \cdot 68 \frac{\text{in}}{2}, b_w + 2 \cdot 8 \cdot h_f, \frac{L}{4}\right) = 85 \text{ in}$$

$$h := 24 \text{ in}$$

$$d_1 := h - 2.5 \text{ in} = 21.5 \text{ in}$$

$$d_2 := d_1 - 3.75 \text{ in} = 17.75 \text{ in}$$

$$A_{s1} := 4 \cdot 1.56 \text{ in}^2 = 6.24 \text{ in}^2$$

$$A_{s2} := 4 \cdot 1.27 \text{ in}^2 = 5.08 \text{ in}^2$$

$$f_y := 33000 \text{ psi}$$

$$d := \frac{(A_{s1} \cdot f_y \cdot d_1 + A_{s2} \cdot f_y \cdot d_2)}{A_{s1} \cdot f_y + A_{s2} \cdot f_y} = 19.817 \text{ in}$$

$$f_c := 6000 \text{ psi}$$

$$\beta_1 := .75$$

$$a := (A_{s1} + A_{s2}) \frac{f_y}{.85 \cdot f_c \cdot b_e} = 0.862 \text{ in} \quad < hf, \text{ OK}$$

Moment Capacity:

$$M_n := (A_{s1} + A_{s2}) \cdot f_y \cdot \left(d - \frac{a}{2}\right) = 603.495 \cdot \text{kip} \cdot \text{ft} \quad \phi_m := .9$$

$$\phi_m \cdot M_n = 543.145 \cdot \text{kip} \cdot \text{ft}$$

$$A_{s_min} := 200 \frac{b_w \cdot d \cdot \text{psi} \cdot \text{in}^2}{\text{in} \cdot f_y \cdot \text{in}} = 2.042 \text{ in}^2 \quad < A_s, \text{ OK}$$

Shear Capacity:

$$A_v := 2 \cdot .2 \text{ in}^2 = 0.4 \text{ in}^2$$

$$s := 15 \text{ in}$$

$$V_c := \frac{2}{1000} \left(\frac{f_c}{\text{psi}}\right)^{\frac{1}{2}} \frac{b_w \cdot d \cdot \text{kip}}{\text{in} \cdot \text{in}} = 52.191 \cdot \text{kip} \quad \phi_v := .75$$

$$V_s := A_v \cdot f_y \cdot \frac{d}{s} = 17.439 \cdot \text{kip}$$

$$V_n := V_c + V_s = 69.63 \cdot \text{kip}$$

$$\phi_v \cdot V_n = 52.223 \cdot \text{kip}$$

Long spans, exterior girder

$$L := 36,1875 \text{ ft}$$

$$b_w := 17 \text{ in}$$

$$h_f := 6 \text{ in}$$

$$b_e := 61 \text{ in}$$

$$h := 24 \text{ in}$$

$$d_1 := h - 2.5 \text{ in} = 21.5 \text{ in} \quad d_2 := d_1 - 3.75 \text{ in} = 17.75 \text{ in}$$

$$A_{s1} := 4 \cdot 1.56 \text{ in}^2 = 6.24 \text{ in}^2 \quad A_{s2} := 4 \cdot 1.27 \text{ in}^2 = 5.08 \text{ in}^2$$

$$f_y := 33000 \text{ psi} \quad d := \frac{(A_{s1} \cdot f_y \cdot d_1 + A_{s2} \cdot f_y \cdot d_2)}{A_{s1} \cdot f_y + A_{s2} \cdot f_y} = 19.817 \text{ in}$$

$$f_c := 6000 \text{ psi}$$

$$\beta_1 := .75$$

$$a := (A_{s1} + A_{s2}) \frac{f_y}{.85 \cdot f_c \cdot b_e} = 1.201 \text{ in} \quad < h_f, \text{ OK}$$

Moment Capacity:

$$M_n := (A_{s1} + A_{s2}) \cdot f_y \cdot \left(d - \frac{a}{2} \right) = 598.217 \cdot \text{kip} \cdot \text{ft} \quad \phi_m := .9$$

$$\phi_m \cdot M_n = 538.396 \cdot \text{kip} \cdot \text{ft}$$

$$A_{s_min} := 200 \frac{b_w \cdot d \cdot \text{psi} \cdot \text{in}^2}{\text{in} \cdot f_y \cdot \text{in}} = 2.042 \cdot \text{in}^2 \quad < A_s, \text{ OK}$$

Shear Capacity:

$$A_v := 2 \cdot 2 \text{ in}^2 = 0.4 \text{ in}^2$$

$$s := 15 \text{ in}$$

$$V_c := \frac{2}{1000} \cdot \left(\frac{f_c}{\text{psi}} \right)^{\frac{1}{2}} \cdot \frac{b_w \cdot d \cdot \text{kip}}{\text{in} \cdot \text{in}} = 52.191 \cdot \text{kip} \quad \phi_v := .75$$

$$V_s := A_v \cdot f_y \cdot \frac{d}{s} = 17.439 \cdot \text{kip}$$

$$V_n := V_c + V_s = 69.63 \cdot \text{kip}$$

$$\phi_v \cdot V_n = 52.223 \cdot \text{kip}$$

APPENDIX C.

PARAMETRIC STUDY OF FLEXURAL STRENGTHENING

Moment Capacity Parametric (12 inch width)			Long Spans	Short Spans
Unstrengthened			543.15	274.05
FRCM-PBO	1 Ply	New ϕM_n	548.975	278.902
		% increase	1.07%	1.77%
	2 Ply	New ϕM_n	558.994	286.871
		% increase	2.92%	4.68%
	3 Ply	New ϕM_n	569.008	294.84
		% increase	4.76%	7.59%
	4 Ply	New ϕM_n	579.018	302.798
		% increase	6.60%	10.49%
FRCM-Carbon	1 Ply	New ϕM_n	551.224	283.09
		% increase	1.49%	3.30%
	2 Ply	New ϕM_n	565.459	295.245
		% increase	4.11%	7.73%
	3 Ply	New ϕM_n	579.685	307.384
		% increase	6.73%	12.16%
	4 Ply	New ϕM_n	593.905	319.518
		% increase	9.35%	16.59%
SRG	1 Ply	New ϕM_n	538.136	274.679
		% increase	-0.92%	0.23%
	2 Ply	New ϕM_n	543.491	280.136
		% increase	0.06%	2.22%
	3 Ply	New ϕM_n	548.849	285.585
		% increase	1.05%	4.21%
	4 Ply	New ϕM_n	554.206	291.032
		% increase	2.04%	6.20%
CFRP	1 Ply	New ϕM_n	585.397	309.759
		% increase	7.78%	13.03%
	2 Ply	New ϕM_n	608.884	333.596
		% increase	12.10%	21.73%
	3 Ply	New ϕM_n	623.38	346.835
		% increase	14.77%	26.56%
	4 Ply	New ϕM_n	635.661	357.986
		% increase	17.03%	30.63%

Moment Capacity Parametric (17 inch width)			Long Spans	Short Spans
Unstrengthened			543.15	274.05
FRCM-PBO	1 Ply	New ϕM_n	553.143	282.22
		% increase	1.84%	2.98%
	2 Ply	New ϕM_n	567.336	293.513
		% increase	4.45%	7.10%
	3 Ply	New ϕM_n	581.525	304.79
		% increase	7.07%	11.22%
	4 Ply	New ϕM_n	595.693	316.062
		% increase	9.67%	15.33%
FRCM-Carbon	1 Ply	New ϕM_n	557.156	288.153
		% increase	2.58%	5.15%
	2 Ply	New ϕM_n	577.319	305.369
		% increase	6.29%	11.43%
	3 Ply	New ϕM_n	597.456	322.55
		% increase	10.00%	17.70%
	4 Ply	New ϕM_n	617.584	339.721
		% increase	13.71%	23.96%
SRG	1 Ply	New ϕM_n	548.541	276.952
		% increase	0.99%	1.06%
	2 Ply	New ϕM_n	560.77	284.675
		% increase	3.24%	3.88%
	3 Ply	New ϕM_n	572.996	292.391
		% increase	5.50%	6.69%
	4 Ply	New ϕM_n	585.218	300.105
		% increase	7.75%	9.51%
CFRP*	1 Ply	New ϕM_n	605.384	325.909
		% increase	11.46%	18.92%
	2 Ply	New ϕM_n	639.411	359.866
		% increase	17.72%	31.31%
	3 Ply	New ϕM_n	660.582	378.857
		% increase	21.62%	38.24%
	4 Ply	New ϕM_n	678.447	394.813
		% increase	24.91%	44.07%

(Highlight = chosen for final design)

*for CFRP, 15 in. (381 mm) strips were used

Bridge P0058 CFRP Design

Michael Janke
Spring 2018

Long spans, interior girder

$$L := 36.1875 \text{ ft}$$

$$b_w := 17 \text{ in}$$

$$h_f := 6 \text{ in}$$

$$b_e := \min\left(b_w + 2 \cdot 68 \frac{\text{in}}{2}, b_w + 2 \cdot 8 \cdot h_f, \frac{L}{4}\right) = 85 \text{ in}$$

$$h := 24 \text{ in}$$

$$d_1 := h - 2.5 \text{ in} = 21.5 \text{ in} \quad d_2 := d_1 - 3.75 \text{ in} = 17.75 \text{ in}$$

$$A_{s1} := 4 \cdot 1.56 \text{ in}^2 = 6.24 \text{ in}^2 \quad A_{s2} := 4 \cdot 1.27 \text{ in}^2 = 5.08 \text{ in}^2$$

$$f_y := 33000 \text{ psi} \quad d := \frac{(A_{s1} \cdot f_y \cdot d_1 + A_{s2} \cdot f_y \cdot d_2)}{A_{s1} \cdot f_y + A_{s2} \cdot f_y} = 19.817 \text{ in}$$

$$f_c := 6000 \text{ psi}$$

$$A_s := A_{s1} + A_{s2} = 11.32 \text{ in}^2$$

$$\beta_1 := .75$$

$$a_0 := (A_{s1} + A_{s2}) \cdot \frac{f_y}{.85 \cdot f_c \cdot b_e} = 0.862 \text{ in} \quad < h_f, \text{ OK}$$

Moment Capacity before strengthening:

$$M_{ns0} := (A_{s1} + A_{s2}) \cdot f_y \cdot \left(d - \frac{a_0}{2}\right) = 603.495 \text{ kip} \cdot \text{ft} \quad \phi_f := .9$$

$$\phi_f \cdot M_{ns0} = 543.145 \text{ kip} \cdot \text{ft}$$

$$A_{s_min} := 200 \frac{b_w}{\text{in}} \cdot \frac{d \cdot \text{psi} \cdot \text{in}^2}{f_y \cdot \text{in}} = 2.042 \text{ in}^2 \quad < A_s, \text{ OK}$$

Shear Capacity before strengthening:

$$A_v := 2 \cdot 2 \text{ in}^2 = 0.4 \text{ in}^2$$

$$s := 15 \text{ in}$$

$$V_c := \frac{2}{1000} \cdot \left(\frac{f_c}{\text{psi}}\right)^2 \cdot \frac{b_w}{\text{in}} \cdot \frac{d \cdot \text{kip}}{\text{in}} = 52.191 \text{ kip} \quad \phi_v := .75$$

$$V_s := A_v \cdot f_y \cdot \frac{d}{s} = 17.439 \text{ kip}$$

$$V_n := V_c + V_s = 69.63 \text{ kip}$$

$$\phi_v \cdot V_n = 52.223 \text{ kip}$$

Fiber Properties

Carbon FRP 5 bridges properties

$$\begin{aligned}
 t_f &:= .0065 \text{ in} & f_{fu0} &:= 550 \text{ ksi} & \varepsilon_{fu0} &:= .0167 \frac{\text{in}}{\text{in}} & E_f &:= 33000 \text{ ksi} & C_E &:= .85 \\
 w_f &:= 15 \text{ in} & f_{fu} &:= C_E \cdot f_{fu0} = 467.5 \text{ ksi} & \varepsilon_{fu} &:= C_E \cdot \varepsilon_{fu0} = 0.014 \\
 n_f &:= 2 \\
 A_f &:= n_f \cdot w_f \cdot t_f = 0.195 \cdot \text{in}^2 & d_f &:= h = 24 \text{ in}
 \end{aligned}$$

Preliminary calcs

$$\begin{aligned}
 \beta_1 &:= .75 & E_c &:= 57000 \cdot (6000)^{.5} \cdot \text{psi} = 4.415 \times 10^6 \cdot \text{psi} & M_{DL} &:= 197.3 \text{ kip ft} \\
 E_s &:= 29000000 \text{ psi}
 \end{aligned}$$

Design

$$\rho := \frac{A_s}{b_w d} = 0.034 \quad n := \frac{E_s}{E_c} = 6.568 \quad k := \left[2 \cdot \rho n + (\rho n)^2 \right]^{.5} - \rho n = 0.479$$

$$I_{cr} := n \cdot A_s \cdot (d - k \cdot d)^2 + \frac{b_w (k \cdot d)^3}{3} = 1.277 \times 10^4 \cdot \text{in}^4$$

Existing Strain on soffit

$$\varepsilon_{bi} := M_{DL} \cdot \frac{(d_f - k \cdot d)}{I_{cr} E_c} = 6.088 \times 10^{-4}$$

Strain on FRP system

$$\varepsilon_{fd1} := .083 \text{ in}^{.5} \cdot \left(\frac{f_c}{n_f E_f t_f} \right)^{.5} = 9.816 \times 10^{-3} \quad \varepsilon_{fd2} := .9 \cdot \varepsilon_{fu} = 0.013$$

$$\varepsilon_{fd} := \min(\varepsilon_{fd1}, \varepsilon_{fd2}) = 9.816 \times 10^{-3}$$

Depth to N.A

$$c := 2.209 \text{ in} \quad \text{*change c here in iterations}$$

Effective strain in FRP and Concrete

$$\varepsilon_{fe1} := .003 \left[\frac{(d_f - c)}{c} \right] = \varepsilon_{bi} = 0.029 \quad \varepsilon_{fe2} := \varepsilon_{fd} = 9.816 \times 10^{-3}$$

$$\varepsilon_{fe} := \min(\varepsilon_{fe1}, \varepsilon_{fe2}) = 9.816 \times 10^{-3} \quad \varepsilon_c := (\varepsilon_{fe} + \varepsilon_{bi}) \cdot \frac{c}{d_f - c} = 1.057 \times 10^{-3}$$

Strain in Steel

$$\varepsilon_s := (\varepsilon_{fc} + \varepsilon_{bi}) \cdot \frac{(d - c)}{d_f - c} = 8.424 \times 10^{-3}$$

Stress in Steel and FRP

$$f_{s1} := E_s \cdot \varepsilon_s = 244.282 \text{ ksi} \quad f_{s2} := f_y = 33 \text{ ksi}$$

$$f_s := \min(f_{s1}, f_{s2}) = 33 \text{ ksi}$$

$$f_{fe} := \min(E_f \cdot \varepsilon_{fe}, f_{fu}) = 323.921 \text{ ksi}$$

Calculate internal force resultants and check equilibrium

$$\varepsilon_c := 1.7 \cdot \frac{f_c}{E_c} = 2.31 \times 10^{-3} \quad \beta_1 := \frac{(4 \cdot \varepsilon_c' - \varepsilon_c)}{6 \cdot \varepsilon_c' - 2 \cdot \varepsilon_c} = 0.697 \quad \alpha_1 := \frac{3 \cdot \varepsilon_c' \cdot \varepsilon_c - \varepsilon_c^2}{(3 \cdot \beta_1 \cdot \varepsilon_c')^2} = 0.556$$

$$c = 2.209 \text{ in} \quad c' := \frac{(A_s \cdot f_s + A_f \cdot f_{fe})}{\alpha_1 \cdot \beta_1 \cdot f_c \cdot b_c} = 2.209 \text{ in} \quad \text{*iterate to force } c=c'$$

Calculate flexural strength components

$$a := \beta_1 \cdot c = 1.539 \text{ in} < hf, \text{ O.K.}$$

$$M_{ns} := A_s \cdot f_s \cdot \left(d - \frac{a}{2} \right) = 592.954 \text{ kip}\cdot\text{ft}$$

$$M_{nf} := A_f \cdot f_{fe} \cdot \left(d_f - \beta_1 \cdot \frac{c}{2} \right) = 122.279 \text{ kip}\cdot\text{ft} \quad \psi_f := .85$$

$$\phi M_n := \phi_f (M_{ns} + \psi_f M_{nf}) = 627.202 \text{ kip}\cdot\text{ft} \quad \frac{(\phi M_n - \phi_f M_{ns0}) \cdot 100}{(\phi_f M_{ns0})} = 15.476$$

Check service stress in FRP and Steel

$$\rho_f := \frac{A_f}{b_w \cdot d} = 5.788 \times 10^{-4}$$

$$k := \left[\left(\rho_f \frac{E_f}{E_c} + \rho \frac{E_s}{E_c} \right)^2 + 2 \cdot \left(\rho_f \frac{E_f \cdot d_f}{E_c \cdot d} + \rho \frac{E_s}{E_c} \right) \right]^{.5} - \left(\rho_f \frac{E_f}{E_c} + \rho \frac{E_s}{E_c} \right) = 0.484$$

$$M_s := 383.9 \text{ kip}\cdot\text{ft} \quad (\text{anticipated service moment})$$

$$f_{ss} := \frac{\left[M_s + \varepsilon_{bi} \cdot A_f \cdot E_f \cdot \left(d_f - k \cdot \frac{d}{3} \right) \right] \cdot (d - k \cdot d) \cdot E_s}{A_s \cdot E_s \cdot \left(d - k \cdot \frac{d}{3} \right) \cdot (d - k \cdot d) + A_f \cdot E_f \cdot \left(d_f - k \cdot \frac{d}{3} \right) \cdot (d_f - k \cdot d)} = 24.085 \text{ ksi}$$

$$.8 \cdot f_y = 26.4 \text{ ksi} > f_{ss}, \text{ O.K.}$$

Check creep rupture limit at service of the FRP

$$f_{fs} := \left[\frac{E_f (d_f - k \cdot d)}{E_s (d - k \cdot d)} \right] \cdot \epsilon_{bf} \cdot E_f = 18.527 \cdot \text{ksi} \quad < \quad .55 \cdot f_{tu} = 257.125 \cdot \text{ksi}$$

stress is well below limit

Shear Design: 3S2 Truck

$$V_u := 57.13 \text{ kip}$$

$$\epsilon_{fv} := \min(\epsilon_{fd}, .004) = 4 \times 10^{-3}$$

$$n_v := 1$$

$$f_{fv} := \epsilon_{fv} \cdot E_f = 132 \cdot \text{ksi}$$

$$d_f := h - h_f = 18 \text{ in}$$

$$t_f = 6.5 \times 10^{-3} \cdot \text{in}$$

$$s_f := 24 \text{ in}$$

$$w_f := 12 \text{ in}$$

$$A_{fv} := 2 \cdot n_v \cdot t_f \cdot w_f = 0.156 \cdot \text{in}^2$$

$$V_f := A_{fv} \cdot f_{fv} \cdot \frac{d_f}{s_f} = 15.444 \cdot \text{kip}$$

$$\phi_{vn} := \phi_v (V_c + V_s + V_f) = 63.806 \cdot \text{kip} > V_u$$

Check limit on FRCM and Steel

$$8 \cdot f_c^{.5} \cdot \text{psi}^{.5} \cdot b_w \cdot d = 208.764 \cdot \text{kip}$$

$$V_s + V_f = 32.883 \cdot \text{kip} \quad < \text{limit, O.K.}$$

Check limit on FRCM

$$V_{n_new} := V_n + V_f = 85.074 \cdot \text{kip}$$

$$.5 \cdot V_{n_new} = 42.537 \cdot \text{kip} \quad > V_f, \text{ O.K.}$$

Bridge P0058 C-FRCM Design

Michael Janke
Spring 2018

Long spans, interior girder

$$L := 36.1875 \text{ ft}$$

$$b_w := 17 \text{ in}$$

$$h_f := 6 \text{ in}$$

$$b_e := \min\left(b_w + 2.68 \frac{\text{in}}{2}, b_w + 2.8 \cdot h_f \cdot \frac{L}{4}\right) = 85 \text{ in}$$

$$h := 24 \text{ in}$$

$$d_1 := h - 2.5 \text{ in} = 21.5 \text{ in}$$

$$d_2 := d_1 - 3.75 \text{ in} = 17.75 \text{ in}$$

$$A_{s1} := 4 \cdot 1.56 \text{ in}^2 = 6.24 \text{ in}^2$$

$$A_{s2} := 4 \cdot 1.27 \text{ in}^2 = 5.08 \text{ in}^2$$

$$f_y := 33000 \text{ psi}$$

$$d := \frac{(A_{s1} \cdot f_y \cdot d_1 + A_{s2} \cdot f_y \cdot d_2)}{A_{s1} \cdot f_y + A_{s2} \cdot f_y} = 19.817 \text{ in}$$

$$f_c := 6000 \text{ psi}$$

$$A_s := A_{s1} + A_{s2} = 11.32 \text{ in}^2$$

$$\beta_1 := .75$$

$$a_0 := (A_{s1} + A_{s2}) \cdot \frac{f_y}{.85 \cdot f_c \cdot b_e} = 0.862 \text{ in} \quad < h_f, \text{ OK}$$

Moment Capacity before strengthening:

$$M_{ns0} := (A_{s1} + A_{s2}) \cdot f_y \cdot \left(d - \frac{a_0}{2}\right) = 603.495 \cdot \text{kip} \cdot \text{ft} \quad \phi_f := .9$$

$$\phi_f \cdot M_{ns0} = 543.145 \cdot \text{kip} \cdot \text{ft}$$

$$A_{s_min} := 200 \frac{b_w}{\text{in}} \cdot \frac{d \cdot \text{psi} \cdot \text{in}^2}{f_y \cdot \text{in}} = 2.042 \cdot \text{in}^2 \quad < A_s, \text{ OK}$$

Shear Capacity before strengthening:

$$A_v := 2 \cdot 2 \text{ in}^2 = 0.4 \text{ in}^2$$

$$s := 15 \text{ in}$$

$$V_c := \frac{2}{1000} \left(\frac{f_c}{\text{psi}}\right)^2 \cdot \frac{b_w}{\text{in}} \cdot \frac{d \cdot \text{kip}}{\text{in}} = 52.191 \cdot \text{kip} \quad \phi_v := .75$$

$$V_s := A_v \cdot f_y \cdot \frac{d}{s} = 17.439 \cdot \text{kip}$$

$$V_n := V_c + V_s = 69.63 \cdot \text{kip}$$

$$\phi_v \cdot V_n = 52.223 \cdot \text{kip}$$

Fiber Properties Carbon FRCM

$$t_f := .00618 \text{ in} \quad f_{fu0} := 202.2 \text{ ksi} \quad \epsilon_{fu0} := .0164 \frac{\text{in}}{\text{in}} \quad E_f := 9210 \text{ ksi} \quad C_E := 1$$

$$w_f := 17 \text{ in} \quad f_{fu} := C_E \cdot f_{fu0} = 202.2 \text{ ksi} \quad \epsilon_{fu} := C_E \cdot \epsilon_{fu0} = 0.016$$

$$n_f := 2$$

$$A_f := n_f \cdot w_f \cdot t_f = 0.21 \cdot \text{in}^2 \quad d_f := h = 24 \text{ in}$$

Preliminary calcs

$$\beta_1 := .75 \quad E_c := 57000 \cdot (6000)^5 \text{ psi} = 4.415 \times 10^6 \text{ psi} \quad M_{DL} := 197.3 \text{ kip} \cdot \text{ft}$$

$$E_s := 29000000 \text{ psi}$$

Design

$$\rho := \frac{A_s}{b_w \cdot d} = 0.034 \quad n := \frac{E_s}{E_c} = 6.568 \quad k := \left[2 \cdot \rho \cdot n + (\rho \cdot n)^2 \right]^{.5} - \rho \cdot n = 0.479$$

$$I_{cr} := n \cdot A_s \cdot (d - k \cdot d)^2 + \frac{b_w \cdot (k \cdot d)^3}{3} = 1.277 \times 10^4 \cdot \text{in}^4$$

Existing Strain on soffit

$$\epsilon_{bi} := M_{DL} \cdot \frac{(d_f - k \cdot d)}{I_{cr} \cdot E_c} = 6.088 \times 10^{-4}$$

Strain on FRP system

$$\epsilon_{fd} := \epsilon_{fu} - .0043 = 0.012$$

STD from Nani

Depth to N.A

$$c := 1.9285 \text{ in} \quad \text{*change c here in iterations}$$

Effective strain in FRP and Concrete

$$\epsilon_{fc1} := .003 \left[\frac{(d_f - c)}{c} \right] = \epsilon_{bi} = 0.034$$

$$\epsilon_{fc2} := \epsilon_{fd} = 0.012$$

$$\epsilon_{fc} := \min(\epsilon_{fc1}, \epsilon_{fc2}, .12) = 0.012$$

$$\epsilon_c := (\epsilon_{fc} + \epsilon_{bi}) \cdot \frac{c}{d_f - c} = 1.11 \times 10^{-3}$$

Strain in Steel

$$\epsilon_s := (\epsilon_{fc} + \epsilon_{bi}) \cdot \frac{(d - c)}{d_f - c} = 0.01$$

Stress in Steel and FRP

$$f_{s1} := E_s \cdot \epsilon_s = 298.708 \text{ ksi} \quad f_{s2} := f_y = 33 \text{ ksi}$$

$$f_s := \min(f_{s1}, f_{s2}) = 33 \text{ ksi}$$

$$f_{fe} := \min(E_f \cdot \epsilon_{fe}, f_{fu}) = 111.441 \text{ ksi}$$

Calculate internal force resultants and check equilibrium

$$\epsilon_c := 1.7 \cdot \frac{f_c}{E_c} = 2.31 \times 10^{-3} \quad \beta_1 := \frac{(4 \cdot \epsilon_c - \epsilon_c)}{6 \cdot \epsilon_c - 2 \cdot \epsilon_c} = 0.698 \quad \alpha_1 := \frac{3 \cdot \epsilon_c \cdot \epsilon_c - \epsilon_c^2}{(3 \cdot \beta_1 \cdot \epsilon_c^2)} = 0.578$$

$$c = 1.929 \text{ in} \quad c' := \frac{(A_s \cdot f_s + A_f \cdot f_{fe})}{\alpha_1 \cdot \beta_1 \cdot \rho \cdot b \cdot c} = 1.928 \text{ in} \quad \text{*iterate to force } c=c'$$

Calculate flexural strength components

$$M_{ns} := A_s \cdot f_s \cdot \left(d - \frac{a}{2} \right) = 595.942 \text{ kip} \cdot \text{ft}$$

$$a := \beta_1 \cdot c = 1.347 \text{ in} < hf, \text{ O.K.}$$

$$M_{nf} := A_f \cdot f_{fe} \cdot \left(d_f - \beta_1 \cdot \frac{c}{2} \right) = 45.518 \text{ kip} \cdot \text{ft}$$

$$\psi_f := 1$$

$$\phi M_n := \phi_f (M_{ns} + \psi_f M_{nf}) = 577.313 \text{ kip} \cdot \text{ft}$$

$$\frac{(\phi M_n - \phi_f M_{ns0}) \cdot 100}{(\phi_f M_{ns0})} = 6.291$$

Check service stress in FRP and Steel

$$\rho_f := \frac{A_f}{b_w \cdot d} = 6.237 \times 10^{-4}$$

$$k := \left[\left(\rho_f \frac{E_f}{E_c} + \rho \frac{E_s}{E_c} \right)^2 + 2 \cdot \left(\rho_f \frac{E_f d_f}{E_c \cdot d} + \rho \frac{E_s}{E_c} \right) \right]^{.5} - \left(\rho_f \frac{E_f}{E_c} + \rho \frac{E_s}{E_c} \right) = 0.481$$

$$M_s := 383.9 \text{ kip} \cdot \text{ft} (\text{anticipated service moment})$$

$$f_{ss} := \frac{\left[\left[M_s + \epsilon_{bi} \cdot A_f \cdot E_f \cdot \left(d_f - k \cdot \frac{d}{3} \right) \right] \cdot (d - k \cdot d) \cdot E_s \right]}{A_s \cdot E_s \cdot \left(d - k \cdot \frac{d}{3} \right) \cdot (d - k \cdot d) + A_f \cdot E_f \cdot \left(d_f - k \cdot \frac{d}{3} \right) \cdot (d_f - k \cdot d)} = 24.332 \text{ ksi}$$

$$.8 \cdot f_y = 26.4 \text{ ksi} > f_{ss}, \text{ O.K.}$$

Check creep rupture limit at service of the FRP

$$f_{fs} := \left[f_{ss} \frac{E_f (d_f - k \cdot d)}{E_g (d - k \cdot d)} \right] = \epsilon_{bi} E_f = 5.262 \text{ ksi} < .55 \cdot f_{fu} = 111.21 \text{ ksi}$$

stress is well below limit

Shear Design: 3S2 Truck

$$V_u := 57.13 \text{ kip}$$

$$\epsilon_{fv} := \min(\epsilon_{fd}, .004) = 4 \times 10^{-3}$$

$$f_{fv} := \epsilon_{fv} \cdot E_f = 36.84 \text{ ksi}$$

$$n_v := 1$$

$$d_f := h - h_f = 18 \text{ in}$$

$$t_f = 6.18 \times 10^{-3} \text{ in}$$

$$s_f := 12 \text{ in}$$

$$w_f := 12 \text{ in}$$

$$A_{fv} := 2 \cdot n_v \cdot t_f \cdot w_f = 0.148 \text{ in}^2$$

$$V_f := A_{fv} \cdot f_{fv} \cdot \frac{d_f}{s_f} = 8.196 \text{ kip}$$

$$\phi_{vn} := \phi_v \cdot (V_c + V_s + V_f) = 58.37 \text{ kip} > V_u$$

Check limit on FRCM and Steel

$$8 \cdot f_c \cdot S \cdot \text{psi} \cdot b_w \cdot d = 208.764 \text{ kip}$$

$$V_s + V_f = 25.635 \text{ kip} < \text{limit, O.K.}$$

Check limit on FRCM

$$V_{n_new} := V_n + V_f = 77.826 \text{ kip}$$

$$.5 \cdot V_{n_new} = 38.913 \text{ kip} > V_f \text{ O.K.}$$

Bridge P0058 PBO Design

Short spans, interior girder

$$L := 26.375 \text{ ft}$$

$$b_w := 17 \text{ in}$$

$$h_f := 6 \text{ in}$$

$$b_e := \min\left(b_w + 2.68 \frac{\text{in}}{2}, b_w + 2.8 \cdot h_f, \frac{L}{4}\right) = 79.125 \text{ in}$$

$$h := 20.5 \text{ in}$$

$$d := h - 2.5 \text{ in} = 18 \text{ in}$$

$$f_c := 6000 \text{ psi}$$

$$\beta_1 := .75$$

$$f_y := 33000 \text{ psi}$$

$$A_s := 4 \cdot 1.56 \text{ in}^2 = 6.24 \text{ in}^2$$

$$a := A_s \frac{f_y}{.85 \cdot f_c \cdot b_e} = 0.51 \text{ in} \quad < h_f, \text{ OK}$$

Moment Capacity before strengthening:

$$M_{ns0} := A_s \cdot f_y \cdot \left(d - \frac{a}{2}\right) = 304.502 \text{ kip} \cdot \text{ft} \quad \phi_f := .9$$

$$\phi_f \cdot M_{ns0} = 274.052 \text{ kip} \cdot \text{ft}$$

$$A_{s_min} := 200 \frac{b_w}{\text{in}} \cdot \frac{d \cdot \text{psi} \cdot \text{in}^2}{f_y \cdot \text{in}} = 1.855 \text{ in}^2 \quad < A_s, \text{ OK}$$

Shear Capacity before strengthening:

$$A_v := 2 \cdot 2 \text{ in}^2 = 0.4 \text{ in}^2$$

$$s := 12 \text{ in}$$

$$V_c := \frac{2}{1000} \left(\frac{f_c}{\text{psi}}\right)^{\frac{1}{2}} \cdot \frac{b_w}{\text{in}} \cdot \frac{d \cdot \text{kip}}{\text{in}} = 47.405 \text{ kip} \quad \phi_v := .75$$

$$V_s := A_v \cdot f_y \cdot \frac{d}{s} = 19.8 \text{ kip}$$

$$V_n := V_c + V_s = 67.205 \text{ kip}$$

$$\phi_v \cdot V_n = 50.404 \text{ kip}$$

Fiber Properties PBO FRCM *Ce for FRP only
 $C_E := 1$

$$t_f := .002 \text{ in} \quad f_{fu0} := 241.343 \text{ ksi} \quad \epsilon_{fu0} := .0176 \frac{\text{in}}{\text{in}} \quad E_f := 18656 \text{ ksi}$$

$$w_f := 17 \text{ in} \quad f_{fu} := C_E \cdot f_{fu0} = 241.343 \cdot \text{ksi} \quad \epsilon_{fu} := C_E \cdot \epsilon_{fu0} = 0.018$$

$$n_f := 2$$

$$A_f := n_f \cdot w_f \cdot t_f = 0.068 \cdot \text{in}^2 \quad d_f := b$$

Preliminary calcs

$$\beta_1 := .75 \quad E_c := 57000 \cdot (6000)^{-5} \cdot \text{psi} = 4.415 \times 10^6 \cdot \text{psi} \quad M_{DL} := 94.3 \text{ kip} \cdot \text{ft}$$

$$E_s := 29000000 \text{ psi}$$

Design

$$\rho := \frac{A_s}{b_w \cdot d} = 0.02 \quad n := \frac{E_s}{E_c} = 6.568 \quad k := \left[2 \cdot \rho \cdot n + (\rho \cdot n)^2 \right]^{.5} - \rho \cdot n = 0.401$$

$$I_{cr} := n \cdot A_s \cdot (d - k \cdot d)^2 + \frac{b_w \cdot (k \cdot d)^3}{3} = 6.896 \times 10^3 \cdot \text{in}^4$$

Existing Strain on soffit

$$\epsilon_{bi} := M_{DL} \cdot \frac{(d_f - k \cdot d)}{I_{cr} \cdot E_c} = 4.939 \times 10^{-4}$$

Strain on FRP system

$$\epsilon_{fd} := \epsilon_{fu} - .0013 = 0.016$$

STD from Nanni

Depth to N.A

$$c := 1.3755 \text{ in} \quad \text{*change c here in iterations}$$

Effective strain in FRP and Concrete

$$\epsilon_{fc1} := .003 \left[\frac{(d_f - c)}{c} \right] - \epsilon_{bi} = 0.041 \quad \epsilon_{fc2} := \epsilon_{fd} = 0.016$$

$$\epsilon_{fc} := \min(\epsilon_{fc1}, \epsilon_{fc2}, .012) = 0.012$$

$$\epsilon_c := (\epsilon_{fc} + \epsilon_{bi}) \frac{c}{d_f - c} = 8.986 \times 10^{-4}$$

Strain in Steel

$$\epsilon_s := (\epsilon_{fc} + \epsilon_{bi}) \frac{(d - c)}{d_f - c} = 0.011$$

Stress in Steel and FRP

$$f_{s1} := E_s \cdot \epsilon_s = 314.959 \cdot \text{ksi} \quad f_{s2} := f_y = 33 \cdot \text{ksi}$$

$$f_s := \min(f_{s1}, f_{s2}) = 33 \cdot \text{ksi}$$

$$f_{fc} := \min(E_f \cdot \epsilon_{fc}, f_{fu}) = 223.872 \cdot \text{ksi}$$

Calculate internal force resultants and check equilibrium

$$\epsilon_{c'} := 1.7 \cdot \frac{f_c}{E_c} = 2.31 \times 10^{-3} \quad \beta_1 := \frac{(4 \cdot \epsilon_{c'} - \epsilon_c)}{6 \cdot \epsilon_{c'} - 2 \cdot \epsilon_c} = 0.691 \quad \alpha_1 := \frac{3 \cdot \epsilon_{c'} \cdot \epsilon_c - \epsilon_c^2}{(3 \cdot \beta_1 \cdot \epsilon_{c'}^2)} = 0.49$$

$$c = 1.375 \cdot \text{in} \quad c' := \frac{(A_s \cdot f_s + A_f \cdot f_{fc})}{\alpha_1 \cdot \beta_1 \cdot f_c \cdot b_e} = 1.376 \cdot \text{in} \quad \text{*iterate to force } c=c'$$

Calculate flexural strength components

$$a := \beta_1 \cdot c = 0.951 \cdot \text{in} < hf, \text{ O.K.}$$

$$M_{ns} := A_s \cdot f_s \cdot \left(d - \frac{a}{2} \right) = 300.719 \cdot \text{kip} \cdot \text{ft} \quad \psi_f := 1$$

$$M_{nf} := A_f \cdot f_{fc} \cdot \left(d_f - \beta_1 \cdot \frac{c}{2} \right) = 25.403 \cdot \text{kip} \cdot \text{ft} < .5 \cdot M_{ns0} = 152.251 \cdot \text{kip} \cdot \text{ft} \quad \text{O.K.}$$

$$\phi M_n := \phi_f (M_{ns} + \psi_f M_{nf}) = 293.51 \cdot \text{kip} \cdot \text{ft} \quad \frac{(\phi M_n - \phi_f M_{ns0}) \cdot 100}{(\phi_f M_{ns0})} = 7.1$$

$$\frac{\phi M_n}{\phi_f} = 326.122 \cdot \text{kip} \cdot \text{ft} \quad \rho_f := \frac{A_f}{b_w \cdot d} = 2.222 \times 10^{-4}$$

Check service stress in FRP and Steel

$$k := \left[\left(\rho_f \frac{E_f}{E_c} + \rho \frac{E_s}{E_c} \right)^2 + 2 \cdot \left(\rho_f \frac{E_f \cdot d_f}{E_c \cdot d} + \rho \frac{E_s}{E_c} \right) \right]^{.5} = \left(\rho_f \frac{E_f}{E_c} + \rho \frac{E_s}{E_c} \right) = 0.402$$

$$M_s := 214.53 \text{kip} \cdot \text{ft} \quad (\text{anticipated service moment})$$

$$f_{ss} := \frac{\left[M_s + \epsilon_{bf} A_f E_f \left(d_f - k \cdot \frac{d}{3} \right) \right] (d - k \cdot d) E_s}{A_s E_s \left(d - k \cdot \frac{d}{3} \right) (d - k \cdot d) + A_f E_f \left(d_f - k \cdot \frac{d}{3} \right) (d_f - k \cdot d)} = 26.319 \cdot \text{ksi}$$

$$.8 \cdot f_y = 26.4 \text{ ksi} > f_{ss}, \text{ O.K.}$$

Check creep rupture limit at service of the FRP

$$f_{fs} := f_{ss} \cdot \frac{E_f (d_f - k \cdot d)}{E_s (d - k \cdot d)} - \epsilon_{br} \cdot E_f = 11.65 \cdot \text{ksi} < .3 \cdot f_{fu} = 72.403 \cdot \text{ksi}$$

stress is well below limit

Shear Design: H20 Legal truck

$$V_u := 46.52 \text{ kip} \quad \text{Shear strengthening not needed, but provided for anchorage}$$

$$\epsilon_{fv} := \min(\epsilon_{fd}, .004) = 4 \times 10^{-3}$$

$$n_v := 2$$

$$d_f := h - h_f = 14.5 \text{ in}$$

$$f_{fv} := \epsilon_{fv} \cdot E_f = 74.624 \text{ ksi}$$

$$t_f = 2 \times 10^{-3} \text{ in}$$

$$s_f := 18 \text{ in}$$

$$w_f := 12 \text{ in}$$

$$A_{fv} := 2 \cdot n_v \cdot t_f \cdot w_f = 0.096 \cdot \text{in}^2$$

$$V_c = 210.869 \cdot \text{kN}$$

$$V_s = 88.075 \cdot \text{kN}$$

$$V_f := A_{fv} \cdot f_{fv} \cdot \frac{d_f}{s_f} = 5.771 \cdot \text{kip}$$

$$V_f = 25.67 \cdot \text{kN}$$

$$\phi_{vn} := \phi_v (V_c + V_s + V_f) = 54.732 \cdot \text{kip} > V_u$$

Check limit on FRCM and Steel

$$8 \cdot f_c^5 \cdot \text{psi}^5 \cdot b_w \cdot d = 189.621 \cdot \text{kip}$$

$$V_s + V_f = 25.571 \cdot \text{kip} < \text{limit, O.K.}$$

Check limit on FRCM

$$V_{n_new} := V_n + V_f = 72.976 \cdot \text{kip}$$

$$.5 \cdot V_{n_new} = 36.488 \cdot \text{kip} > V_f, \text{ O.K.}$$

Bridge P0058 SRG Design

Short spans, interior girder

$$L := 26.375 \text{ ft}$$

$$b_w := 17 \text{ in}$$

$$h_f := 6 \text{ in}$$

$$b_c := \min\left(b_w + 2 \cdot 68 \frac{\text{in}}{2}, b_w + 2 \cdot 8 \cdot h_f, \frac{L}{4}\right) = 79.125 \text{ in}$$

$$h := 20.5 \text{ in}$$

$$d := h - 2.5 \text{ in} = 18 \text{ in}$$

$$f_c := 6000 \text{ psi}$$

$$\beta_1 := .75$$

$$f_y := 33000 \text{ psi}$$

$$A_s := 4 \cdot 1.56 \text{ in}^2 = 6.24 \text{ in}^2$$

$$a := A_s \frac{f_y}{.85 \cdot f_c \cdot b_c} = 0.51 \text{ in} < hf, \text{ OK}$$

Moment Capacity before strengthening:

$$M_{ns0} := A_s \cdot f_y \cdot \left(d - \frac{a}{2}\right) = 304.502 \cdot \text{kip} \cdot \text{ft} \quad \phi_f := .9$$

$$\phi_f \cdot M_{ns0} = 274.052 \cdot \text{kip} \cdot \text{ft}$$

$$A_{s_min} := 200 \frac{b_w}{\text{in}} \cdot \frac{d \cdot \text{psi} \cdot \text{in}^2}{f_y \cdot \text{in}} = 1.855 \cdot \text{in}^2 < A_s, \text{ OK}$$

Shear Capacity before strengthening:

$$A_v := 2 \cdot 2 \text{ in}^2 = 0.4 \text{ in}^2$$

$$s := 12 \text{ in}$$

$$V_c := \frac{2}{1000} \left(\frac{f_c}{\text{psi}}\right)^2 \cdot \frac{1}{\text{in}} \cdot \frac{b_w}{\text{in}} \cdot \frac{d \cdot \text{kip}}{\text{in}} = 47.405 \cdot \text{kip} \quad \phi_v := .75$$

$$V_s := A_v \cdot f_y \cdot \frac{d}{s} = 19.8 \cdot \text{kip}$$

$$V_n := V_c + V_s = 67.205 \cdot \text{kip}$$

$$\phi_v \cdot V_n = 50.404 \cdot \text{kip}$$

Fiber Properties

SRG

$$t_f := .00333 \text{ in} \quad f_{fu0} := 194.54 \text{ ksi} \quad \epsilon_{fu0} := .0101 \frac{\text{in}}{\text{in}} \quad E_f := 13058 \text{ ksi} \quad C_E := 1$$

$$w_f := 17 \text{ in} \quad f_{fu} := C_E \cdot f_{fu0} = 194.54 \text{ ksi} \quad \epsilon_{fu} := C_E \cdot \epsilon_{fu0} = 0.01$$

$$n_f := 2$$

$$A_f := n_f \cdot w_f \cdot t_f = 0.113 \cdot \text{in}^2 \quad d_f := h = 20.5 \text{ in}$$

Preliminary calcs

$$\beta_1 := .75 \quad E_c := 57000 \cdot (6000)^{-5} \cdot \text{psi} = 4.415 \times 10^6 \cdot \text{psi} \quad M_{DL} := 94.3 \text{ kip} \cdot \text{ft}$$

$$E_s := 29000000 \text{ psi}$$

Design

$$\rho := \frac{A_s}{b_w \cdot d} = 0.02 \quad n := \frac{E_s}{E_c} = 6.568 \quad k := \left[2 \cdot \rho \cdot n + (\rho \cdot n)^2 \right]^{.5} - \rho \cdot n = 0.401$$

$$I_{cr} := n \cdot A_s \cdot (d - k \cdot d)^2 + \frac{b_w \cdot (k \cdot d)^3}{3} = 6.896 \times 10^3 \cdot \text{in}^4$$

Existing Strain on soffit

$$\epsilon_{bi} := M_{DL} \cdot \frac{(d_f - k \cdot d)}{I_{cr} \cdot E_c} = 4.939 \times 10^{-4}$$

Strain on FRP system

$$\epsilon_{fd} := \epsilon_{fu} - .003 = 7.1 \times 10^{-3}$$

STD from Nani

Depth to N.A

$$c := 1.701 \text{ in} \quad \text{*change c here in iterations}$$

Effective strain in FRP and Concrete

$$\epsilon_{fc1} := .003 \left[\frac{(d_f - c)}{c} \right] - \epsilon_{bi} = 0.033 \quad \epsilon_{fc2} := \epsilon_{fd} = 7.1 \times 10^{-3}$$

$$\epsilon_{fc} := \min(\epsilon_{fc1}, \epsilon_{fc2}, .012) = 7.1 \times 10^{-3} \quad \epsilon_c := (\epsilon_{fc} + \epsilon_{bi}) \cdot \frac{c}{d_f - c} = 6.871 \times 10^{-4}$$

Strain in Steel

$$\epsilon_s := (\epsilon_{fc} + \epsilon_{bi}) \cdot \frac{(d - c)}{d_f - c} = 6.584 \times 10^{-3}$$

Stress in Steel and FRP

$$f_{s1} := E_s \cdot \epsilon_s = 190.936 \text{ ksi} \quad f_{s2} := f_y = 33 \text{ ksi}$$

$$f_s := \min(f_{s1}, f_{s2}) = 33 \text{ ksi}$$

$$f_{fc} := \min(E_f \cdot \epsilon_{fc}, f_{fu}) = 92.712 \text{ ksi}$$

Calculate internal force resultants and check equilibrium

$$\epsilon_{c'} := 1.7 \cdot \frac{f_c}{E_c} = 2.31 \times 10^{-3} \quad \beta_1 := \frac{(4 \cdot \epsilon_{c'} - \epsilon_c)}{6 \cdot \epsilon_{c'} - 2 \cdot \epsilon_c} = 0.685 \quad \alpha_1 := \frac{3 \cdot \epsilon_{c'} \cdot \epsilon_c - \epsilon_c^2}{(3 \cdot \beta_1 \cdot \epsilon_{c'}^2)} = 0.391$$

$$c = 1.701 \text{ in} \quad c' := \frac{(A_s \cdot f_s + A_f \cdot f_{fc})}{\alpha_1 \cdot \beta_1 \cdot f_c \cdot b_e} = 1.701 \text{ in} \quad \text{*iterate to force } c=c'$$

Calculate flexural strength components

$$a := \beta_1 \cdot c = 1.165 \text{ in} < hf, \text{ O.K.}$$

$$M_{ns} := A_s \cdot f_s \cdot \left(d - \frac{a}{2}\right) = 298.883 \text{ kip}\cdot\text{ft} \quad \psi_f := 1$$

$$M_{nf} := A_f \cdot f_{fc} \cdot \left(d_f - \beta_1 \cdot \frac{c}{2}\right) = 17.422 \text{ kip}\cdot\text{ft} < .5 \cdot M_{ns0} = 152.251 \text{ kip}\cdot\text{ft} \quad \text{O.K.}$$

$$\phi M_n := \phi_f (M_{ns} + \psi_f M_{nf}) = 284.675 \text{ kip}\cdot\text{ft} \quad \frac{(\phi M_n - \phi_f \cdot M_{ns0}) \cdot 100}{(\phi_f \cdot M_{ns0})} = 3.876$$

Check service stress in FRP and Steel

$$\rho_f := \frac{A_f}{b_w \cdot d} = 3.7 \times 10^{-4}$$

$$k := \left[\left(\rho_f \frac{E_f}{E_c} + \rho \frac{E_s}{E_c} \right)^2 + 2 \cdot \left(\rho_f \frac{E_f \cdot d_f}{E_c \cdot d} + \rho \frac{E_s}{E_c} \right) \right]^{.5} - \left(\rho_f \frac{E_f}{E_c} + \rho \frac{E_s}{E_c} \right) = 0.402$$

$$M_s := 214.53 \text{ kip}\cdot\text{ft} \quad (\text{anticipated service moment})$$

$$f_{ss} := \frac{\left[M_s + \varepsilon_{bi} A_f E_f \left(d_f - k \cdot \frac{d}{3} \right) \right] (d - k \cdot d) E_s}{A_s E_s \left(d - k \cdot \frac{d}{3} \right) (d - k \cdot d) + A_f E_f \left(d_f - k \cdot \frac{d}{3} \right) (d_f - k \cdot d)} = 26.297 \text{ ksi}$$

$$.8 \cdot f_y = 26.4 \text{ ksi} > f_{ss}, \text{ O.K.}$$

Check creep rupture limit at service of the FRP

$$f_{fs} := f_{ss} \frac{E_f (d_f - k \cdot d)}{E_s (d - k \cdot d)} = \varepsilon_{bi} E_f = 8.143 \text{ ksi} < .3 \cdot f_{fu} = 58.362 \text{ ksi}$$

stress is well below limit

Shear Design: H20 Legal truck

$$V_u := 46.52 \text{ kip} \quad \text{Shear strengthening not needed, but provided for anchorage}$$

$$\varepsilon_{fv} := \min(\varepsilon_{fd}, .004) = 4 \times 10^{-3} \quad n_v := 2$$

$$f_{fv} := \varepsilon_{fv} E_f = 52.232 \text{ ksi} \quad d_f := h - h_f = 14.5 \text{ in}$$

$$t_f = 3.33 \times 10^{-3} \text{ in} \quad s_f := 18 \text{ in}$$

$$w_f := 12 \text{ in} \quad A_{fv} := 2 \cdot n_v \cdot t_f \cdot w_f = 0.16 \text{ in}^2$$

$$V_f := A_{fv} f_{fv} \frac{d_f}{s_f} = 6.725 \text{ kip}$$

$$\phi_{vn} := \phi_v (V_c + V_s + V_f) = 55.448 \text{ kip} > V_u$$

Check limit on FRCM and Steel

$$8 \cdot f_c^{.5} \cdot \text{psi}^{.5} \cdot b_w \cdot d = 189,621 \text{ kip}$$

$$V_s + V_f = 26.525 \text{ kip} < \text{limit}, \text{ O.K.}$$

Check limit on FRCM

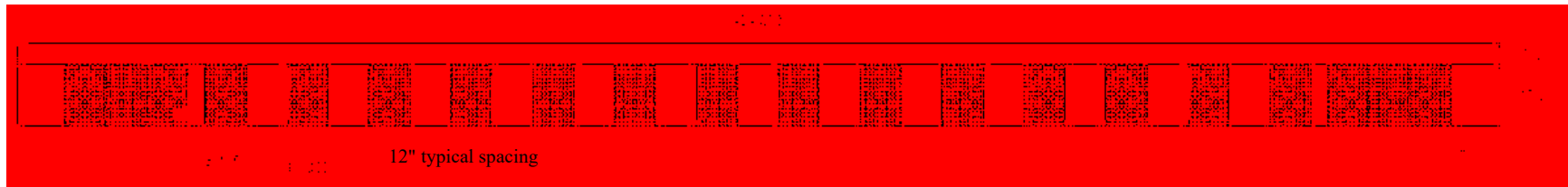
$$V_{n_new} := V_n + V_f = 73.931 \text{ kip}$$

$$.5 \cdot V_{n_new} = 36.965 \text{ kip} > V_f, \text{ O.K.}$$

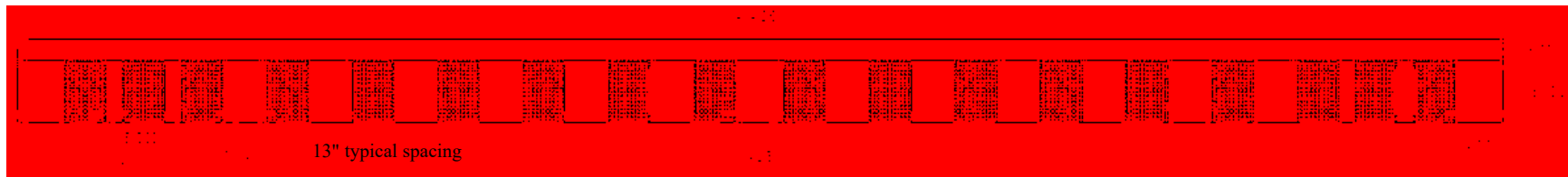
APPENDIX D.

SHEAR STRENGTHENING WRAPPING SCHEME

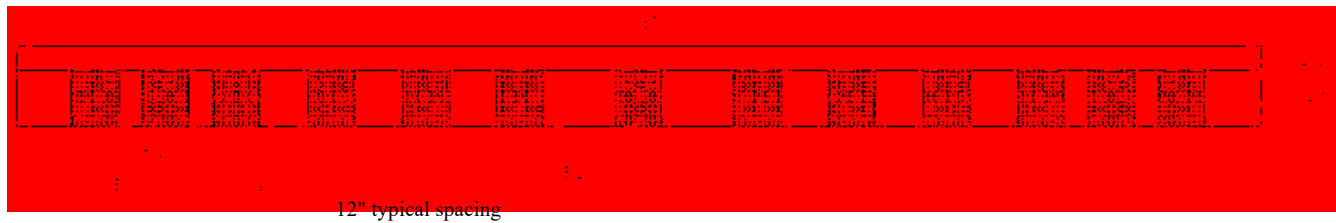
C-FRCM: (2 girders, 1 ply)



CFRP: (1 girder, 1 ply)



SRG: (2 girders, 2 ply) and PBO: (1 girder, 2 ply)



All wraps 12" wide
All schemes symmetric about center line
Dimensions shown in inches. 1 in. = 25.4 mm

APPENDIX E.
BILL OF MATERIALS

Detailed Bill of Materials

Michael Janke
Spring 2018

1) Carbon FRCM:

1.1) Flexural reinforcement: 2 girders, 2 plies

$$A_{fl} := 2 \cdot 2 \cdot 17in \cdot 36.1875ft = 205.062 ft^2$$

$$I_{fl} := 2 \cdot 2 \cdot 36.1875ft = 144.751 (linear)$$

1.2) Shear Reinforcement: 2 girders, 1 ply

$$A_{sh} := 2 \cdot 1 \cdot 20 \cdot 12in \cdot 4.41666ft = 176.666 ft^2$$

$$I_{sh} := 2 \cdot 1 \cdot 20 \cdot 4.41666ft = 176.66 (linear)$$

Total:

$$A := A_{fl} + A_{sh} = 381.729 ft^2$$

$$I := I_{fl} + I_{sh} = 321.414 ft (linear)$$

2) Carbon FRP:

2.1) Flexural reinforcement: 1 girders, 2 plies

$$A_{fl} := 1 \cdot 2 \cdot 15in \cdot 36.1875ft = 90.469 ft^2$$

$$I_{fl} := 1 \cdot 2 \cdot 36.1875ft = 72.3751 (linear)$$

2.2) Shear Reinforcement: 1 girders, 1 ply

$$A_{sh} := 1 \cdot 1 \cdot 18 \cdot 12in \cdot 4.41666ft = 79.5 ft^2$$

$$I_{sh} := 1 \cdot 1 \cdot 18 \cdot 4.41666ft = 79.499 f (linear)$$

Total:

$$A := A_{fl} + A_{sh} = 169.969 ft^2$$

$$I := I_{fl} + I_{sh} = 151.874 ft (linear)$$

3) SRG:

3.1) Flexural reinforcement: 2 girders, 2 plies

$$A_{fl} := 2 \cdot 2 \cdot 17in \cdot 26.37ft = 149.458ft^2$$

$$I_{fl} := 2 \cdot 2 \cdot 26.37ft = 105.5ft (linear)$$

3.2) Shear Reinforcement: 2 girders, 2 ply

$$A_{sh} := 2 \cdot 2 \cdot 13 \cdot 12in \cdot 3.8333ft = 199.333ft^2$$

$$I_{sh} := 2 \cdot 2 \cdot 13 \cdot 3.8333ft = 199.333ft (linear)$$

Total:

$$A := A_{fl} + A_{sh} = 348.791ft^2$$

$$I := I_{fl} + I_{sh} = 304.833ft (linear)$$

4) PBO:

4.1) Flexural reinforcement: 1 girders, 2 plies

$$A_{fl} := 1 \cdot 2 \cdot 17 \text{ in} \cdot 26.375 \text{ ft} = 74.729 \text{ ft}^2$$

$$I_{fl} := 1 \cdot 2 \cdot 26.375 \text{ ft} = 52.75 \text{ ft (linear)}$$

4.2) Shear Reinforcement: 1 girders, 2 ply

$$A_{sh} := 1 \cdot 2 \cdot 13 \cdot 12 \text{ in} \cdot 3.83333 \text{ ft} = 99.667 \text{ ft}^2$$

$$I_{sh} := 1 \cdot 2 \cdot 13 \cdot 3.83333 \text{ ft} = 99.667 \text{ (linear)}$$

Total:

$$A := A_{fl} + A_{sh} = 174.396 \text{ ft}^2$$

$$I := I_{fl} + I_{sh} = 152.417 \text{ ft (linear)}$$

APPENDIX F.

MANUFACTURER'S MATERIAL INFORMATION

DEFINITION: / Steel fiber reinforced sheets for structural strengthening of reinforced concrete and masonry structures.

GeoSteel G600

GeoSteel G600 Hardwire™ is a unidirectional sheet made of ultra-high strength galvanized steel micro-cords, fixed to a fibreglass micromesh to facilitate installation, which can be installed using a GeoCalce® Fino or GeoLite® or GeoLite® Gel matrix according to project and building site requirements.

The structural strengthening GeoSteel sheet is thus extremely easy to handle and shape, and combines excellent mechanical and installation properties with high durability thanks to galvanization of the individual wires. Galvanized steel fiber sheets guarantee unique structural and mechanical properties, much higher than traditional carbon-glass-epoxy fiber sheets, making them particularly effective in the various structural strengthening and seismic upgrade or compliance retrofit solutions, as well as the creation of suitable connection systems, when combined with GeoSteel Injección Connector.



PRODUCT STRENGTHS

- High durability thanks to the special steel wire galvanization process, tested using strict durability tests in a chloride, freeze-thaw and high humidity environment
- Specifically intended for structural strengthening using:
 - GeoCalce® Fino, with pure natural hydraulic NHL 3.5 lime and mineral geo-binder base, ideal for retrofitting structural elements made of brick, natural stone, and tuff masonry and substrates that require advanced breathability along with high mechanical adhesion
 - GeoLite®, with mineral geo-binder base, ideal for retrofitting structural elements in reinforced concrete, prestressed reinforced concrete or good consistency masonry
 - GeoLite® Gel epoxy-based mineral adhesive, ideal for structural retrofitting sections made of reinforced concrete, prestressed reinforced concrete, wood and steel
- Can be tensioned to create structural reinforcements and active devices using particular mechanical anchoring systems, thanks to the unique characteristics of the textile which do not require advance impregnation of the sheet, and at the same time allow it to be anchored and fastened with metal plates without having to take particular precautions, as is necessary for all the other types of fibre and textile on the market
- Can be shaped using GeoSteel Bender which allows the sheet to be modelled easily without altering its mechanical properties to create surround brackets for beams and pilae and other bent elements required during structural consolidation works

AREAS OF USE

Use

- Static and seismic upgrade or compliance retrofit of structural elements in brick, natural stone, tuff, reinforced concrete, prestressed reinforced concrete, wood, and steel walls
- Consolidation of brick masonry, natural stone and tuff arches, vaults and domes
- Confinement and wrapping of masonry and reinforced concrete structural elements
- Flexural shear and confinement strengthening of brick, natural stone, tuff, and masonry panels and reinforced concrete sections
- Flexural shear and confinement strengthening for timber elements
- Flexural strengthening for steel girders
- Execution of top ring beams or in breach in reinforced masonry
- Execution of special single- or double-flap thinned connections for anchoring sheets and grids and executing reinforced injections

INSTRUCTIONS FOR USE

Preparation

The ultra-high strength galvanized steel fibre sheet, GeoSteel G600 Hardwire™, is ready-to-use. The sheet can be cut at right angles to the cords with manual or electric shears, or parallel with the cords using a normal box cutter. The sheet, cut into strips even just a few cm wide and a number of metres long, ensures perfect stability without in any way compromising the workability of the material and its application.

Preparation of substrates

The substrate must be properly prepared and cleaned, always in accordance with the instructions dictated by the construction supervisor.

When the substrates are not damaged, simply clean and remove any dust or oils that could compromise the adhesion of the system, using compressed air or pressure water.

When the substrate is clearly degraded, uneven, or damaged by significant events, proceed as follows, always in accordance with the construction supervisor:

1. For masonry, tuff, and natural stone substrates:
 - Completely remove residues from previous processes that could compromise adhesion, and any quantity of inconsistent rendering mortars from between the stones;

KERA KOLL
The Green Building Company

INSTRUCTIONS FOR USE

- Saturation, spray, or brush application, if required, of certified natural stabilizing cortical consolidant with base of pure stabilized potassium silicate in aqueous solution such as BioCalc® Silicate Consolidants or water-based eco-friendly solvent-free stabilizing agent, such as Resobuild® Eco Consolidant.
 - Reconstruction, if necessary, of material according to design instructions and the construction supervisor.
 - Levelling previously consolidated surfaces with geo-mortar with a base of pure natural hydraulic lime NHL 3.5 and mineral geo-binder such as GeoCalce® or GeoCalce® Fino, depending on the thickness required.
2. For substrates in masonry concrete or prestressed reinforced concrete:
- Thorough removal of weakened concrete if necessary, through mechanical scarification or hydro-demolition, making sure to roughen the substrate to a depth of at least 5 mm.
 - Removal of rust, if any, from reinforcing bars, which must be cleaned by brushing (manual or mechanical) or sandblasting.
 - Monolithic reconstruction or smoothing of the surface, if needed, using geo-mortar based on a mineral geo-binder such as GeoLite®.
 - When applying the reinforcing system with an inorganic matrix, make sure that the substrate is appropriately dampened (follow the directions on the GeoLite® or GeoCalce® data sheets).
 - When applying the reinforcing system with an organic matrix, the substrate must be dry and free of humidity (follow the instructions on the GeoLite® Gel data sheet).

Application

Execution of steel fibre structural reinforcement in Steel Reinforced Mortar (combination of steel fibre and GeoCalce® Fino or GeoLite®) or Steel Reinforced Polymer (combination of steel fibre and GeoLite® Gel) epoxy mineral adhesive will be followed by application of a first layer of geo-mortar, making sure there is sufficient material for the substrate (average thickness = 3 - 5 mm) to even it out and to lay and incorporate the reinforcing sheet. When using an epoxy mineral adhesive matrix, the substrate can be levelled using GeoLite® or GeoCalce®, taking care to allow the geo-mortar to cure for long enough to ensure that the humidity of the substrate is appropriate for application of GeoLite® Gel. The first layer of adhesive must be an average thickness of 1 - 2 - 3 mm. Afterward, working over the matrix while it is still wet, apply the ultra-high strength galvanized steel fibre sheet GeoSteel G800 Hardwire™, making sure that the sheet is perfectly incorporated into the matrix by pressing with a squeegee or steel roller and also checking that it comes out between the joints to ensure optimum adhesion between the first and second layers of matrix. At longitudinal overlapping points, overlap two layers of steel fibre sheet by least 15 cm for epoxy matrix and 30 cm for inorganic matrices. For organic and inorganic matrix, working wet on wet, perform the final protective smoothing (= 1 - 2 mm thick for organic matrix, = 2 - 3 mm thick for inorganic), in order to fully incorporate the reinforcement and fill in any underlying voids. If there are additional layers after the first, proceed with laying of the second layer of steel fibre over the matrix while it is still wet, repeating the steps described above. In the event that the system installed with a epoxy matrix must be plastered or concealed by smoothing, we recommend that, while the resin is still wet, you apply a spray of mineral quartz to provide better adhesion for subsequent layers.

If the reinforcing system is installed in especially aggressive environments, or you otherwise wish to ensure additional protection beyond that already provided by the matrix, we recommend applying:

- GeoLite® Microsilica on reinforcement systems with GeoLite® or GeoCalce® Fino matrix.
- Kerakoll Eco Acrylics Flex on reinforcement systems with GeoLite® Geo matrix.

If the work area is permanent or occasional contact with water, the cycles described above must be replaced with a polyurethane epoxy cycle or an anionic cement depending on the needs of the work area and the design specifications.

For technical specifications, application, and preparation of the matrix, as well as protective systems, adaptions for the matrix type, consult the relevant data sheets.

Creating a GeoSteel Connector

A steel-fibre thread connector system is created by including a band of fabric of appropriate width from the GeoSteel Hardwire™ line to provide the minimum number of cords in the connector according to the design, in order to achieve the required tensile strength; make sure to ensure the end of the fabric band by cutting the supportive mesh, making the cut parallel to the cords themselves, to the length of the edge you want to create on the masonry. In the event of a connector with threads on both sides, this operation must be performed on both ends of the duly arranged fibre strip. Once the sheet is cut, roll the band onto itself, taking care to create a cylinder of an appropriate diameter compared to the hole.

Insert the connector that has been created into the hole, and then insert the GeoSteel glass fibre-reinforced polypropylene GeoSteel Tape Cord Connector, so that the end of the fibre bends 90°. Finally, using the special hole located on the band of the piece, inject the pourable mortar, such as GeoCalce® Fluida, to grout the fibre-thread connector system. When this phase is complete, the GeoSteel Tape Cord Connector must be duly sealed with the cap provided.

Depending on the type of substrate (concrete or masonry) for grouting the connector, as an alternative to the use of pourable natural hydraulic lime, the designer may choose to use pourable cement-based mortar Kerakoll® Eco Binder, thixotropic epoxy resin GeoLite® Gel or superfluid Kerakoll® EpoFill.

Provided below is a table listing the tensile strength of a connector as a function of the type of GeoSteel Hardwire™ sheet and the corresponding widths of the band adopted:

Sheet	Width of the band (cm)	Number of Cords*	Tensile breaking load
GeoSteel G800	10	18	> 24 kN
GeoSteel G800	15	23	> 36 kN

*If cords/cm = 1.5;
tensile breaking load of a cord > 1500 N.

In the event that a connector with another strength or a different number of cords from those listed is required, simply calculate the appropriate width of the band by dividing the required strength by the strength of one cord and then by the number of cords present per unit of width in the type of sheet selected.

Test reports are available upon request to determine the calculation parameters.

ABSTRACT

SRM-GeoCulce® GeoSteel G600

Execution of structural reinforcement or repair, seismic upgrade of masonry, full or partial stone elements and structures using a composite system based on ultra-high strength galvanized steel fibre sheet GeoSteel G600 Hardware™ from Kerakoll Spa, with net fibre weight of ~ 400 g/m², with the following mechanical characteristics: sheet tensile strength > 2600 MPa; sheet elastic modulus > 190 GPa; sheet break deformation > 1.50%; nominal area of a cord 3x2 (3 wires) = 0.536 mm²; no. cords per cm = 1.52; sheet equivalent thickness = 0.064 mm, impregnated with certified inorganic matrix of natural, structural, breathable, eco-friendly geo-mortar based on pure natural hydraulic lime NHL 3.5 and mineral geo-binders such as GeoCulce® Fino by Kerakoll Spa, to be applied directly on the structure requiring reinforcement.

The procedure is conducted as follows:

1. Any restoration of degraded, weakened, non-cohesive, or non-planar surfaces with GeoCulce® by Kerakoll Spa, in the case of masonry substrates, or GeoLite® by Kerakoll Spa, in the case of reinforced concrete substrates, and in all cases as dictated and approved by the construction supervisor.
2. Lay a first layer of approximately average thickness of ~ 3-5 mm thick dry or mortar with pure natural NHL 3.5 and mineral geo-binder base, such as GeoCulce® Fino by Kerakoll Spa.
3. While the mortar is still wet, lay the ultra-high strength galvanized steel fibre sheet GeoSteel G600 Hardware™ by Kerakoll Spa, and by pressing firmly with a smooth spreader or metal roller, make sure that the sheet is completely impregnated and avoid allowing any gaps or air bubbles to form, because these can compromise the adhesion of the sheet to the matrix or to the substrate.
4. Working wet on wet, apply the second layer of geo-mortar based on pure natural lime NHL 3.5 and mineral geo-binder, such as GeoCulce® Fino by Kerakoll Spa, ~ 2-3 mm thick to fully incorporate the reinforcing sheet and fill in any remaining underlying gaps.
5. Repeat steps 3 and 4 if necessary for all subsequent reinforcing layers called for by the design.

Delivery and installation of all the materials described above as well as everything else required to finish the job is included. The following are included: restoration of degraded areas and repair of the substrate; anchoring devices using connectors or metal plates; material acceptance tests; pre- and post-procedure testing; all aids required to perform the work. The price is by unit of reinforcing surfaces actually laid, including overlaps and anchoring sections.

SRM-GeoLite® GeoSteel G600

Execution of structural reinforcement or repair or seismic upgrade or compliance retrofit of reinforced cement, masonry, full or partial stone elements and structures using a composite system based on ultra-high strength galvanized steel fibre sheet GeoSteel G600 Hardware™ from Kerakoll Spa, with net fibre weight of ~ 400 g/m², with the following mechanical characteristics: sheet tensile strength > 2600 MPa; sheet elastic modulus > 190 GPa; sheet break deformation > 1.50%; nominal area of a cord 3x2 (3 wires) = 0.536 mm²; no. cords per cm = 1.52; sheet equivalent thickness = 0.064 mm, impregnated with inorganic matrix of eco-friendly, bioactive, mineral setting certified mineral geo-mortar based on crystalline reaction geo-binder and zirconium, with very low petrochemical polymer content and free of organic fibres, specifically for positioning, restoration, smoothing, and guaranteed, long-lasting monolithic protection of structures in concrete, such as GeoLite® by Kerakoll Spa, to be applied directly on the structure requiring reinforcement.

The procedure is conducted as follows:

1. Any restoration of degraded, weakened, non-cohesive, or non-planar surfaces shall be performed with GeoCulce® by Kerakoll Spa, in the case of masonry substrates, or GeoLite® by Kerakoll Spa, in the case of reinforced concrete substrates, and in all cases as dictated and approved by the construction supervisor.
2. Spread a first layer of approximate average thickness of ~ 3-5 mm of geo-mortar with mineral geo-binder base, such as GeoLite® by Kerakoll Spa.
3. While the mortar is still wet, lay the ultra-high strength galvanized steel fibre sheet GeoSteel G600 Hardware™ by Kerakoll Spa, and by pressing firmly with a smooth spreader or metal roller, make sure that the sheet is completely impregnated and avoid allowing any gaps or air bubbles to form, because these can compromise the adhesion of the sheet to the matrix or to the substrate.
4. Working wet on wet, apply the second layer of geo-mortar, such as GeoLite® by Kerakoll Spa, approximately ~ 2-3 mm thick, until the reinforcing sheet is fully incorporated and any underlying voids are filled.
5. Repeat steps 3 and 4 if necessary for all subsequent reinforcing layers called for by the design.

Delivery and installation of all the materials described above as well as everything else required to finish the job is included. The following are included: restoration of degraded areas and repair of the substrate; anchoring devices using connectors or metal plates; material acceptance tests; pre- and post-procedure testing; all aids required to perform the work. The price is by unit of reinforcing surfaces actually laid, including overlaps and anchoring sections.

SRP GeoSteel G600

Execution of structural reinforcement or repair, or seismic upgrade or compliance retrofit of reinforced cement, masonry, wood and steel using a composite system based on ultra-high strength galvanized steel fibre sheet GeoSteel G600 Hardware™ from Kerakoll Spa, with net fibre weight of ~ 400 g/m², with the following mechanical characteristics: sheet tensile strength > 2600 MPa; sheet elastic modulus > 190 GPa; sheet break deformation > 1.50%; nominal area of a cord 3x2 (3 wires) = 0.536 mm²; no. cords per cm = 1.52; sheet equivalent thickness = 0.064 mm, impregnated with epoxy mineral matrix such as GeoLite® Gel by Kerakoll Spa to be applied directly on the structure requiring reinforcement without any need for primer.

The procedure is conducted as follows:

1. Any restoration of degraded, weakened, non-cohesive, or non-planar surfaces shall be performed with GeoCulce® by Kerakoll Spa, in the case of masonry substrates, or GeoLite® by Kerakoll Spa, in the case of reinforced concrete substrates, and in all cases as dictated and approved by the construction supervisor.
2. Application of a first layer approximately average thickness of ~ 2-3 mm of epoxy mineral adhesive such as GeoLite® Gel by Kerakoll Spa.
3. While the epoxy mineral adhesive is still wet, lay the ultra-high strength galvanized steel fibre sheet GeoSteel G600 Hardware™ by Kerakoll Spa, and by pressing firmly with a smooth spreader or metal roller, make sure that the sheet is completely impregnated and avoid allowing any gaps or air bubbles to form, because these can compromise the adhesion of the reinforcing system to the substrate.
4. Working wet on wet, lay the second layer of matrix, such as GeoLite® Gel by Kerakoll Spa, at an average thickness of ~ 1-2 mm, until the reinforcing sheet is completely covered.
5. Repeat steps 3 and 4 if necessary for all subsequent reinforcing layers called for by the design.

Delivery and installation of all the materials described above as well as everything else required to finish the job is included. The following are included: restoration of degraded areas and repair of the substrate; anchoring devices using connectors or metal plates; material acceptance tests; pre- and post-procedure testing; all aids required to perform the work. The price is by unit of reinforcing surfaces actually laid, including overlaps and anchoring sections.

KERAKOLL
The GreenBuilding Company

TECHNICAL DATA COMPLIANT WITH KERAKOLL QUALITY STANDARD

Wire			
- characteristic tensile stress	σ_{tens}		> 2500 MPa
- elastic modulus	E_{tens}		> 205 GPa
- area	A_{tens}		8.1076 mm ²
Drysheet/Cord			
Cord 3x2 obtained by joining 5 filaments, of which 3 straight and 2 wrapped with a high torque angle			
- characteristic area of a cord 3x2 (5 wires)	A_{3x2}		0.508 mm ²
- n° conductor			1.57 conductors
- mass inclusion at the final welding			- 678 g/m ²
- equivalent thickness of sheet	t_{equiv}		> 0.054 mm
- tensile breaking load of a cord			> 1580 N
- tensile strength of the sheet	σ_{sheet}		> 2800 MPa
- tensile strength by unit of width	σ_{sheet}		> 2.35 kN/cm
- normal elastic modulus of sheet	E_{sheet}		> 190 GPa
- final warp of the sheet	δ_{sheet}		> 1.50%
Pack			50 m rolls of 30 cm
Weight of 1 roll			- 24 kg (including packaging)

WARNING

- Product for professional use
- abide by any standards and national regulations
- when handling the sheet wear protective clothing and goggles, and follow the instructions regarding methods for applying the material
- contact with the skin; no special measures required
- storage on the work site: store under cover in a dry place, well away from substances that might damage it or its ability to adhere to the chosen matrix
- if necessary, ask for the safety data sheet
- for any other issues, contact the Kerakoll Worldwide Global Service +39 0536 811 510 - global.service@kerakoll.com

0536-0361 (000) Curve 010201007

The information was last updated in July 2016. Please note that additional or further information may be made available by 01000 011334, for the whole of Italy, via www.kerakoll.com. KERAKOLL is a registered trademark of Kerakoll S.p.A. All other trademarks belong to their respective owners. © Kerakoll is provided only when used strictly in accordance with the instructions. The Kerakoll brand does not guarantee any specific performance. No liability is accepted for any damage caused by the use of the product. The Kerakoll brand does not guarantee any specific performance. No liability is accepted for any damage caused by the use of the product. The Kerakoll brand does not guarantee any specific performance. No liability is accepted for any damage caused by the use of the product.



KERAKOLL
The Green Building Company

KERAKOLL S.p.A.
Via de'FARIGNETTI, 9 - 41049 Sassuolo (MO) Italy
Tel. +39 0536 811 511 - Fax +39 0536 811 521
info@kerakoll.com - www.kerakoll.com

المنارة للاستشارات

Ruredil X Mesh Gold

PBO (Polyparaphenylenebenzobisoxazole) mesh in a stabilised inorganic matrix for flexural and shear strength reinforcement of concrete

Product description

RUREDIL X MESH GOLD is a patented new FRCM (Fibre Reinforced Cementitious Matrix) system, a ground-breaking application of FRP or high performance fibre structural reinforcement systems called FRP.

The RUREDIL X MESH GOLD system consists of a Polyparaphenylene benzobisoxazole (PBO) mesh and a stabilised inorganic matrix designed to connect the mesh with the concrete substrate.

Its outstanding mechanical performance allows this composite material to equal the performance of conventional carbon fibre FRP's with epoxy binders.

Typical applications

RUREDIL X MESH GOLD is suitable for reinforcement of reinforced concrete and pre-compressed reinforced concrete structures, including those subject to the simultaneous action of fire and high temperatures.

RUREDIL X MESH GOLD is applied to reinforced concrete and pre-compressed reinforced concrete structures for:

- Flex reinforcement;
- Shear strength;
- Tension reinforcement;
- Confinement of beam columns with low eccentricity;
- Confinement and longitudinal reinforcement of beam columns with high eccentricity.

RUREDIL X MESH GOLD is suitable for work in seismic zones for:

- increasing resistance to simple flex fatigue or combined pressing and bending action of pillars and beams;
- increasing resistance to shear stress of pillars and beams;
- increasing the flexibility of the terminal portions of beams and pillars by binding;
- increasing the resistance to tensile stress of the panels of beam-pillar nodes with fibres aligned with tensile stress isostatics.

Packaging, storage, dosage and yield

- RUREDIL X MESH GOLD: roll of PBO fibre mesh 100 cm wide and 15 m long.
Store in a dry place away from heat.
- RUREDIL X MESH M750: inorganic stabilised matrix, 25 Kg bags.
- For 1 15 m roll of RUREDIL X MESH GOLD about 5 bags of RUREDIL X MESH M750 mortar are required.
- As RUREDIL X MESH M750 is inorganic it is sensitive to damp, and must be kept indoors in a dry place. Use up the whole package once it has been opened.
Store at temperatures between +5°C and +35°C.

Benefits as compared to conventional FRPs

RUREDIL X MESH GOLD offers the following benefits over an FRP system employing epoxy or polyester resins:

Same resistance to high temperatures as substrate

The structural properties of FRP systems depend on temperature. The glassy transition temperature (T_g) of epoxy resins – normally between 40 and 80 °C – is the chemical/physical quantity determining the performance of an FRP system, independently of the fiber used (carbon, aramid, etc.)

When the outdoor temperature exceeds the glassy transition temperature, the epoxy resin is no longer capable of serving the function of transferring stress from the structure to the high modulus fiber buried in it, making it ineffective as structural reinforcement. This behavior is attributable to total loss of the adhesive bond between the resin and the fiber and/or between the resin and the support.

RUREDIL X MESH GOLD is not influenced by outdoor temperature after it hardens, and is fire-resistant because it is inorganic, like the concrete base. FRP systems not only fail to resist fire, but contribute to it by emitting toxic fumes.

Moisture resistance

RUREDIL X MESH GOLD's adhesion to concrete is not affected by relative humidity, unlike FRP systems. Epoxy resin degrades with prolonged exposure to moisture, losing its adhesive properties and therefore its ability to transfer stress to structural fiber.

Applicability of inorganic material to damp substrates

FRP systems can only be applied to dry substrates; as polyester and epoxy resins will not catalyse in the presence of water.

Ease of handling

The premixed substance is mixed with the amount of water specified in the instructions and applied like a conventional cement mortar, with the PBO structural mesh buried in it.

Workability

There are essentially no differences in workability time between 5 °C and 40 °C. Resins' pot life depends on temperature, which limits applicability of FRPs under unfavourable temperature and humidity conditions.

It is not toxic like the resins used in FRPs

RUREDIL X MESH GOLD is applied under ordinary working conditions applicable to cement mortars.

Tools may be cleaned with water

FRPs require cleaning with special solvents and, in many cases, tools cannot be used again.

1/6

Ruredil



Ruredil X Mesh Gold

PBO (Poliparafenilenbenzobisoxazolo) mesh in a stabilised inorganic matrix for flexural and shear strength reinforcement of concrete

Recommendations for use

a) Preparing the substrate

Eliminate dust and loose parts, then gently sand mechanically or with a high-pressure water jet cleaner to completely eliminate the thin layer of cement grout. Be careful to remove residues from surface treatments such as paint, release agents, insulation, etc. Make sure the surface is flat after this operation. In the presence of macroscopic surface defects, correct with mortars from the EXOCEM line. Always bevel corners if they are to be bound with composite material.

b) Preparing RUREDIL X MESH M750 matrix

Pour about 90% of the required amount of water into the mixer, then start the mixer and add RUREDIL X MESH M750 uninterruptedly to prevent lumps from forming. Mix for 2-3 minutes; add the rest of the water up to the quantity specified in the technical information sheet and mix for 1-2 minutes more. Let the mix rest for about 2-3 minutes, then mix again and apply.

c) Applying the RUREDIL X MESH GOLD system

Dampen the substrate, saturating it with water and being sure to remove excess water. Apply RUREDIL X MESH M750 with a smooth metal trowel in a layer about 3-4 mm thick; wait a couple of minutes and then bury RUREDIL X MESH GOLD in it. Apply a second layer of RUREDIL X MESH M750 about 3-4 mm thick to cover the mesh completely.

If the mortar becomes unworkable, do not add any more water, but mix for about 1-2 minutes and then continue applying.

The RUREDIL X MESH GOLD system should not be applied in sunshine, during the hot hours of the day in summer, or with moderate or strong winds.

If it is raining, shelter the structure from the rain.

d) Effect of temperature

The product should be applied at temperatures of between +5 °C and +35 °C; low temperatures (4-10 °C) will slow down setting considerably; while high temperatures (35-50 °C) will rapidly cause the mortar to become unworkable.

e) Curing

In environments exposed to sun and wind, protection may be required (CURING S or wet non-woven fabric). If it is about to rain, shelter the reinforcement appropriately.

Properties of system RUREDIL X MESH GOLD

PBO fibres properties

Density (g/cm ³)	1,36
Tensile strength (GPa)	5,6
Modulus of elasticity (GPa)	235
Ultimate deformation (%)	2,15
Breakdown temperature (°C)	650
Coefficient of thermal dilation (10 ⁻⁶ °C ⁻¹)	16

Mesh properties

Weight of PBO fibres in the mesh	88 g/m ²
Equivalent dry fabric thickness in the direction of the warp	0,0455 mm
Equivalent dry fabric thickness in the direction of the weft	0,0115 mm
Ultimate tensile stress of the warp per unit of width	264,0 kN/m
Ultimate tensile stress of the weft per unit of width	92,5 kN/m
Mesh weight (Substrate + PBO fibres)	110 ± 10 g/m ²

Inorganic matrix properties

Compressive strength (UNI EN 12390-1)	115
Specific weight of fresh mortar	1,90 ± 0,20 g/cm ³
Water (litres) for 100 kg of Ruredil X Mesh M750	25 - 27
Yield strength (dry product)	1,400
Compressive strength (UNI EN 12601)	≥ 20,0 MPa (at 28 days)
Tensile strength (UNI EN 12601)	≥ 4,0 MPa (at 28 days)
Flexural modulus of elasticity (UNI EN 12601)	≥ 7000 MPa (at 28 days)

Durability of the RUREDIL X MESH GOLD system

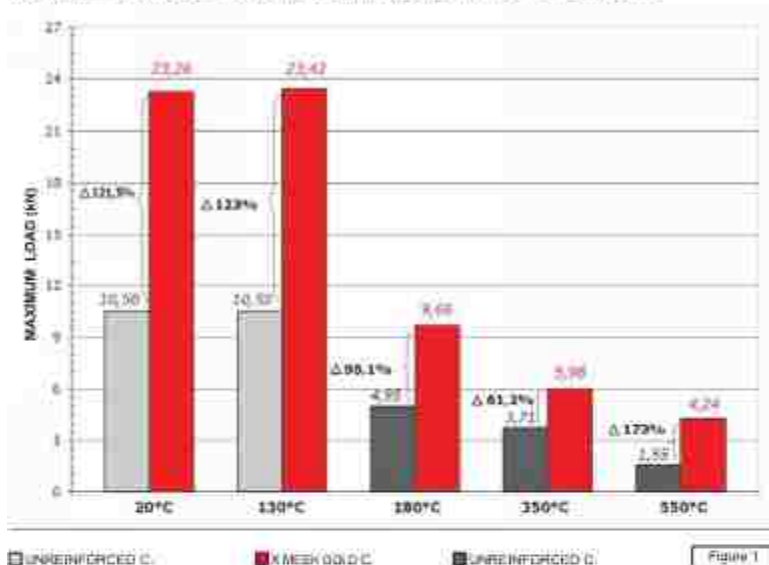
The mechanical properties of the RUREDIL X MESH GOLD system are not influenced by high temperatures and fire since the binding matrix is inorganic, as in all FRCM systems. The graphic shown in figure N.1 illustrates the load increase of samples reinforced with RUREDIL X MESH GOLD exposed to different temperatures; compared with samples without reinforcement. It should be pointed out that bending strength of concrete drastically decreases at temperatures exceeding +130 °C.



Ruredil X Mesh Gold

PBO (Poliparafenilenbenzobisoxazolo) mesh in a stabilised inorganic matrix for flexural and shear straight reinforcement of concrete

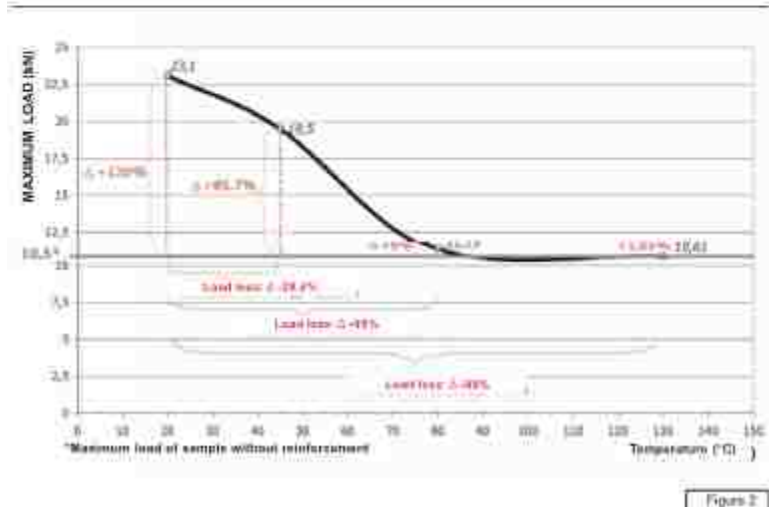
RUREDIL X MESH GOLD: LOAD INCREASE ACCORDING TO TEMPERATURE



In fact, traditional FRP systems completely lose their mechanical properties after one hour of exposure to +50°C because rigid resin becomes gummy. In addition, resin becomes unable to transfer concrete stress to carbon fibre as from +45°C (Figure N.2).

According to the accelerated tests performed at +80°C thermohygrometric conditions and 100% relative humidity, PBO-FRCM reinforcement does not have any chemical or mechanical alterations whereas C-FRP loses 100% of its efficiency (Figure N.3).

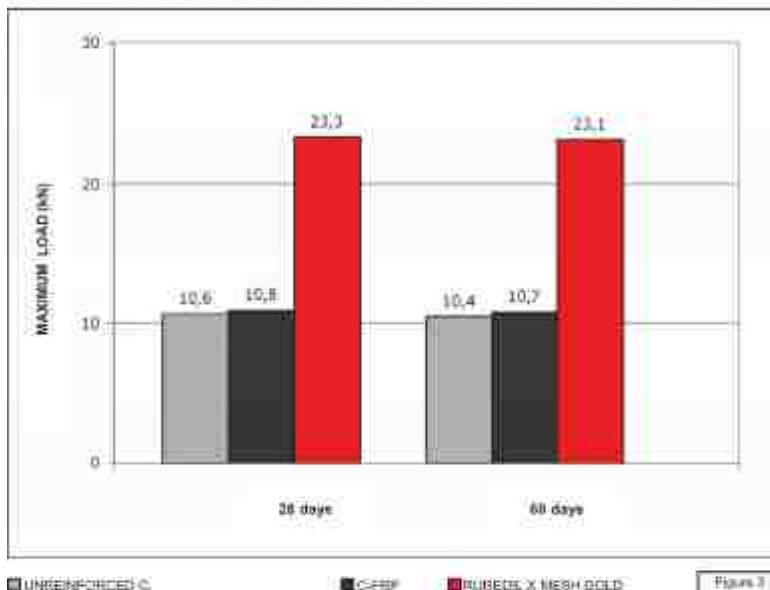
C- FRP: Maximum load according to temperature with equal period of exposure (1h)



Ruredil X Mesh Gold

PBO (Poliparafenilenbenzobisoxazolo) mesh in a stabilised inorganic matrix for flexural and shear strength reinforcement of concrete

RUREDIL X MESH GOLD vs. C-FRP: Maximum load at +80°C - 100% relative humidity



Bending stress reinforcement for concrete beams

The efficiency of concrete beams reinforced with RUREDIL X MESH GOLD has been carefully studied and tested. In fact, bending stress tests were performed on three or four points of concrete beams (40cm x 25cm) with 1.6 and 2.2m clearance. Different types of reinforcement were tested, similar to the ones referred to in figures N.4, N.5, N.6 and N.7. Certain test results concerning load - centre line displacement diagrams have been included in the above mentioned figures. The benefits of fibre reinforcement can be appreciated by the collapse load increase when compared with samples without reinforcement.

- Flex reinforcement of reinforced concrete beams with RUREDIL X MESH GOLD may be achieved with application to areas under tension and bracketing, resulting in an increase in distributed collapse load of around 10-50% or more of the current value.

- The typical reinforcement morphology consists of strips of variable length in the intrados, possibly folded over onto lateral surfaces and, where possible, with at least one U-shaped bracketing strip at the end of the longitudinal cover.

Figures N.4, N.5, N.6 and N.7 represent three possible reinforcement configurations for which the number of intrados layers required must be determined by calculating beam flexing. Some experimental load-arrow charts are illustrated in the same figures. Those charts have been obtained by means of bending tests on reinforced concrete beams, adopting similar configurations as those illustrated.

The first configuration (figure N.4) has an intrados reinforcement layer with U-shaped strips at the ends, while the second (figures N.5 and N.6) have two layers of intrados strips and U-shaped strips at the ends, and the third and last configuration (figure N.7) has intrados strips, intrados strips extended to the side surfaces and U-shaped strips for shear strength.

Use of the configuration shown in figure N.7, where possible.

4/5

Ruredil



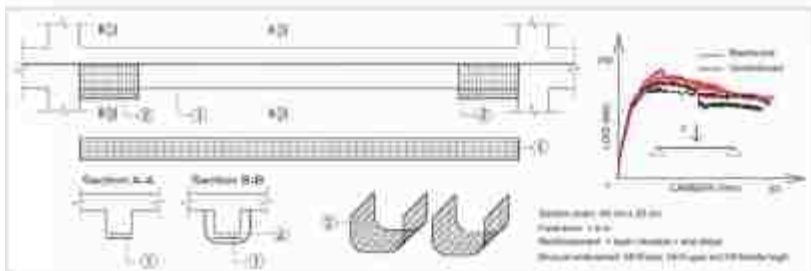


Figure 4

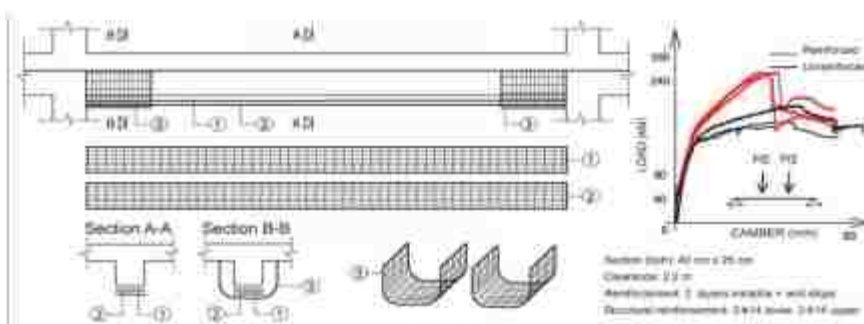


Figure 5

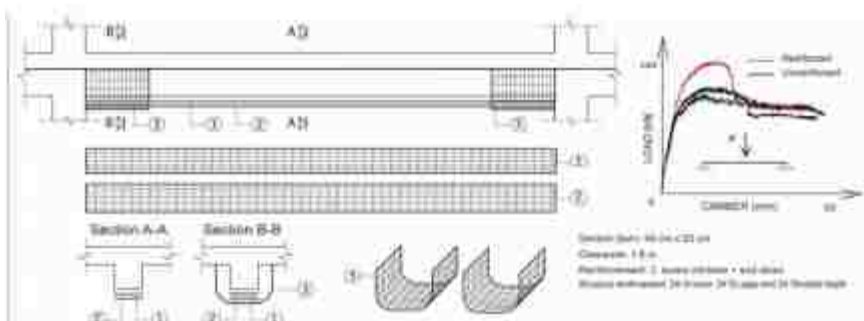


Figure 6

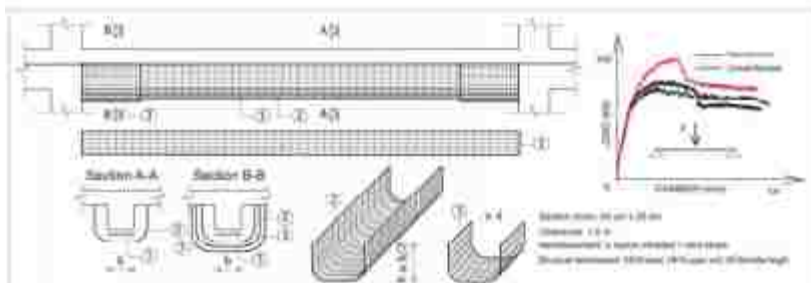


Figure 7

Ruredil X Mesh Gold

PBO (Poliparafenilenbenzobisoxazolo) mesh in a stabilised inorganic matrix for flexural and shear strength reinforcement of concrete

Design criteria for reinforcement with RUREDIL X Mesh GOLD for inflected reinforced concrete beams



According to the technical document CNR-DT 200/2004, the dimensioning of the flexural reinforcement can be performed at the ultimate state by considering a design resistance of the reinforcement taking the "intermediate peeling" crisis into account. With RUREDIL X MESH GOLD, usually this happens by sliding between fibres and cementitious matrix.

On the basis of these experiments performed, the following figures may be suggested for calculated tensile strength of the reinforcement (taking also the intermediate peeling crisis into account):

- with one reinforcement layer and U-shaped strips at the end (as shown in figure N.4):
 $F_{Rd} = 157.5 \text{ kN/m}$ (force per width unit of the reinforcement), corresponding to the calculated (warp) tensile strength $f_{Rk} = 3500 \text{ N/mm}^2$ and the calculated ultimate dilatation $\epsilon_{Rk} = 1.29\%$.
- with two reinforcement layers and U-shaped strips on the ends (as shown in figures N.5, N.6 and N.7):
 $F_{Rd} = 291.6 \text{ kN/m}$ (force per width unit of the reinforcement), corresponding to the calculated (warp) tensile strength $f_{Rk} = 3240 \text{ N/mm}^2$ and the calculated ultimate dilatation $\epsilon_{Rk} = 1.20\%$.

These figures are to be used exclusively for assessment of the ultimate momentum of reinforced sections.

The verification of peeling at the ends at the ultimate state can be carried out according to the technical document CNR-DT 200/2004, considering, for the various configurations, peeling tensions at the reinforcement end of about 20% of the calculated resistances indicated above.

The peeling of the reinforcement at the end can be prevented with U-shaped bracketing strips shown as  in figure 5 (which also improve shear strength) and the conformation shown as  in figure 7 in the surface layer of reinforcement.

The calculated resistances above can be achieved only if the concrete of the metal rod has suitable mechanical properties. Premature breakages of the metal rod might occur, also causing the crisis with sliding of the fibres in the cementitious matrix might not be achieved.

Careful assessment of the mechanical properties of the surface layer of the concrete is therefore recommended, as is reconstruction of the entire area covering the reinforcement rod if it is found to be inadequate and if the metal rods reveal a state of advanced corrosion.

Once the reinforcement section meeting the ultimate state has been determined, it is possible to check the operating limit and that concerning stresses.

Generally the pre-existing stress state (due to the existing loads upon reinforcement application) should be considered, from which a differential dilatation between support and reinforcement derives.

M.B. Reinforcement projects must in all cases, as for all composite materials, be based on careful assessment of the properties of the structure to be reinforced. Specifically, it is important to study the quality of the materials used (concrete and steel), the amount of metal reinforcement present, the condition of the concrete covering the reinforcement rods and corrosion of the rods. It is also essential to assess how the structure reacts to loads before and after reinforcement.

Designers should be acquainted with the mechanical properties and durability of the structural reinforcement under the different thermohygrometric conditions it will be used.

Before handing over the executive project, the designer must estimate, on the basis of essential tests conducted on the structure, the mechanical properties of the concrete and local damage (cracking and peeling) to be repaired. A total load test is strongly recommended both before and after reinforcement to verify the functioning of the composite-concrete joint.

Before accepting the work the supervisor of works must carefully check the composite material, taking into consideration the mechanical properties and stability under the different environmental conditions of application, compliance with the conditions specified by the engineer on the surfaces for adhesion, and conduct a preventive test in addition to the usual inspections of the installation, including application of the composite material.

Revision 06/2012. The present leaflet, covers, and replaces all the previous ones. This information contained in the present leaflet may be used as an indication and does not constitute any form of liability on the part of our companies. Ruredil and its logo are registered trademarks of the Ruredil Group. All other trademarks are the property of their respective owners.

Ruredil spa

Headquarters and plant: Via R. Bianco, 1 - I-20097 San Felice Milanese - Milan (ITALY)

Phone: +39 02 5076941 E-mail: info@ruredil.it Fax: +39 02 5072195 e-mail: info@ruredil.it website: www.ruredil.it

Branches: Algeria, Austria, Canada, Costa Rica, Chile, Cuba, Cyprus, Dominican Republic, Ecuador, Egypt, France, Greece, Iran, Morocco, Panama, Poland, Portugal, Qatar, Romania, Russia, Spain, Switzerland, Tunisia, Ukraine, U.S.A.

6/6



Strengthening Solutions

V-Wrap™ C200HM

High Modulus Carbon Fiber Fabric

struc'tural
TECHNOLOGIES

structuraltechnologies.com

+1-410-859-6539

Typical Data for V-Wrap C200HM

Storage Conditions:	Store dry at 40°F – 90°F (4°C – 32°C)
Color:	Black
Primary Fiber Direction:	0° (unidirectional)
Weight:	17.7 oz/yd ² (600 g/m ²)
Shelf life:	10 years

Fiber Properties (Dry)

Tensile Strength:	790,000 psi (5,440 MPa)
Tensile Modulus:	42 x 10 ⁶ psi (289,550 MPa)
Elongation:	1.9 %

Cured Laminate Properties

	Average Values
Tensile Strength:	180,000 psi (1,241 MPa)
Modulus of Elasticity:	14.24 x 10 ⁶ psi (98,181 MPa)
Elongation at Break:	1.27%
Thickness:	0.04 in. (1.02 mm)
Strength per Unit Width:	7,200 lbs/in. (1.26 kN/mm)

Design Values*

Tensile Strength:	155,000 psi (1,068 MPa)
Modulus of Elasticity:	14.0 x 10 ⁶ psi (96,527 MPa)
Elongation at Break:	1.1%
Thickness:	0.04 in. (1.02 mm)
Strength per Unit Width:	6,200 lbs/in. (1.09 kN/mm)



*Design properties are based on ACI 440 2R using average minus three standard deviations.

Description:

V-Wrap C200HM is a unidirectional carbon fiber fabric with fiber oriented in the 0° direction. V-Wrap C200HM system is field laminated using environmentally friendly, two-part 100% solids and high strength structural adhesives to form a carbon fiber reinforced polymer (CFRP) system used to reinforce structural elements.

Product Uses:

V-Wrap strengthening systems can be used to resolve strength deficiencies and increase the load carrying capacity of building, bridges, silos, chimneys, and other structures.

Loading Increases:

- Increasing the live loads capacity of floor systems
- Increasing shear and flexural strengths of reinforced and prestressed beams
- Increasing the axial capacity of columns
- Increasing the live load capacity of parking garages

Seismic Strengthening:

- Column confinement for ductility improvement
- Masonry and concrete shear walls strengthening

Damage to Structural Parts:

- Correct strength deficiency due to deterioration and corrosion
- Restore strength of structural elements damaged by fire

Change in Structural System:

- Load redistribution due to removal of walls, beams or columns
- Removal of slab sections for new openings

Design or Construction Defects:

- Insufficient amount of shear or flexural reinforcement
- Insufficient size and/or layout of reinforcement
- Insufficient reinforcing bar or lap splice length
- Low compressive strength in beams, slabs, and columns

Advantages:

- ICC-ES ESR-3606 listed product
- 0% VOC
- 100% Solvent free
- Non-corrosive reinforcement system
- Lightweight flexible fabric can be wrapped around complex shapes
- Used for shear, confinement or flexural strengthening
- High strength and high modulus
- Light weight
- Reduces crack width
- Alkali resistant
- Low aesthetic impact

Packaging:

Fabric: 24 in. width x 150 ft rolls
0.61 m width x 45.7 m rolls

Strengthening Solutions

V-Wrap™ C200HM

High Modulus Carbon Fiber Fabric

structural
TECHNOLOGIES

structuraltechnologies.com

+1-410-859-6539

How To Use:

Design:

Design should comply with ACI 440.2R or recognized design/specification entity, and is typically based on CFRP contribution determined by detailed analysis. Design values will vary based on project requirements and applicable environmental and strength reduction factors. Contact STRUCTURAL TECHNOLOGIES to determine applicable design factors.

Surface Preparation:

Surfaces to receive V-Wrap C200HM must be clean and sound. It must be dry and free of frost. All dust, laitance, grease, curing compounds, waxes, deteriorated materials, and other bond inhibiting materials must be removed from the surface prior to application. Existing uneven surfaces must be filled with appropriate epoxy putty or repair mortar. Use abrasive blasting, pressure wash, shotblast, grind or other approved mechanical means to achieve an open-pore texture with a concrete surface profile of CSP-3 or better (ICRI). In certain applications and at the engineer's discretion, the bond between the substrate and the fabric may be determined to be non-critical (such as in column confinement applications). All corners must be rounded to 1/2" radius minimum. A minimum overlap (or lap splice) of 6" is required to achieve continuity. The adhesive strength of the concrete may be verified after surface preparation by random pull-off testing (ASTM D7522) at the discretion of the engineer. Minimum tensile strength of 200 psi must be achieved.

Cutting V-Wrap C200HM:

Fabric can be cut to appropriate length by using a commercial quality heavy-duty scissors.

Application:

Installation of the V-Wrap C200HM strengthening system should be performed only by a specially trained, approved contractor. The V-Wrap C200HM strengthening system shall consist of V-Wrap C200HM carbon fabric and V-Wrap epoxy resins such as: V-Wrap 600, V-Wrap 700S, and V-Wrap 770.

Note the specified number of plies, ply widths, and fiber orientation. Mix resin components using recommended procedures on product datasheet. Apply one coat of V-Wrap epoxy as a primer to the surface using a nap roller. Fill minor

concrete defects such as bug holes and other imperfections with V-Wrap epoxy putty or V-Wrap epoxy mixed with fumed silica (thickened epoxy). Apply V-Wrap putty or thickened epoxy using a roller or trowel to primed surface. Adjust the gap between saturator rollers to approximately 42 mils. Using a saturator machine, pre-saturate the appropriate length of V-Wrap C200HM with V-Wrap epoxy adhesive as a saturant. Install the saturated FRP sheet. Use a rib roller to remove all air pockets and ensure intimate contact with the surface. If a splice is needed, a minimum 6" overlap is required. On multiple plies with splices, stagger the splice locations. If required, apply topcoat material.

Limitations:

- Design calculations must be approved by a licensed professional engineer.
- System is a vapor barrier.
- Concrete deterioration and steel corrosion must be resolved prior to application.
- Minimum application temperature is 40°F.

Storage:

Store material in a cool, dark space. Low humidity is recommended.

Handling:

Approved personal protection equipment should be worn at all times. Particle mask is recommended for possible airborne particles. Gloves are recommended when handling fabrics and resins to avoid skin irritation. Safety glasses are recommended to prevent eye irritation. Wear chemical resistant clothing/gloves/goggles. Ventilate area. In absence of adequate ventilation, use properly fitted NIOSH respirator.

Cleanup:

Dispose of material in accordance with local disposal regulations. Uncured material can be removed with approved solvents. Cured materials can only be removed mechanically.

First Aid:

In case of skin contact, wash thoroughly with soap and water. For eye contact, flush immediately with plenty of water; contact physician immediately. For respiratory problems, remove to fresh air. Wash clothing before reuse.

STRUCTURAL TECHNOLOGIES, LLC warrants its products to be free from manufacturing defects and to meet STRUCTURAL TECHNOLOGIES' current published properties when applied in accordance with STRUCTURAL TECHNOLOGIES' directions and tested in accordance with ASTM and STRUCTURAL TECHNOLOGIES Standards. User determines suitability of product for use and assumes all risks. Buyer's sole remedy shall be limited to the purchase price or replacement of product and excludes labor or the cost of labor. Any claim for breach of this warranty must be brought within one year of the date of purchase.

No other warranties expressed or implied including any warranty of merchantability or fitness for a particular purpose shall apply. STRUCTURAL TECHNOLOGIES shall not be liable for any consequential or special damages of any kind, resulting from any claim or breach of warranty, breach of contract, negligence or any legal theory. STRUCTURAL TECHNOLOGIES assumes no liability for use of this product in a manner to infringe on another's patent.

Page 2 of 2 • V-Wrap C200HM • Rev11/17/16

© 2016 Structural Technologies, LLC

Strengthening Solutions

V-Wrap™ 770

Epoxy Adhesive


structural
TECHNOLOGIES

 structuraltechnologies.com
+1-410-859-6539
Physical Properties⁽¹⁾:

Tensile Strength (ASTM D638):	8,800psi (60.7 MPa)
Tensile Modulus (ASTM D638):	400,000 psi (2,760 MPa)
Elongation at Break (ASTM D638):	4.4%
Flexural Strength (ASTM D790):	13,780 psi (95 MPa)
Flexural Modulus (ASTM D790):	380,000 psi (2,620 MPa)
Compressive Strength (ASTM D695):	12,450 psi (85.8 MPa)
Compressive Modulus (ASTM D695):	387,000 psi (2,670 MPa)
T_g (ASTM D4065):	180°F (82°C)
Density:	
Mixed Product:	9.17 lbs/gal (1.11 kg/L)
Part A:	9.7 lbs/gal (1.16 kg/L)
Part B:	7.9 lbs/gal (0.95 kg/L)
VOC Content (ASTM D2369):	0% VOC

(1) Curing schedule: 72 hours post cure at 140°F (60°C)

DESCRIPTION:

V-Wrap 770 is a two-part, 100% solids, epoxy for high strength composite bonding applications. V-Wrap 770 matrix material is combined with V-Wrap carbon and glass fabrics to provide a wet-layup composite for strengthening of structural members. It is formulated to provide high elongation to optimize properties of the V-Wrap composite systems. It provides a long working time for application, with no offensive odor. V-Wrap 770 may be thickened with fumed silica to produce a tack coat/putty or a finishing coat, depending upon the project requirements.

V-Wrap 770 is an environmentally friendly product with no Volatile Organic Compounds (VOC) or solvents.

PRODUCT USES:

V-Wrap 770 is a multi use epoxy that performs as a primer, tack coat/putty, and saturating resin for the V-Wrap carbon and glass fiber systems. For detailed uses see installation guides for V-Wrap strengthening systems. Fumed silica may be added to thicken the resin. The maximum ratio by volume is 1.5 of fumed silica to 1 part of resin.

ADVANTAGES:

- ICC-ES ESR-3606 listed product
- NSF/ANSI Standard 61 listed product for drinking water systems
- 100% solvent free
- Good high / low temperature properties
- High elongation

APPLICATION INFORMATION

Please refer to the NSF Listing for the NSF/ANSI 61 Listed Application.

SURFACE PREPARATION:

V-Wrap 770 should be applied to substrates that are free of protrusions, dry, exhibit an open pore structure, and are free of dust, oils or other surface contaminants or bond inhibiting materials.

BASIC APPLICATION EQUIPMENT:

Application processes for V-Wrap 770 will require mixing drill, mixing paddle, 1/4" nap rollers, steel rollers, paint brushes, trowels and saturator.

MIXING:

Mix ratio: Premix Part A for 2 minutes. Add the full contents of Part B pail to the full contents of Part A pail, or use equal fractions of each pail. Blend Part A and Part B with a mechanical mixer for 3 minutes until uniformly blended.

APPROXIMATE POT LIFE:

3 to 6 hours at 88°F (20°C)

COVERAGE RATES:**AS A PRIMER:**

Concrete:	225 ft ² /gal (5.5 m ² /L)
Masonry: (Concrete)	125 ft ² /gal (3.0 m ² /L)
Masonry: (Clay)	200 ft ² /gal (4.9 m ² /L)

AS PUTTY/TACK COAT:

Filler: 60 ft²/gal (1.5 m²/L)
(Depending on surface roughness)

Strengthening Solutions

V-Wrap™ 770

Epoxy Adhesive


structural
 TECHNOLOGIES

structuraltechnologies.com

+1-410-859-6539

AS SATURANT:

V-Wrap C100	80 ft ² /gal (1.9 m ² /L)
V-Wrap C200	60 ft ² /gal (1.5 m ² /L)
V-Wrap C200H	60 ft ² /gal (1.5 m ² /L)
V-Wrap C400H	40 ft ² /gal (1 m ² /L)
V-Wrap EG50	60 ft ² /gal (1.5 m ² /L)

Coverage rates may vary based on installation procedure and fabric type. Contact STRUCTURAL TECHNOLOGIES for coverage rates.

LIMITATIONS:

Only apply V-Wrap 770 when the ambient temperature is between 40°F and 100°F (4°C to 38°C). Topcoat selection should be based upon requirements for protection from environmental exposures, aesthetics, and fire protection/burn characteristics.

CLEAN UP:

Use methyl ethyl ketone or acetone. Observe fire and health precautions when using solvents. Dispose of in accordance with local regulations.

OBSERVE WORKING TIME LIMITATIONS:

Mix no more material than can be applied within the work time period. Available work time, temperature and complexity of the application will determine how much material should be mixed at one time. Keep material cool and in shaded area, away from direct sunlight in warm weather. During hot weather, work time can be extended by keeping the material cool before and after mixing or by immersing the pot in ice water.

HANDLING PROPERTIES:

Color:	
Mixed	Clear
Part A	Clear
Part B	Clear

SHELF LIFE:

Stored at 70°F (21°C); 24 months (Parts A and B)

PACKAGING:

	Volume	Weight	Package
Part A	2.8 gal	27.3 lbs	5 gal pail
Part B	1.15 gal	9.1 lbs	5 gal pail

STORAGE:

Store in a cool, dry area (40°F and 90°F [4°C to 32°C]) away from direct sunlight, flame or other hazards.

SAFETY:

WARNING: Vapor may be harmful. Contains epoxy adhesive and curing agent. May cause skin sensitivity or other allergic responses. Keep away from heat, sparks or open flame. In enclosed areas or where ventilation is poor use an approved air mask and utilize adequate safety precautions to prevent fire or explosion. In case of skin contact, wash with soap and water. For eyes, flush immediately (seconds count) with water for 15 minutes and CALL A PHYSICIAN. If swallowed, CALL A PHYSICIAN IMMEDIATELY.

HANDLING:

Approved personal protection equipment should be worn at all times. Particles mask is recommended when handling airborne particles. Gloves are recommended when handling fabrics and resins to avoid skin irritation. Safety glasses are recommended to prevent eye irritation. Wear chemical resistant clothing /gloves/goggles. Ventilate area. In absence of adequate ventilation, use properly fitted NIOSH respirator. Product Material Safety Data Sheets (MSDS) are available and should be consulted and on hand whenever handling these products.

These products are for professional and industrial use only and are to be installed by trained and qualified applicators. Trained applicators must follow installation instructions.

MAINTENANCE:

Periodically inspect the applied material and repair localized areas as needed.

STRUCTURAL TECHNOLOGIES, LLC warrants its products to be free from manufacturing defects and to meet STRUCTURAL TECHNOLOGIES' current published properties when applied in accordance with STRUCTURAL TECHNOLOGIES' directions and tested in accordance with ASTM and STRUCTURAL TECHNOLOGIES Standards. User determines suitability of product for use and assumes all risks. Buyer's sole remedy shall be limited to the purchase price or replacement of product and excludes labor or the cost of labor. Any claim for breach of this warranty must be brought within one year of the date of purchase.

No other warranties expressed or implied including any warranty of merchantability or fitness for a particular purpose shall apply. STRUCTURAL TECHNOLOGIES shall not be liable for any consequential or special damages of any kind, resulting from any claim or breach of warranty, breach of contract, negligence or any legal theory. STRUCTURAL TECHNOLOGIES assumes no liability for use of this product in a manner to infringe on another's patent.

Page 2 TD-VWR770-770 - Rev. 5-31-2014

© 2014 Structural Technologies, LLC

Simpson Strong-Tie® Composite Strengthening Systems

CSS-CM

Cementitious Matrix



DESCRIPTION

CSS-CM is a one-component, shrinkage-compensated, polypropylene-fiber reinforced cementitious matrix designed to be field installed with CSS-UGG and CSS-BCG carbon grids to create a fabric-reinforced cementitious matrix (FRCM) composite for structural reinforcement applications. This product is part of the tested assembly in UL Design No. NR59, which achieved a four-hour fire rating when subjected to ASTM E119 / UL 263 full-scale fire testing. Please refer to UL Online Certifications Directory for the UL listing.

MATERIAL PROPERTIES

Matrix Properties

Unit Weight	140 lb./ft. ³ (2,240 kg/m ³)
Set Times (ASTM C191)	Initial Set: <5 hr. Final Set: <8 hr.

Matrix Test Properties¹

Property	Design Value
Tensile Modulus (ASTM C469)	3,880,000 psi (26.8 GPa) @ 28 days
Rapid Chloride Penetration (ASTM C1202)	<500 coulombs (very low) @ 28 days
Freeze/Thaw Resistance (ASTM C666, Proc. A)	93.7% RDM @ 300 cycles
Salt Scaling Resistance (ASTM C672)	0.06 lb./ft. ² (very slight) @ 50 cycles
Sulfate Resistance (ASTM C1012)	+0.02% @ 6 mo.
Direct Tensile Bond Strength (ASTM C1583)	28 day: 390 psi (2.7 MPa)
Direct Shear Bond Strength (Michigan DOT)	28 day: 300 psi (2.1 MPa)
Split Shear Bond Strength (ASTM C882, mod.)	28 day: 2,520 psi (18.1 MPa)
Splitting Tensile Strength (ASTM C496)	28 day: 700 psi (4.8 MPa)
Flexural Strength (ASTM C348)	28 day: 1,000 psi (6.9 MPa)
Compressive Strength (ASTM C109)	1 day: 3,000 psi (21 MPa) 7 day: 4,300 psi (43 MPa) 28 day: 7,500 psi (52 MPa)
Drying Shrinkage (ASTM C157, mod.1)	+0.09% @ 28 days

¹ The data herein is based on laboratory testing under controlled conditions. Variations may result from mixing methods and job site conditions. All testing performed at 73°F (23°C) and 50% R.H., unless otherwise noted. Results were obtained using 0.72 lb. galons (2.7 L) water per 25 lb. (23 kg) bag.

² ASTM C109 modified 2'x4'x12" specimens are tested at 50% RH and 73°F.

PERFORMANCE FEATURES

- High strength
- Ambient cure
- Non-corrosive
- Molds to fit various shapes
- Low aesthetic impact
- Compatible with many finish coatings
- UL listed (www.ul.com/database)

APPLICATIONS

Seismic Retrofit

- Shear strengthening
- Displacement/ductility
- Life safety

Load Rating Upgrade

- Increased live loads
- New equipment
- Change of use

STRUCTURES

- Buildings
- Bridges
- Parking garages
- Chimneys
- Piers/wharfs
- Tunnels
- Pipes

ELEMENTS

- Columns
- Beams
- Slabs
- Walls
- Piles
- Pier caps

SUBSTRATES

- Concrete
- Masonry

PACKAGING

Bag Size
55 lb. (24.9 kg)

Model No.
CSS-CM



strongtie.com/RPS | (800) 999-5029

© 2017 Simpson Strong-Tie Company

CSS-CM Cementitious Matrix

2

Design

The number of layers, dimensions, and detailing of CSS-CM system shall be designed in accordance with ACI 549 or another recognized design guideline/code in order to meet the design performance specified for the application. Contact Simpson Strong-Tie for design and technical support.

Surface Preparation

Prepare surface and any exposed reinforcement per ICCI Guideline No. 310.1R. Concrete shall be prepared to achieve a minimum W (6 mm) amplitude (CSP-6-0 in accordance with ICCI Guideline No. 310.2F) by means of sand blasting, shot blasting, or water blasting. Application surfaces shall be clean, sound, and free of standing water at time of application. All dirt, laitance, grease, curing compounds, and other foreign materials that may hinder the bond must be removed before installation. All corners to be covered with grid and matrix shall be rounded to a $3/4"$ (19 mm) minimum radius using a grinder. Wet the substrate for at least 24 hours to a saturated surface dry condition prior to FRCM application.

Mixing

Start with 95% of the total mixing water recommendation depending on the desired consistency of the shot mortar. Consult the printed instructions on the product package for the maximum recommended amount of mixing water. Mix with a mechanical mixer at least 3 minutes adding the remaining 10% of the recommended total water if necessary until a homogeneous mixture with the desired consistency is formed. The mixture should rest 1 minute and then mixed another 10 seconds before applying. Do not add additional water after the setting process is started.

Application

CSS installation shall be performed only by contractors and personnel that have been properly trained by Simpson Strong-Tie. CSS-CM cementitious matrix can be pumped and projected with traditional shotcrete equipment. If required, CSS-CM cementitious matrix may be used to patch voids and defects no deeper than 2" (51 mm). Immediately place $W-12$ (6-13 mm) layer of CSS-CM cementitious matrix, then immediately set CSS grid into wet CSS-CM layer. Follow with additional layers of CSS grid, if required, set into $W-12$ (6-13 mm) layers of CSS-CM. Finish with a final layer of CSS-CM at $W-12$ (6-13 mm) thick and screed/trowel to desired finish. If a layer of matrix is allowed to cure with more layers to follow, the first layer must be cleared with water pressure before the next matrix layer can be applied.

Curing

Installation shall be kept humid and protected against heat and wind for 3 to 5 days by wet curing or using an ASTM C909 compliant water-based curing compound. The use of curing compounds may affect adhesion of subsequent surface treatments. SSD surface conditions and proper curing procedures are critical at minimum application thickness to prevent premature drying or cracking.

Yield

A 55 lb (24.9 kg) bag of CSS-CM will yield approximately 0.43 ft.³ (0.012 m³) of finished material.

Limitations

CSS installation shall take place only when the ambient and substrate temperatures are between 41°F (5°C) and 86°F (30°C).

CAUTION

May cause serious eye and skin irritation or damage. When combined with water may cause moderate to severe alkali burns.

Protective Measures: The use of safety glasses and chemically resistant gloves is recommended. Use appropriate clothing to minimize skin contact. The use of a NIOSH-approved respirator is required to protect respiratory tract when ventilation is not adequate to limit exposure below the permissible exposure limit (PEL). Refer to Safety Data Sheet (SDS) available at strongtie.com/ads for detailed information.

FIRST AID

Eye Contact: Immediately flush eyes with plenty of cool water for at least 15 minutes while holding the eyes open.

If redness, burning, blurred vision, or swelling persists. **CONSULT A PHYSICIAN**

Skin Contact: Remove product and wash affected area with soap and water. Do not apply greases or ointments.

Remove contaminated clothing. Wash clothing with soap and water before reuse. If redness, burning, or swelling persists. **CONSULT A PHYSICIAN**

Ingestion: DO NOT INDUCE VOMITING. **CONSULT A PHYSICIAN OR POISON CONTROL CENTER**

IMMEDIATELY FOR CURRENT INFORMATION. Never administer anything by mouth to an unconscious person.

Place mouth out with water. Never leave affected person unattended. If vomiting occurs spontaneously, lay affected person on their side, keeping head below hips to prevent aspiration of material into lungs.

Inhalation: Remove affected person to fresh air. If affected person continues to experience difficulty breathing. **CONSULT A PHYSICIAN**

CSS-CM Cementitious Matrix

3

CLEAN-UP

Spills: Sweep or vacuum material and place in a suitable container. Keep out of sewers, storm drains, surface waters, and soils.

Surface Clean: Remove any residue with hot soapy water. Cured material can be removed only by mechanical means.

Tools and Equipment: Clean with soap and water immediately after use.

Skin: Use a non-toxic, pH-neutral soap, citrus-based hand cleaner, or waterless hand-cleanser foam. Never use solvents to remove product from skin.

Disposal: Dispose of container and unused contents in accordance with federal, state, and local requirements. Containers may be recycled; consult local regulations for exceptions.

SHELF LIFE

1 year in unopened packaging.

STORAGE

Store material in a dry area with no exposure to moisture.

LIMITED WARRANTY

See strongtie.com for information.



IMPORTANT INFORMATION

It is the responsibility of each purchaser and user of each Product to determine the suitability of each Product for its intended use. Prior to using any Product, consult a qualified design professional for advice regarding the suitability and use of the Product, including whether the code(s) for any structural building element may be amended by a local authority having jurisdiction. The highest local code, applicable and better or similar methods and standards contained in the product label, Product Data Sheet(s), Safety Data Sheet(s) and/or strongtie.com website shall apply. The product is not for use in applications not specified in the label. **KEEP OUT OF REACH OF CHILDREN**. **Preparation 02:** Product mixed with pre-mixed concrete/ready-mix concrete (California as shown) in a ratio (see the label) for application.

strongtie.com/RPS | (800) 999-6099

© 2012 Dowler-Strong-Tie Company, Inc.

T-R-CSSCM | 1/18

Simpson Strong-Tie® Composite Strengthening Systems

CSS-UCG

Unidirectional Carbon Grid



DESCRIPTION

CSS-UCG is a unidirectional, high-strength, non-corrosive carbon grid designed to be field installed with CSS-CM cementitious matrix to create a fabric-reinforced cementitious matrix (FRCM) composite for structural reinforcement applications. This product is part of the listed assembly in UL Design No. N859, which achieved a four-hour fire rating when subjected to ASTM E119 / UL 253 full-scale fire testing. Please refer to UL Online Certifications Directory for the UL listing.

MATERIAL PROPERTIES

Grid Properties

Weight	13 oz./yd. ² (440 g/m ²)
Weight of fibers	8.3 oz./yd. ² (280 g/m ²)
Equivalent Dry Fabric Thickness (in strong direction)	0.0062 in. (0.157 mm)
Ultimate Tensile Strength	21 kip/ft. (450 kN/m)
Ultimate Tensile Strain	1.5%
Axial Stiffness by width unit	2,067 kip/in. (30,000 kN/m)
Area by width unit	0.0062 in. ² /in. (157 mm ² /m)
Color	Gray

Cured Composite Properties¹

Property	Design Value ²
Cracked Tensile Modulus	7.1 x 10 ³ psi (49,000 MPa)
Ultimate Tensile Strain	5.1%
Ultimate Tensile Strength	128,300 psi (885 MPa)
Lap Tensile Strength	121,000 psi; 12" lap (834 MPa; 30 cm)
Thickness per Layer	0.5 in. (13 mm)

1. When installed with CSS-CM cementitious matrix.

2. Average tensile strength and strain minus one standard deviation per ACI 944. Strain values apply on average.



STRUCTURAL CONCRETE
FIBER-REINFORCED COMPOSITE SYSTEM
FIRE RESISTANCE CLASSIFICATION
SEE UL FIRE RESISTANCE DIRECTORY
-R37897-

PERFORMANCE FEATURES

- High strength
- Ambient Cure
- Non-corrosive
- Molds to fit various shapes
- Low aesthetic impact
- Compatible with many finish coatings
- UL listed (www.ul.com/ database)

APPLICATIONS

Selamic Retrofit

- Shear strengthening
- Displacement/ductility
- Life safety

Load Rating Upgrade

- Increased live loads
- New equipment
- Change of use

Damage Repair

- Oxidation/corrosion
- Blast/vibratic impact

Defect Remediation

- Size/layout errors
- Low concrete strengths

Biset Mitigation

- Progressive collapse

STRUCTURES

- Buildings
- Bridges
- Parking garages
- Chimneys
- Piers/wharfs
- Tunnels
- Pipes

ELEMENTS

- Columns
- Beams
- Slabs
- Walls
- Piles
- Pier caps

SUBSTRATES

- Concrete
- Masonry

PACKAGING

Roll Size (Width x Length)	Model No.
77 in. (1.96 m) x 164 ft. (50 m)	CSS-UCG19650

strongtie.com/RPS / (800) 999-5099

© 2018 Simpson Strong-Tie Company Inc.

APPENDIX G.

TEE-BEAM ANALYSIS DEFLECTION CALCULATIONS

Theoretical Model Calculations Summary

Theoretical deflections in in. w/ barrier	Location on span				
	0	L/4	L/2	3L/4	L
	0	9.05	18.1	27.15	36.2
Stop 1, Interior	0	-0.0759	-0.0993	-0.0645724	0
Stop 1, Exterior	0	-0.0606	-0.0793	-0.0515959	0
Stop 2, Interior	0	-0.0756	-0.0986	-0.0641064	0
Stop 2, Exterior	0	-0.0604	-0.0788	-0.0512235	0
Stop 3, Interior	0	-0.0758	-0.0992	-0.0645251	0
Stop 3, Exterior	0	-0.0606	-0.0792	-0.051558	0

Theoretical deflections in in. no barrier	Location on span				
	0	L/4	L/2	3L/4	L
	0	9.05	18.1	27.15	36.2
Stop 1, Interior	0	-0.1901	-0.2487	-0.1617997	0
Stop 1, Exterior	0	-0.2167	-0.2835	-0.1844205	0
Stop 2, Interior	0	-0.1894	-0.2471	-0.160632	0
Stop 2, Exterior	0	-0.2158	-0.2817	-0.1830895	0
Stop 3, Interior	0	-0.1899	-0.2485	-0.161681	0
Stop 3, Exterior	0	-0.2165	-0.2832	-0.1842852	0

I with curb		no curb	with curb	difference	Adjusted I
Long Span	Interior	37332	-	-	93543
	Exterior	32753	157666	124914	117070
Short Span	Interior	22790	-	-	77432
	Exterior	20523	129807	109284	102486

E	L (in)	DF (one wheel)	DF/2
4415201	434.1	1.181	0.590

				Theoretical Δ Locations (x)				
Stop 1, Interior 50% barrier contribution				0	L/4	L/2	3L/4	L
Load	P (lbs)	a (in)	b (in.)	0.0	108.5	217.1	325.6	0.0
B1	14180	0	434.1	0	0.0000	0	0	0
B2	12010	121.05	313.05	0	0.0298	0.0372	0.0238	0
B3	12010	177.05	257.05	0	0.0344	0.0472	0.0312	0
A3	12140	173.05	261.05	0	0.0347	0.0472	0.0311	0
A2	12140	117.05	317.05	0	0.0296	0.0366	0.0234	0
A1	13900	0	434.1	0	0.0000	0	0	0
total Δ (in.)				0.0000	0.1285	0.1682	0.1094	0.0000
total Δ * DF (in.)				0	0.07587637	0.0993	0.0646	0
total Δ * DF (mm)				0	1.92725967	2.5212	1.6401	0

				Theoretical Δ Locations (x)				
Stop 2, Interior 50% barrier contribution				0	L/4	L/2	3L/4	L
Load	P (lbs)	a (in)	b (in.)	0.0	108.5	217.1	325.6	0.0
B1	14180	0	0	0	0	0	0	0
B2	12010	117.05	317.05	0	0.02925065	0.0362	0.0231	0
B3	12010	173.05	261.05	0	0.03432379	0.0467	0.0308	0
A3	12140	174.05	260.05	0	0.03472838	0.0473	0.0312	0
A2	12140	118.05	316.05	0	0.02971907	0.0368	0.0235	0
A1	13900	0	434.1	0	0	0	0	0
total Δ (in.)				0.0000	0.1280	0.1671	0.1086	0.0000
total Δ * DF (in.)				0	0.07556847	0.0986	0.0641	0
total Δ * DF (mm)				0	1.91943926	2.5052	1.6283	0

				Theoretical Δ Locations (x)				
Stop 3, Interior 50% barrier contribution				0	L/4	L/2	3L/4	L
Load	P (lbs)	a (in)	b (in.)	0.0	108.5	217.1	325.6	0.0
B1	14180	0	0	0	0	0	0	0
B2	12010	125.05	309.05	0	0.03038814	0.0381	0.0244	0
B3	12010	181.05	253.05	0	0.03453291	0.0476	0.0316	0
A3	12140	169.05	265.05	0	0.03454382	0.0467	0.0307	0
A2	12140	113.05	321.05	0	0.02893668	0.0356	0.0227	0
A1	13900	0	434.1	0	0	0	0	0
total Δ (in.)				0.0000	0.1284	0.1680	0.1093	0.0000
total Δ * DF (in.)				0	0.07579259	0.0992	0.0645	0
total Δ * DF (mm)				0	1.92513172	2.5189	1.6389	0

$$\Delta_x \text{ (when } x > a) = \frac{Pa(L-x)}{6EI} (2Lx - x^2 - a^2)$$

$$\Delta_x \text{ (when } x < a) = \frac{Pbx}{6EI} (L^2 - b^2 - x^2)$$

Stop 1, Exterior 75% barrier contribution				Theoretical Δ Locations (x)				
Load	P (lbs)	a (in)	b (in.)	0	L/4	L/2	3L/4	L
B1	14180	0	0	0.0	108.5	217.1	325.6	0.0
B2	12010	121.05	313.05	0	0.0238414	0.02969	0.01899	0
B3	12010	177.05	257.05	0	0.0275215	0.0377	0.02491	0
A3	12140	173.05	261.05	0	0.0277229	0.03773	0.02485	0
A2	12140	117.05	317.05	0	0.0236254	0.02924	0.01867	0
A1	13900	0	434.1	0	0	0	0	0
total Δ (in.)				0.0000	0.1027	0.1344	0.0874	0.0000
total Δ * DF (in.)				0	0.0606282	0.07931	0.0516	0
total Δ * DF (mm)				0	1.5399551	2.01451	1.31054	0

Stop 2, Exterior 75% barrier contribution				Theoretical Δ Locations (x)				
Load	P (lbs)	a (in)	b (in.)	0	L/4	L/2	3L/4	L
B1	14180	0	0	0	108.5	217.1	325.6	0.0
B2	12010	117.05	317.05	0	0.0233724	0.02893	0.01847	0
B3	12010	173.05	261.05	0	0.027426	0.03732	0.02458	0
A3	12140	174.05	260.05	0	0.0277493	0.03783	0.02493	0
A2	12140	118.05	316.05	0	0.0237467	0.02944	0.0188	0
A1	13900	0	434.1	0	0	0	0	0
total Δ (in.)				0.0000	0.1023	0.1335	0.0868	0.0000
total Δ * DF (in.)				0	0.0603821	0.07881	0.05122	0
total Δ * DF (mm)				0	1.5337063	2.00172	1.30108	0

Stop 3, Exterior 75% barrier contribution				Theoretical Δ Locations (x)				
Load	P (lbs)	a (in)	b (in.)	0	L/4	L/2	3L/4	L
B1	14180	0	0	0	108.5	217.1	325.6	0.0
B2	12010	125.05	309.05	0	0.0242813	0.03043	0.01949	0
B3	12010	181.05	253.05	0	0.0275931	0.03805	0.02522	0
A3	12140	169.05	265.05	0	0.0276018	0.03731	0.0245	0
A2	12140	113.05	321.05	0	0.0231215	0.02844	0.01813	0
A1	13900	0	434.1	0	0	0	0	0
total Δ (in.)				0.0000	0.1026	0.1342	0.0873	0.0000
total Δ * DF (in.)				0	0.0605612	0.07924	0.05156	0
total Δ * DF (mm)				0	1.5382548	2.01267	1.30957	0

Step 1, Interior no barrier contribution				Theoretical Δ Locations (x)				
Load	P (lbs)	a (in.)	b (in.)	0	L/4	L/2	3L/4	L
B1	14180	0	0	0.0	108.5	217.1	325.6	0.0
B2	12010	121.05	313.05	0	0.07476	0.09311	0.05954	0
B3	12010	177.05	257.05	0	0.0863	0.11824	0.07811	0
A3	12140	173.05	261.05	0	0.08694	0.11831	0.07792	0
A2	12140	117.05	317.05	0	0.07409	0.09169	0.05854	0
A1	13900	0	434.1	0	0	0	0	0
total Δ (in.)				0.0000	0.3221	0.4213	0.2741	0.0000
total Δ * DF (in.)				0	0.19012	0.24871	0.1618	0
total Δ * DF (mm)				0	4.82915	6.3173	4.10971	0

Step 2, Interior no barrier contribution				Theoretical Δ Locations (x)				
Load	P (lbs)	a (in.)	b (in.)	0	L/4	L/2	3L/4	L
B1	14180	0	0	0.0	108.5	217.1	325.6	0.0
B2	12010	117.05	317.05	0	0.07329	0.09071	0.05791	0
B3	12010	173.05	261.05	0	0.08601	0.11704	0.07708	0
A3	12140	174.05	260.05	0	0.08702	0.11862	0.07818	0
A2	12140	118.05	316.05	0	0.07447	0.09231	0.05895	0
A1	13900	0	434.1	0	0	0	0	0
total Δ (in.)				0.0000	0.3208	0.4187	0.2721	0.0000
total Δ * DF (in.)				0	0.18935	0.24713	0.16063	0
total Δ * DF (mm)				0	4.80955	6.27721	4.08005	0

Step 3, Interior no barrier contribution				Theoretical Δ Locations (x)				
Load	P (lbs)	a (in.)	b (in.)	0	L/4	L/2	3L/4	L
B1	14180	0	0	0.0	108.5	217.1	325.6	0.0
B2	12010	125.05	309.05	0	0.07614	0.09544	0.06113	0
B3	12010	181.05	253.05	0	0.08653	0.11934	0.07909	0
A3	12140	169.05	265.05	0	0.08656	0.11699	0.07683	0
A2	12140	113.05	321.05	0	0.07251	0.0892	0.05686	0
A1	13900	0	434.1	0	0	0	0	0
total Δ (in.)				0.0000	0.3217	0.4210	0.2739	0.0000
total Δ * DF (in.)				0	0.18991	0.24849	0.16168	0
total Δ * DF (mm)				0	4.82382	6.31155	4.1067	0

Step 1, Exterior no barrier contribution				Theoretical Δ Locations (x)				
				0	L/4	L/2	3L/4	L
Load	P (lbs)	a (in.)	b (in.)	0.0	108.5	217.1	325.6	0.0
B1	14180	0	0	0	0	0	0	0
B2	12010	121.05	313.05	0	0.08522	0.10613	0.06786	0
B3	12010	177.05	257.05	0	0.09837	0.13477	0.08903	0
A3	12140	173.05	261.05	0	0.09909	0.13485	0.08881	0
A2	12140	117.05	317.05	0	0.08444	0.10451	0.06672	0
A1	13900	0	434.1	0	0	0	0	0
total Δ (in.)				0.0000	0.3671	0.4803	0.3124	0.0000
total Δ * DF (in.)				0	0.2167	0.28348	0.18442	0
total Δ * DF (mm)				0	5.5043	7.20051	4.68428	0

Step 2, Exterior no barrier contribution				Theoretical Δ Locations (x)				
				0	L/4	L/2	3L/4	L
Load	P (lbs)	a (in.)	b (in.)	0.0	108.5	217.1	325.6	0.0
B1	14180	0	0	0	0	0	0	0
B2	12010	117.05	317.05	0	0.08354	0.10339	0.06601	0
B3	12010	173.05	261.05	0	0.09803	0.1334	0.08786	0
A3	12140	174.05	260.05	0	0.09919	0.1352	0.08911	0
A2	12140	118.05	316.05	0	0.08488	0.10521	0.0672	0
A1	13900	0	434.1	0	0	0	0	0
total Δ (in.)				0.0000	0.3656	0.4772	0.3102	0.0000
total Δ * DF (in.)				0	0.21583	0.28169	0.18309	0
total Δ * DF (mm)				0	5.48197	7.15481	4.65047	0

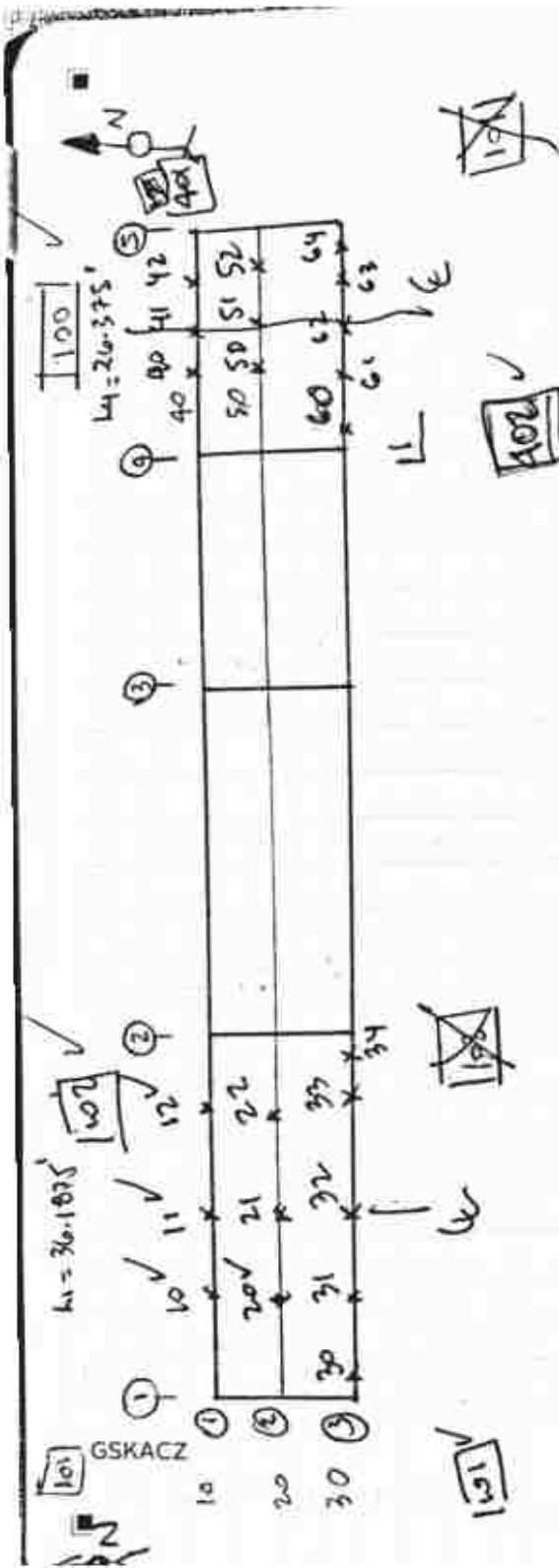
Step 3, Exterior no barrier contribution				Theoretical Δ Locations (x)				
				0	L/4	L/2	3L/4	L
Load	P (lbs)	a (in.)	b (in.)	0.0	108.5	217.1	325.6	0.0
B1	14180	0	0	0	0	0	0	0
B2	12010	125.05	309.05	0	0.08679	0.10878	0.06968	0
B3	12010	181.05	253.05	0	0.09863	0.13602	0.09015	0
A3	12140	169.05	265.05	0	0.09866	0.13335	0.08757	0
A2	12140	113.05	321.05	0	0.08264	0.10167	0.06481	0
A1	13900	0	434.1	0	0	0	0	0
total Δ (in.)				0.0000	0.3667	0.4798	0.3122	0.0000
total Δ * DF (in.)				0	0.21647	0.28323	0.18429	0
total Δ * DF (mm)				0	5.49822	7.19395	4.68084	0

Load Test Data Summary

Test 1	Round	Point #	Location	Corrected Delta (in/mm)		
	1	101	---	0.000	0.0	Reference
	1	10	9.3	-0.051	-1.3	Girder 1
	1	11	18.1	-0.067	-1.7	
	1	12	26.9	-0.048	-1.2	
	1	20	9.2	-0.052	-1.3	Girder 2
	1	21	18.1	-0.077	-2.0	
	1	22	27.0	-0.063	-1.6	
	1	30	1.6	-0.008	-0.2	Girder 3
	1	31	9.1	-0.034	-0.9	
	1	32	18.1	-0.045	-1.1	
	1	33	27.0	-0.031	-0.8	
	1	34	34.9	0.000	0.0	
	1	102	---	0.000	0.0	Reference

Test 2	Round	Point #	Location	Corrected Delta (in/mm)		
	15	101	---	0.000	0.0	Reference
	15	10	9.3	-0.040	-1.0	Girder 1
	15	11	18.1	-0.045	-1.1	
	15	12	26.9	-0.033	-0.8	
	15	20	9.2	-0.0524	-1.3	Girder 2
	15	21	18.1	-0.0708	-1.8	
	15	22	27.0	-0.0564	-1.4	
	15	30	1.6	-0.007	-0.2	Girder 3
	15	31	9.1	-0.040	-1.0	
	15	32	18.1	-0.054	-1.4	
	15	33	27.0	-0.040	-1.0	
	15	34	34.9	0.000	0.0	
	15	102	---	0.000	0.0	Reference

Test 3	Round	Point #	Location	Corrected Delta (in/mm)		
	16	101	---	0.000	0.0	Reference
	16	10	9.3	-0.017	-0.4	Girder 1
	16	11	18.1	-0.024	-0.6	
	16	12	26.9	-0.021	-0.5	
	16	20	9.2	-0.0468	-1.2	Girder 2
	16	21	18.1	-0.0616	-1.6	
	16	22	27.0	-0.0508	-1.3	
	16	30	1.6	-0.002	-0.1	Girder 3
	16	31	9.1	-0.042	-1.1	
	16	32	18.1	-0.059	-1.5	
	16	33	27.0	-0.042	-1.1	
	16	34	34.9	-0.003	-0.1	
	16	102	---	0.000	0.0	Reference



P0058
7/3/19

marks

- 71 POINT RELOADING
- 73 NO LOAD RUN
- 73 NO LOAD RUN
- 73 STOP 1
- 73 STOP 2
- 73 STOP 3
- 73 NO LOAD RUN

FILE 02.GSI

July 3, 2018

P=058

STATIC (SPAN 1-2)

TIME	DESCRIPTION	METHOD	LECT
10:06-10:19	NO LOAD RUN	>	3
10:33-10:46	STOP 1	>	3
10:54-11:09	STOP 2	>	3
11:17-11:30	STOP 3	>	3
	NO LOAD RUN	>	3

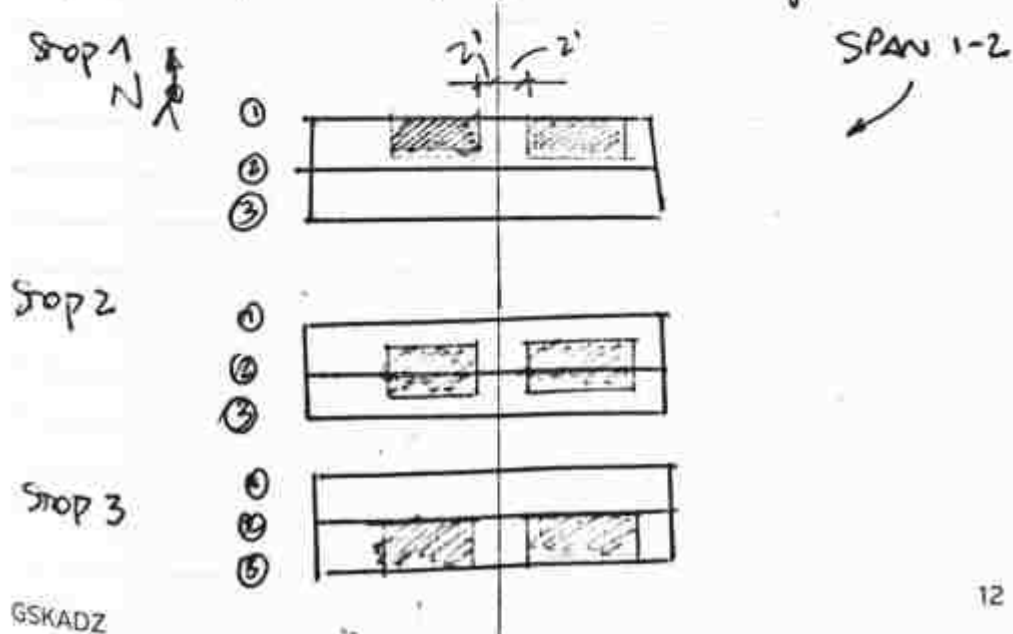
Michael removed t/s before finishing

DYNAMIC

- ✓ 10 mph
- ✓ 20 mph
- ✓ 30 mph
- ✓ 40 mph
- ✓ 50 mph
- X 60 mph

✓ MARK (✓ or X)

- Dynamic 1-WE ✓ Dynamic 1-EW ✓
- Dynamic 2-WE ✓ Dynamic 2-EW ✓
- Dynamic 3-WE ✓ Dynamic 3-EW ✓
- Dynamic 4-WE ✓ Dynamic 4-EW ✓
- Dynamic 5-WE ✓ Dynamic 5-EW X
- Dynamic 6-WE ✓ Dynamic 6-EW ✓



GSKADZ

12

FILE

.GSI

REFERENCES

- AC434. (2013). "Proposed acceptance criteria for masonry and concrete strengthening using fiber-reinforced cementitious matrix (FRCM) composite systems." ICC-Evaluation Service, Whittier, CA.
- ACI Committee 318. (2014). *Building Code Requirements for Structural Concrete and Commentary*. American Concrete Institute. Farmington Hills, Michigan.
[https://doi.org/10.1016/0262-5075\(85\)90032-6](https://doi.org/10.1016/0262-5075(85)90032-6)
- ACI Committee 440. (2008). *ACI 440.2R-08 Guide for the Design and Construction of Externally Bonded FRP Systems. Guide for the Design and Construction of Externally Bonded FRP Systems for Strengthening Concrete Structures*.
- ACI Committee 440. ACI 440.2R-17: Guide for the design and construction of externally bonded FRP systems for strengthening existing structures, American Concrete Institute § (2017).
- ACI Committee 549. (2013). *ACI 549.4R-13: Guide to Design and Construction of Externally Bonded Fabric-Reinforced Cementitious Matrix (FRCM) Systems for Repair and Strengthening Concrete and Masonry Structures*. American Concrete Institute. Farmington Hills, Michigan.
- Aram, M. R., Czaderski, C., & Motavalli, M. (2008). Debonding failure modes of flexural FRP-strengthened RC beams. *Composites Part B: Engineering*, 39(5), 826–841. <https://doi.org/10.1016/j.compositesb.2007.10.006>
- Arboleda, D. (2014). *Fabric Reinforced Cementitious Matrix (FRCM) Composites for Infrastructure Strengthening and Rehabilitation : Characterization Methods*.
- ASCE. (2017). 2017 Infrastructure Report Card.
<https://doi.org/10.1017/CBO9781107415324.004>
- Babaeidarabad, S., Loreto, G., & Nanni, A. (2014). Flexural Strengthening of RC Beams with an Externally Bonded Fabric-Reinforced Cementitious Matrix. *Journal of Composites for Construction*, 18(5), 04014009.
[https://doi.org/10.1061/\(ASCE\)CC.1943-5614.0000473](https://doi.org/10.1061/(ASCE)CC.1943-5614.0000473)
- Barton, B., Wobbe, E., Dharani, L. R., Silva, P., Birman, V., Nanni, A., ... Tunis, G. (2005). Characterization of reinforced concrete beams strengthened by steel reinforced polymer and grout (SRP and SRG) composites. *Materials Science and Engineering A*, 412(1–2), 129–136. <https://doi.org/10.1016/j.msea.2005.08.151>
- Brameshuber, W. (2006). *Textile Reinforced Concrete - State-of-the-Art Report of RILEM TC 201-TRC*. RILEM.

- D'Ambrisi, A., & Focacci, F. (2011). Flexural Strengthening of RC Beams with Cement-Based Composites. *Journal of Composites for Construction*, 15(5), 707–720. [https://doi.org/10.1061/\(ASCE\)CC.1943-5614.0000218](https://doi.org/10.1061/(ASCE)CC.1943-5614.0000218).
- Di Tommaso, A., Focacci, F., & Mantegazza, G. (2008). *PBO-FRCM composites to strengthen R . C . beams : mechanics of adhesion and efficiency. Fourth International Conference on FRP Composites in Civil Engineering*.
- Gonzalez-Libreros, J. H., Sabau, C., Sneed, L. H., Pellegrino, C., & Sas, G. (2017). State of research on shear strengthening of RC beams with FRCM composites. *Construction and Building Materials*, 149, 444–458. <https://doi.org/10.1016/j.conbuildmat.2017.05.128>
- Hernandez, & Myers. (2018). Diagnostic Test for Load Rating of a Prestressed SCC Bridge. *Evaluation of Concrete Bridge Behavior Through Load Testing - International Perspective*, ACI SP 323 11.1-11.16.
- Hind, M. K., Özakçab, M., & Ekmekyaparc, T. (2016). A Review on Nonlinear Finite Element Analysis of Reinforced Concrete Beams Retrofitted with Fiber Reinforced Polymers. *Journal of Advanced Research in Applied Mechanics*, 22(1), 13–48.
- Holdener, D. J., Myers, J. J., & Nanni, A. (2004). *Field Strengthening and Validation of FRP Composites Technology in Missouri*.
- Huang, X., Birman, V., Nanni, A., & Tunis, G. (2003). Properties and potential for application of steel reinforced polymer and steel reinforced grout composites. *Composites Part B: Engineering*, 36(1), 73–82. [https://doi.org/10.1016/S1359-8368\(03\)00080-5](https://doi.org/10.1016/S1359-8368(03)00080-5)
- Kerakoll S.p.A. (2014). GeoSteel G600, 1–4.
- Loreto, G., Babaeidarabad, S., Leardini, L., & Nanni, A. (2015). RC beams shear-strengthened with fabric-reinforced-cementitious-matrix (FRCM) composite. *International Journal of Advanced Structural Engineering*, 7(4), 341–352. <https://doi.org/10.1007/s40091-015-0102-9>
- Loreto, G., Leardini, L., Arboleda, D., & Nanni, A. (2013). Performance of RC Slab-Type Elements Strengthened with Fabric-Reinforced Cementitious-Matrix Composites. *Journal of Composites for Construction*, 18(3), A4013003. [https://doi.org/10.1061/\(ASCE\)CC.1943-5614.0000415](https://doi.org/10.1061/(ASCE)CC.1943-5614.0000415)
- Merkle, W. J. (2004). *LOAD DISTRIBUTION AND RESPONSE OF BRIDGES RETROFITTED WITH VARIOUS FRP SYSTEMS*. University of Missouri- Rolla.
- Missouri Department of Transportation. (2005). Preservation of Missouri Transportation Infrastructures : Validation of FRP Composite Technology. *Missouri Department of Transportation Research, Development and Technology*.

- Myers, J. J., Holdener, D., & Merkle, W. (2012). Load testing and load distribution of fiber reinforced, polymer strengthened bridges: Multi-year, post construction/post retrofit performance evaluation. *Fiber Reinforced Polymer (FRP) Composites for Infrastructure Applications: Focusing on Innovation, Technology Implementation and Sustainability*, 163–191. https://doi.org/10.1007/978-94-007-2357-3_9
- Myers, J. J., Holdener, D., Merkle, W., & Hernandez, E. (2008). *PRESERVATION OF MISSOURI TRANSPORTATION INFRASTRUCTURES: IN-SITU LOAD TESTING OF BRIDGES P-962, T-530, X-495, X-596 AND Y-298*.
- Nanni, Antonio. "Properties of Materials - Southern Mo Bridge Strengthening: RECAST." 7 Mar. 2018.
- Ombres, L. (2015). Structural performances of reinforced concrete beams strengthened in shear with a cement based fiber composite material. *Composite Structures*, 122, 316–329. <https://doi.org/10.1016/j.compstruct.2014.11.059>
- Petrou, M. F., Parler, D., Harries, K. A., & Rizos, D. C. (2008). Strengthening of Reinforced Concrete Bridge Decks Using Carbon Fiber-Reinforced Polymer Composite Materials. *Journal of Bridge Engineering*, 13(5), 455–467. [https://doi.org/10.1061/\(ASCE\)1084-0702\(2008\)13:5\(455\)](https://doi.org/10.1061/(ASCE)1084-0702(2008)13:5(455))
- Pino, V. A. (2016). Fabric Reinforced Cementitious Matrix (FRCM) Composites as a Repair System for Transportation Infrastructure.
- Rahman, A. H., Kingsley, C. Y., & Kobayashi, K. (2000). SERVICE AND ULTIMATE LOAD BEHAVIOR OF BRIDGE DECK REINFORCED WITH CARBON FRP GRID. *Journal of Composites for Construction*, 45(February), 16–23.
- Ruredil. (2012). Ruredil X Mesh Gold, 1–6. Retrieved from www.ruredil.it
- Simpson Strong-Tie. (2017). CSS-CM Product Guide. Retrieved from strongtie.com
- Simpson Strong-Tie. (2018). CSS-UCG Product Guide. Retrieved from strongtie.com
- Structural Technologies. (2016a). V-Wrap™ 770 Product Guide, 4–5. Retrieved from structuraltechnologies.com
- Structural Technologies. (2016b). V-Wrap™ C200HM Product Guide, 1–2. Retrieved from structuraltechnologies.com
- Wight, J. K., & Macgregor, J. G. (2012). *Reinforced concrete: mechanics and design* (6th ed.). Upper Saddle River, New Jersey: Pearson Education, Inc. <https://doi.org/10.1139/100-087>

Wobbe, E., Silva, P., Barton, B. L., Dharani, L. R., Birman, V., Nanni, A., ... Tunis, G. (2004). Flexural capacity of RC beams externally bonded with SRP and SRG. *International SAMPE Symposium and Exhibition (Proceedings)*, 49, 2995–3002. Retrieved from <http://www.scopus.com/inward/record.url?eid=2-s2.0-23844538743&partnerID=tZOtx3y1>

VITA

Michael Andrew Janke was born in St. Louis, Missouri on September 9, 1994. He grew up in Rolla, Missouri, and thus was exposed to Missouri University of Science and Technology (Missouri S&T) at a young age. A love for physics, encouragement from family and friends, and an interest in structures led him to pursue a degree in civil engineering at Missouri S&T.

Michael was involved in many student organizations at Missouri S&T. He was a part of the inaugural class of the Greenberg Scholars Program, which was established to help passionate students get undergraduate research experience, and accelerate their M.S. programs. Michael also joined the Missouri S&T American Society of Civil Engineers student chapter as a freshman, where he held several positions, including chapter president in spring 2016. He was inducted into the civil engineering honor society, Chi Epsilon, as well as the general engineering honors fraternity, Tau Beta Pi. Other organizations Michael was a part of include Delta Sigma Phi fraternity, Steel Bridge Design Team, and Miner Challenge alternative spring breaks. In the spring of 2017, Michael dual enrolled in order to begin master's courses as he finished his B.S. In May of 2017, Michael graduated summa cum laude with a Bachelor of Science degree in Civil Engineering.

Michael continued his education at Missouri S&T, later earning his Master of Science degree in Civil Engineering with an emphasis in Structural Engineering in December of 2018. He chose to start his professional career with KPFF in St. Louis, Missouri, and was very grateful for his time spent at Missouri S&T in Rolla, Missouri.